星形成における磁場について------ALMAに向けて

Contraction of Magnetized Rotating Clouds and Outflows

Kohji Tomisaka

with collaborators: M. N. Machida (Kyoto U.), K. Saigo (NAOJ), T. Matsumoto (Hosei U.), Hanawa (Chiba U.)

星形成の概念図

太陽質量程度の星の形成過程

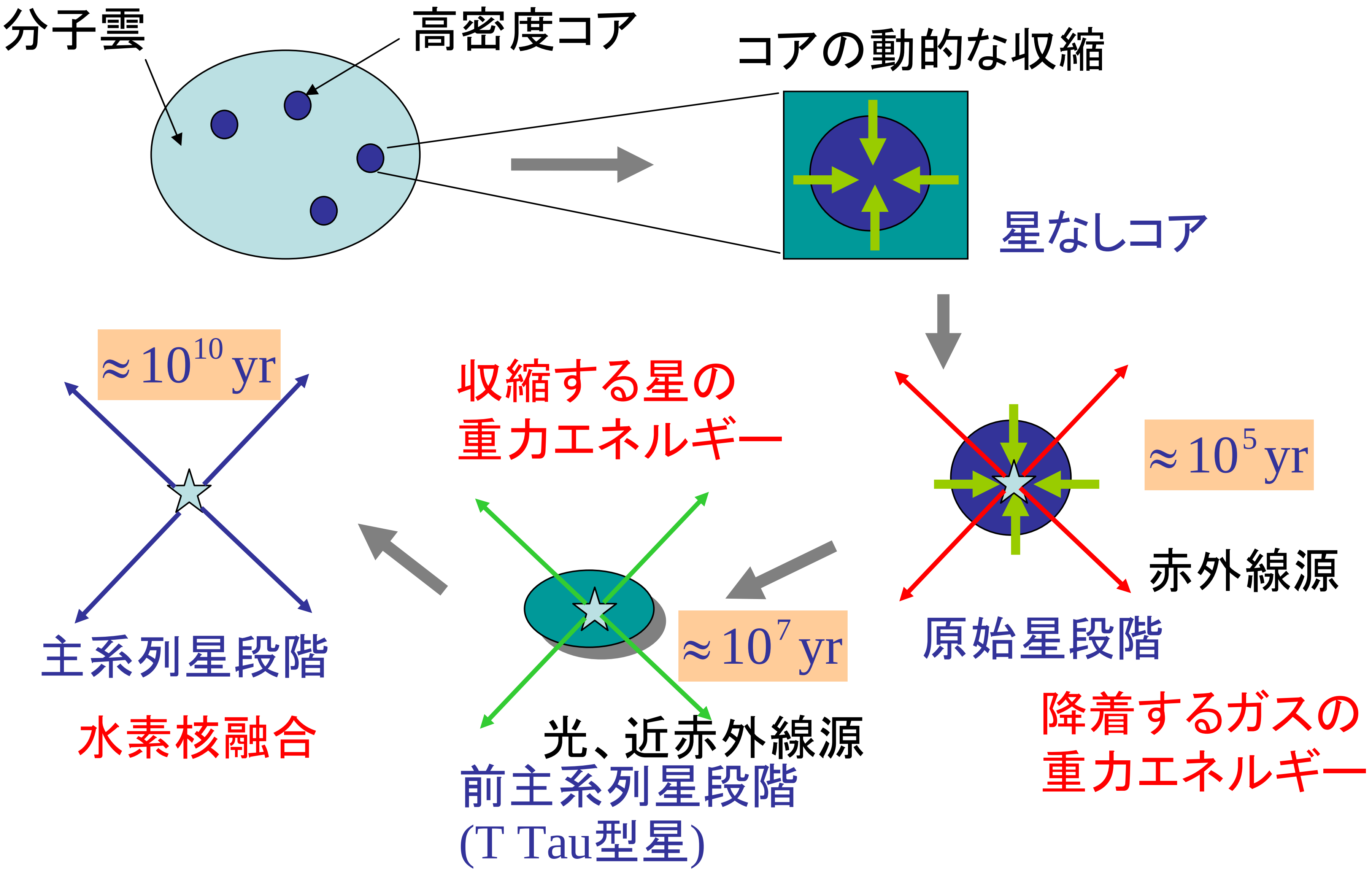

ビリアル定理

- ビリアル定理から、球状の雲が力学平衡状態にある条件が決められる。
- 運動方程式に $\mathbf{r}$ を内積して雲全体にわたって体積積分すると、

$$\rho\left(\frac{\partial \mathbf{u}}{\partial t}+(\mathbf{u}\cdot\nabla)\mathbf{u}\right)=-\nabla p-\rho\nabla\phi+\frac{1}{4\pi}(\nabla\times\mathbf{B})\times\mathbf{B}$$

- ビリアル関係式

$$\frac{1}{2}\frac{d^2 I}{dt^2}=2(T-T_0)+\mathrm{M}+W$$

星形成の条件

ビリアル定理

- 慣性モーメント $$I = \int \rho r^2 dV$$
- 運動エネルギー $$T = \int \left(\frac{3}{2} p_{th} + \frac{1}{2} \rho v^2 \right) dV = \frac{3}{2} \overline{P} V_{cl}$$
- 表面圧力項 $$T_0 = \int_S P_{th} \mathbf{r} \cdot \mathbf{n} dS = \frac{3}{2} P_0 V_{cl}$$
- 磁場項

$$\mathrm{M} = \int \frac{B^2}{8\pi} dV + \int_S (\mathbf{r} \cdot \mathbf{B}) \mathbf{B} \cdot \mathbf{n} dS - \int_S \frac{B^2}{8\pi} \mathbf{r} \cdot \mathbf{n} dS$$

$$\approx \int \frac{B^2 - {B_0}^2}{8\pi} dV \approx \frac{1}{6\pi^2} \left(\frac{\Phi_B^2}{R} - \frac{\Phi_B^2}{R_0} \right)$$

$$\Phi_B = \pi R_0^2 B_0$$

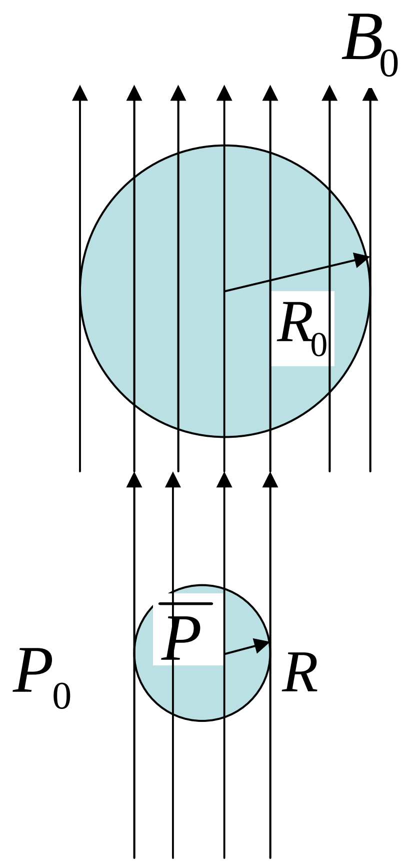

- 重力項

$$W = -\int \rho \mathbf{r} \cdot \nabla \phi dV = -\frac{3}{5} a \frac{GM^2}{R}$$

星形成の条件

ビリアル定理

B＝0の場合（ジーンズ質量）

- 平衡条件

$$\frac{1}{2}\frac{d^2I}{dt^2}=2(T-T_0)+W$$

- 等温を仮定

$$4\pi\overline{P}R^3-4\pi P_0R^3-\frac{3}{5}a\frac{GM^2}{R}=0$$

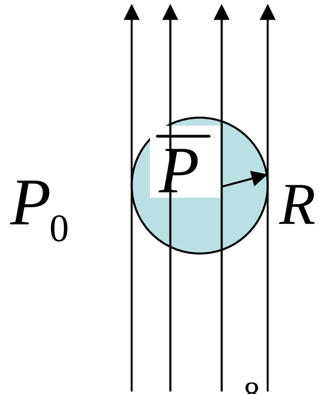

- 外圧に関する条件

$$\overline{P}=c_s^2\overline{\rho}=c_s^2\frac{3M}{4\pi R^3}$$

$$P_{0,\max}=3.15\frac{c_s^8}{G^3M^2}$$

$$P_0=\frac{3c_s^2M}{4\pi R^3}-\frac{3aGM^2}{20\pi R^4}$$

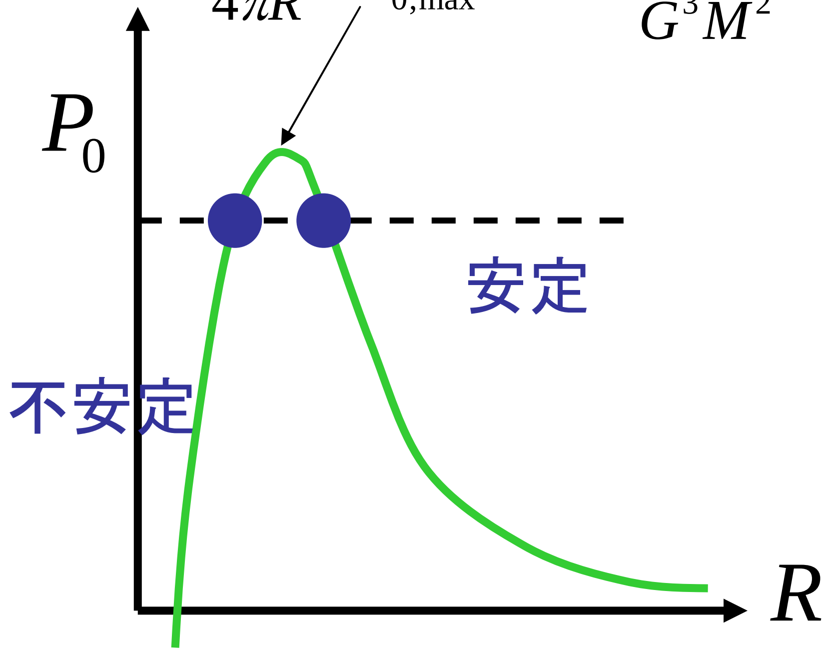

- ジーンズ質量

$$M<M_J=1.77\frac{c_s^4}{G^{3/2}P_0^{1/2}}$$

磁場が存在する場合

$$\frac{1}{2}\frac{d^2 I}{dt^2} = 2(T - T_0) + \mathrm{M} + W$$

- 星間雲を貫く磁束 $\Phi_B \equiv B_0 \pi R_0^2$ が一定
- 磁場の項 $\int B^2 dV \approx \dfrac{\Phi_B^2}{R} \propto \dfrac{GM^2}{R}$ 重力の項
- 初期に磁場が収縮を止められなければ、その後も収縮を止めることは出来ない。
- 平衡条件

$$4\pi \overline{P} R^3 - 4\pi P_0 R^3 - \frac{3G}{5R}\left(M^2 - M_\Phi^2\right) = 0$$

$$\frac{3GM_\Phi^2}{5R} = \frac{\Phi_B^2}{3\pi^2 R}$$

星形成の条件

ビリアル定理

- 準臨界雲

$M < M_\Phi \quad M_\Phi < M < M_{cr}$

- 超臨界雲 $\begin{cases} M > M_\Phi \\ M > M_{cr} \end{cases}$

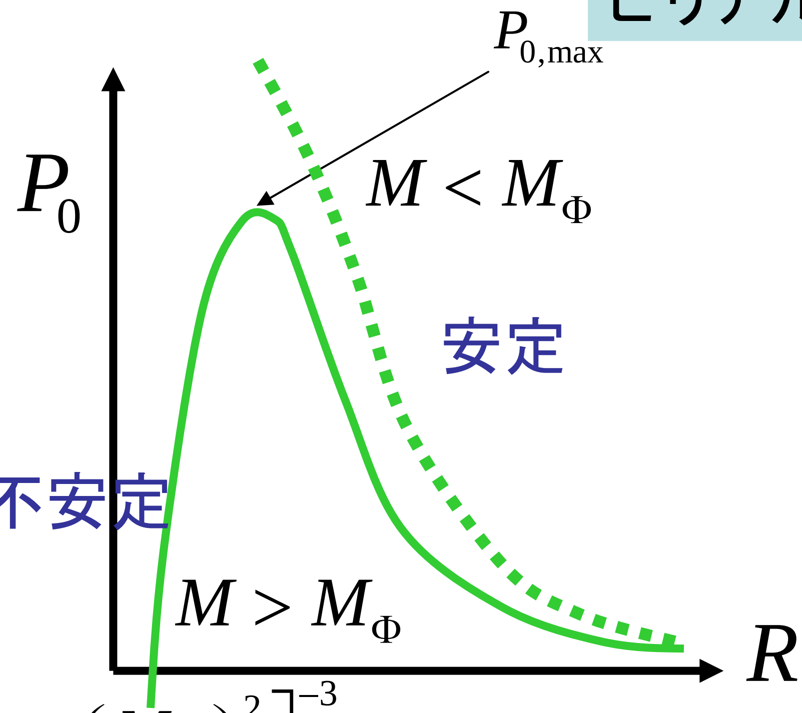

- 外圧に関する条件

$$P_0 < P_{0,\max} = 3.15 \frac{c_s^8}{G^3 M^2} \left[1 - \left(\frac{M_\Phi}{M} \right)^2 \right]^{-3}$$

- ジーンズ質量

$$M < M_{cr} = 1.77 \frac{c_s^4}{G^{3/2} P_0^{1/2} \left[1 - \left(M_\Phi / M \right)^2 \right]^{3/2}} \quad (M > M_\Phi)$$

臨界雲 $M_\Phi = \dfrac{1}{3\pi} \sqrt{\dfrac{5}{G}} \Phi_B \approx 55 M \left(R / 0.2\mathrm{pc} \right)^2 \left(B / 100\,\mu\mathrm{G} \right)$

$$\left. \sqrt{G} M / \Phi_B \right|_c \simeq \sqrt{5} / 3\pi = 0.24$$

磁気静水圧平衡

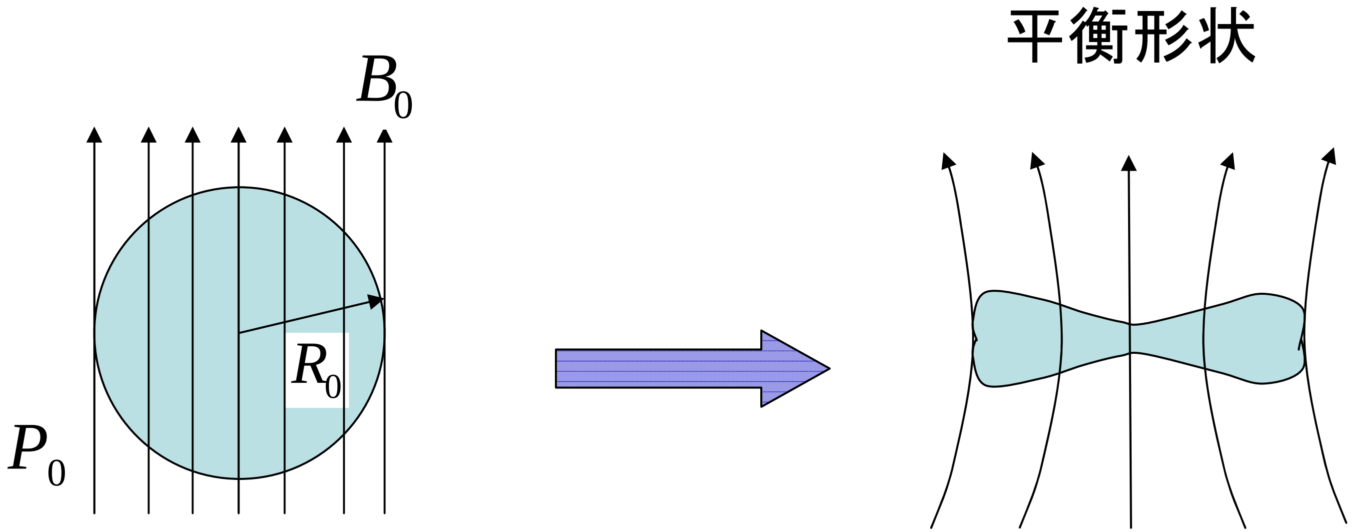

磁束管内の質量と角運動量を保存

Mass Loading　　Angular Momentum Loading

≈プラズマの閉じ込め

中心密度の異なる一連の解（外圧、磁束＝一定）

ρ_c: $2 \Rightarrow 10^3$

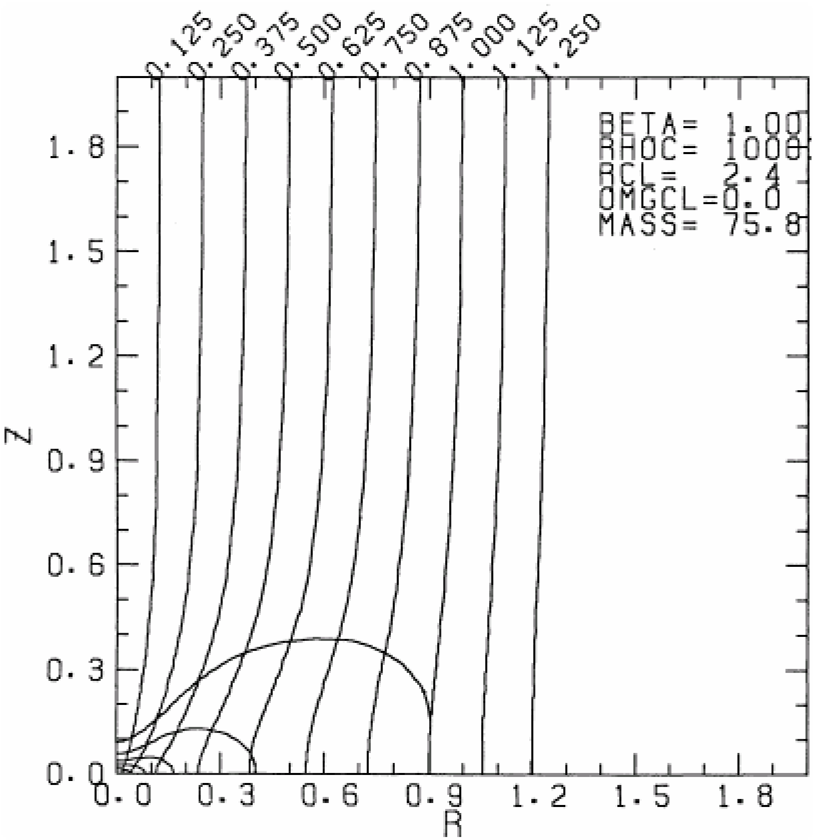

$\beta = 1$

ρ_c: $2 \Rightarrow 10^3$

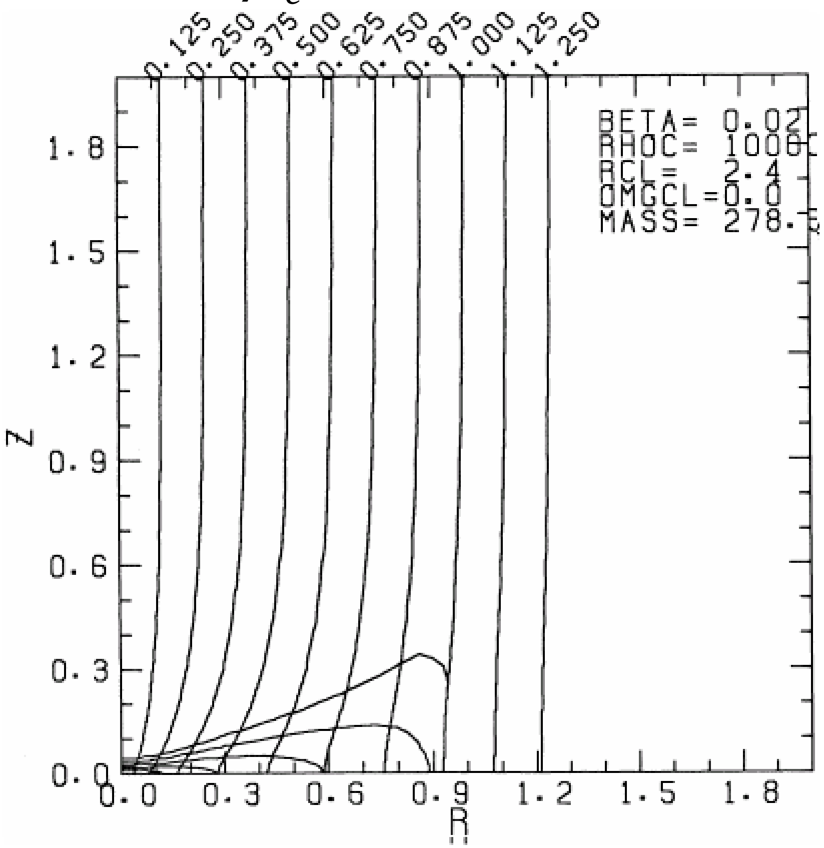

$\beta = 0.02$

最大質量

$$\beta_0 = p_{ext} / (B_0^2 / 8\pi)$$

p_{ext} 一定

星間雲を貫く磁束

$\Phi_B \Uparrow$

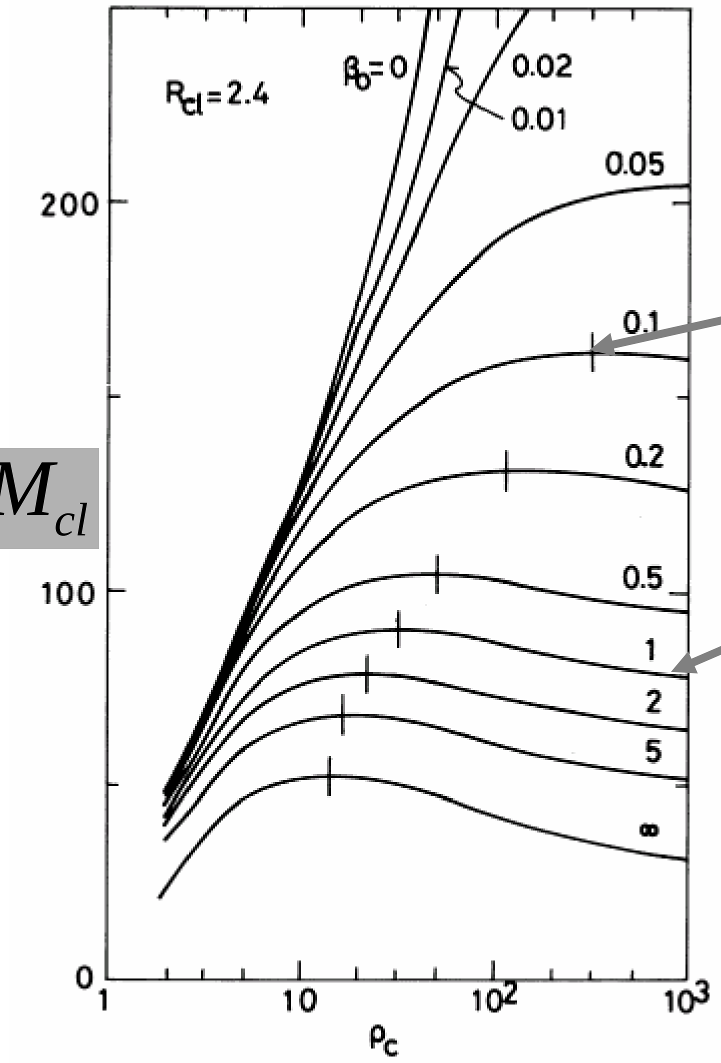

最大質量

M_{cl}

$\Phi_B = \mathrm{const}$

ρ_c / ρ_s

磁場は自己重力を支えることができる

星形成の条件

磁気雲の重力収縮

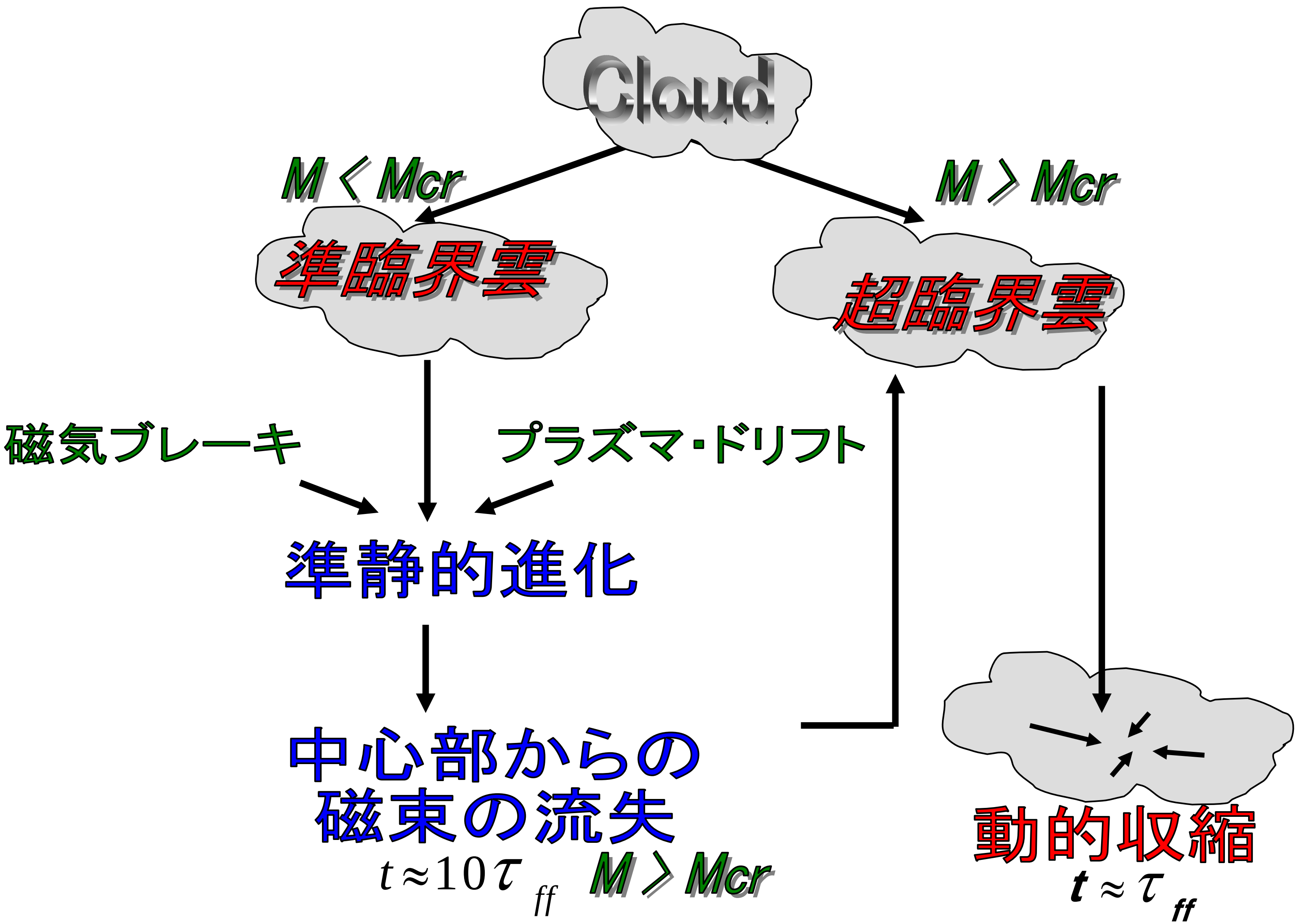

$$\sqrt{G}M/\Phi_B\big|_c \simeq 0.17 \simeq 1/2\pi$$

$$M < M_{cr} = 1.39\left[1-\left(\frac{0.17}{G^{1/2}\sigma_c/B_c}\right)^2\right]^{-3/2}\frac{c_s^4}{G^{3/2}P_0^{1/2}}$$

$1/2\pi$

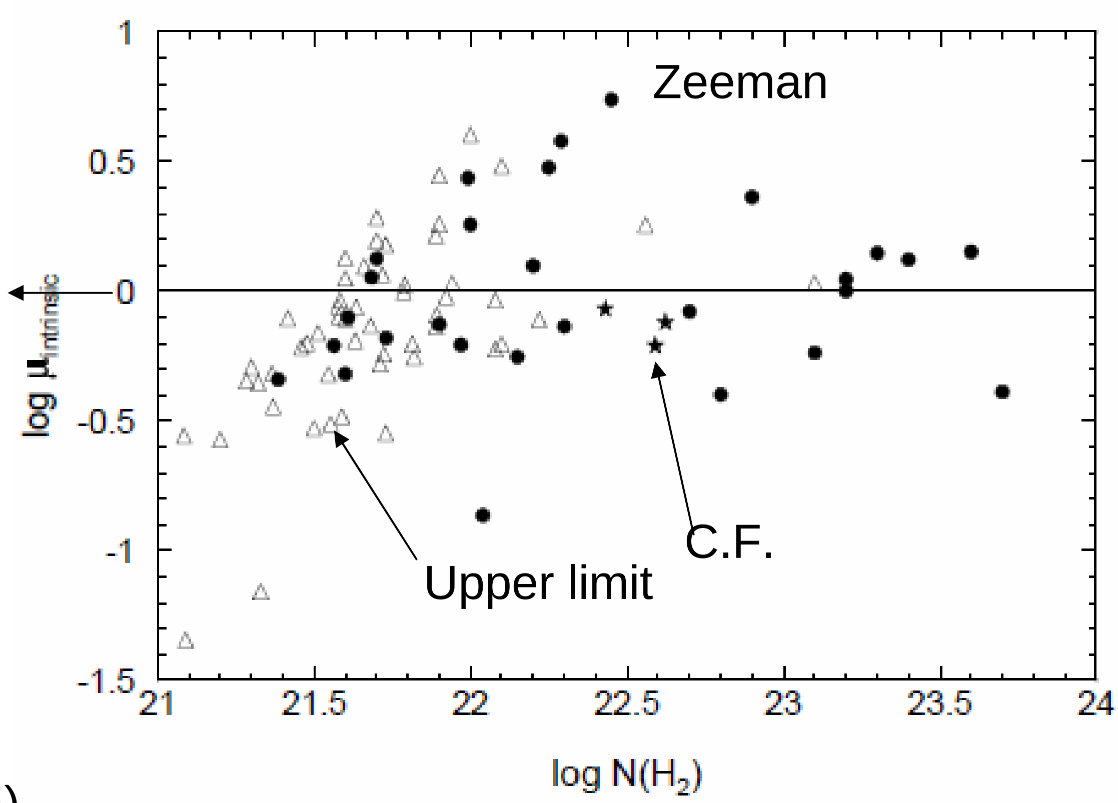

Heiles & Crutcher (2005)

Taurus Molecular Cloud

^{13}CO

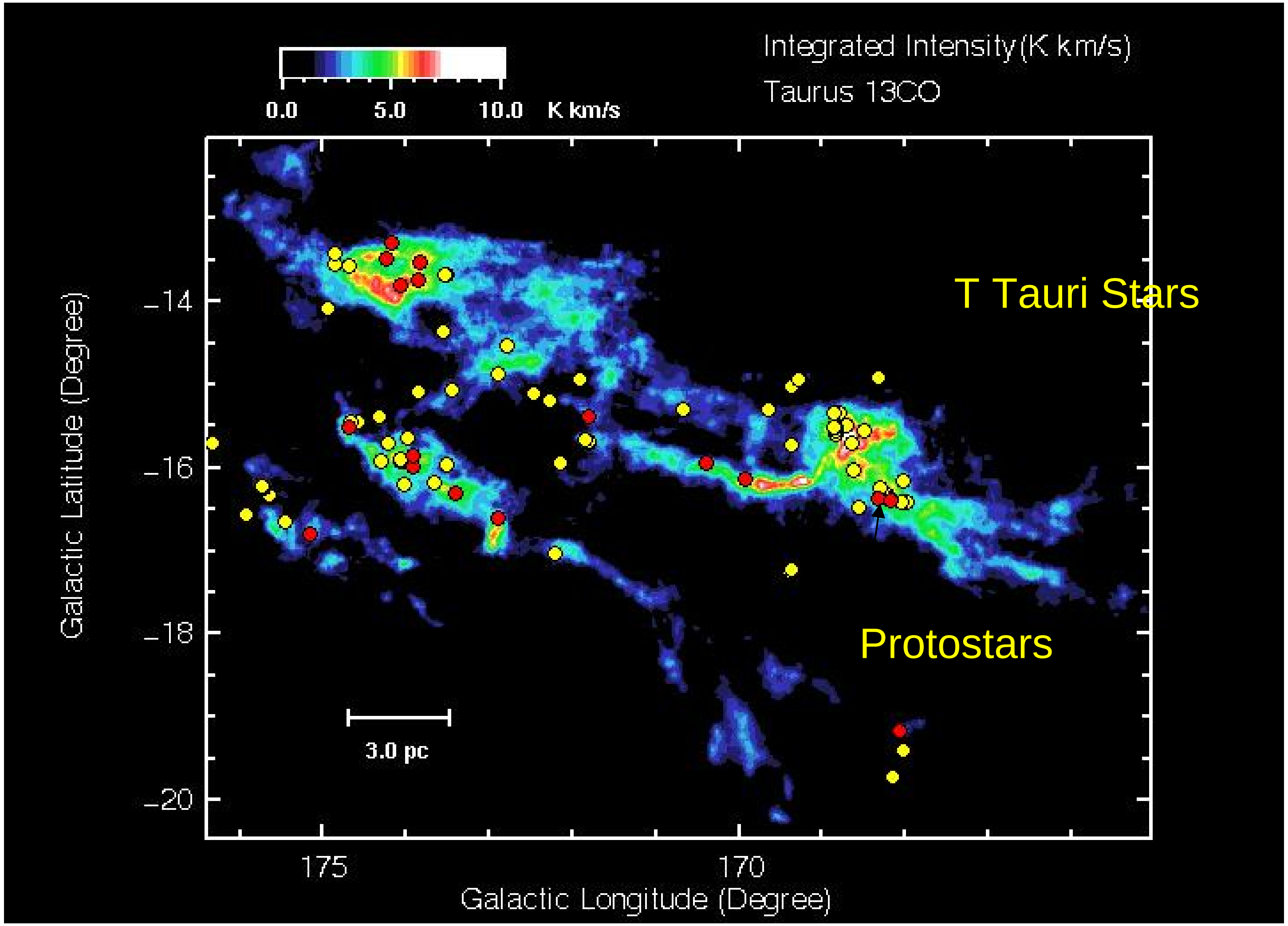

^{13}CO map of Taurus molecular cloud observed by Nagoya 4m radio telescope.

Star Formation in Molecular Cloud

Molecular Cores

$C^{18}O$

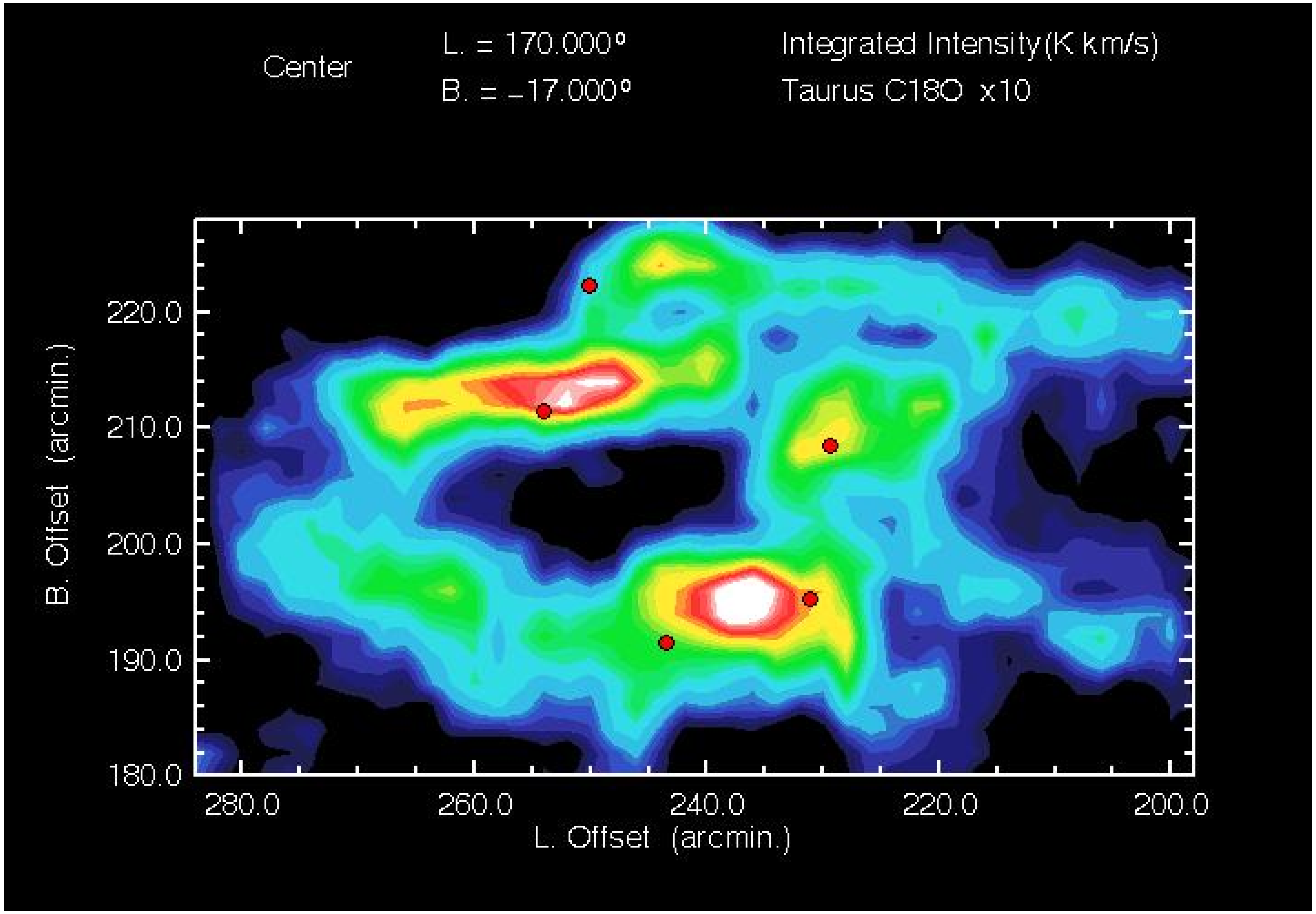

$C^{18}O$ integrated intensity map of HLC2 in Taurus molecular cloud.
This shows the molecular cloud consists of many molecular cores.

Cores with/without Protostars

$H^{13}CO$

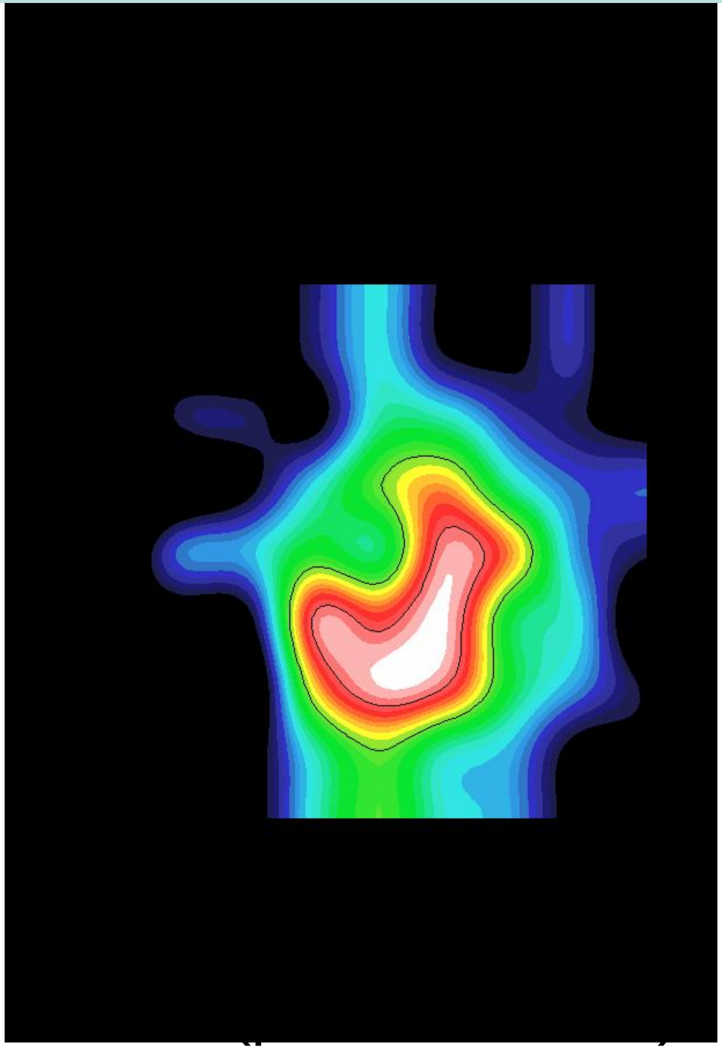

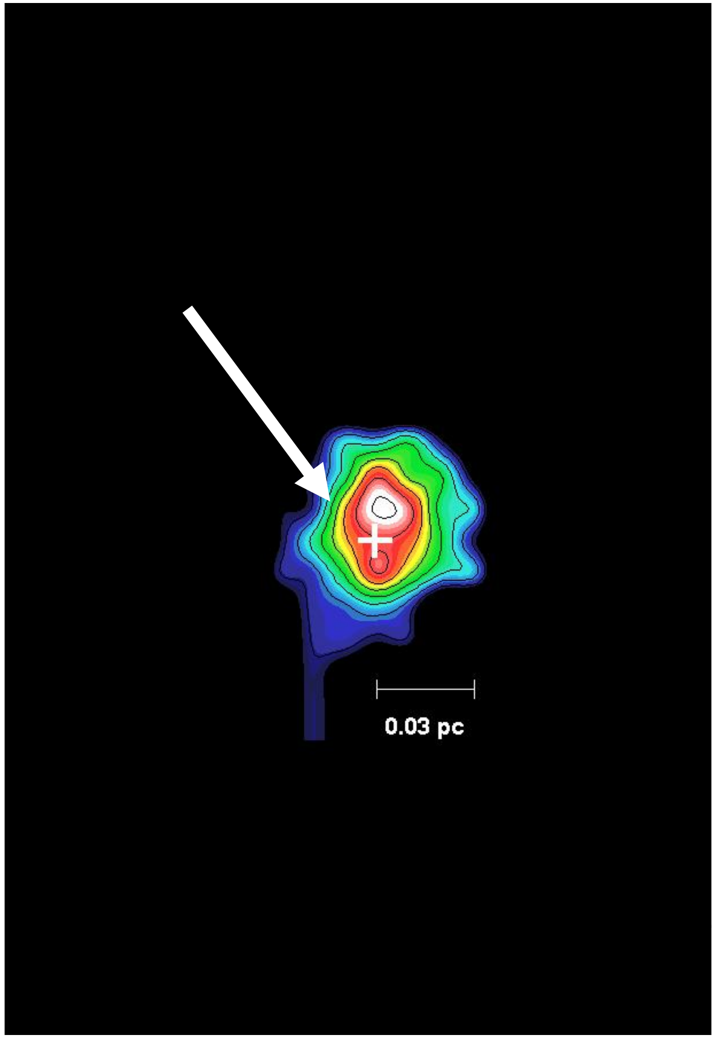

$H^{13}CO$ integrated intensity map of prestellar (left) and protostellar (right) cores in Taurus molecular cloud observed by Nobayama 45m radio telescope

Star Formation of ~$M_\odot$ stars

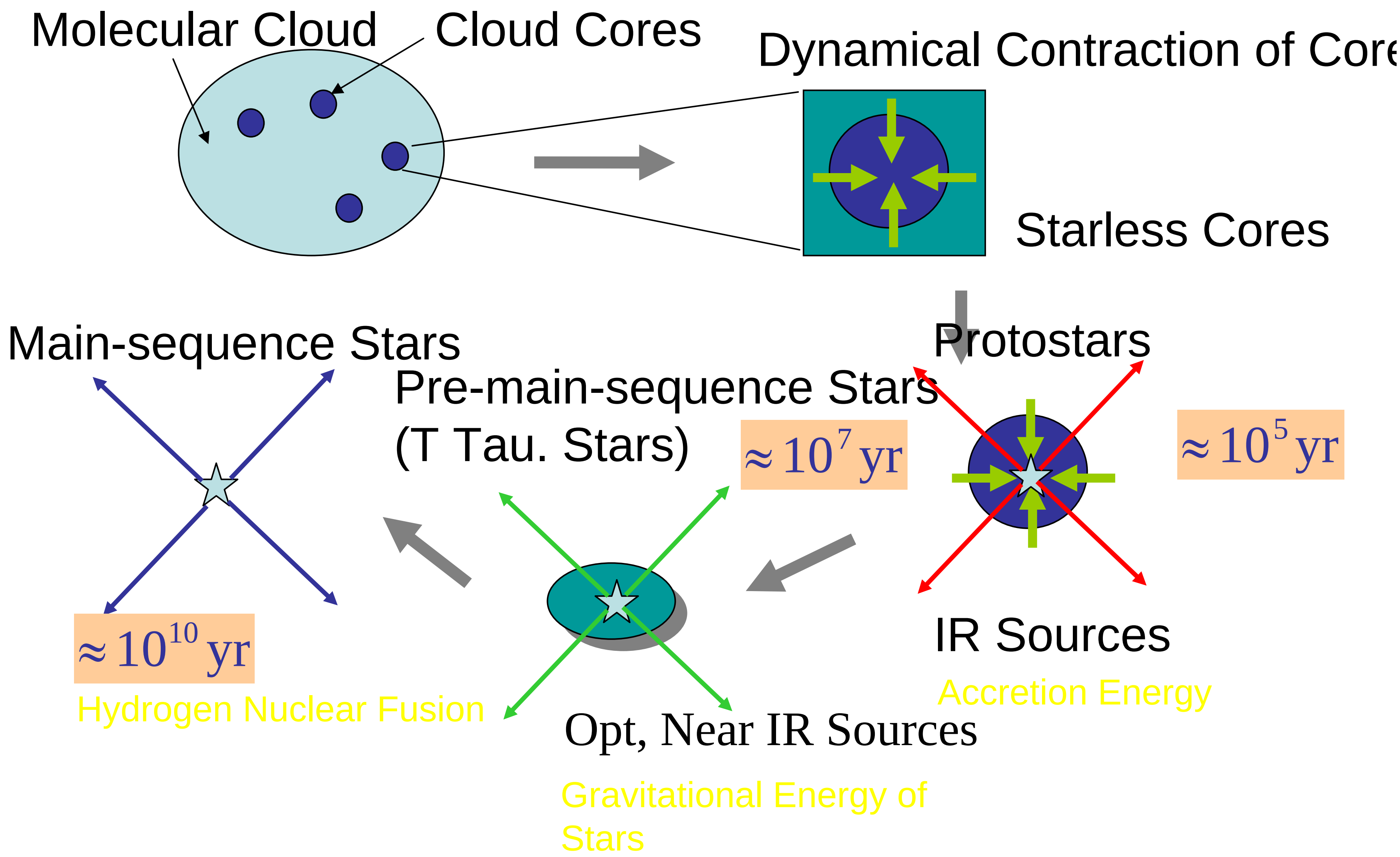

Spherical Collapse

Gas $(\mathbf{B}=0,\ \Omega=0)$ contracting under the self-gravity

Larson (1969)

- isothermal $\gamma = 1$ $\rho < \rho_A = 10^{-13}$ g cm^{-3}
  - ✓run-away collapse
  - ✓first collapse
- adiabatic $\gamma = 7/5$ $\rho_A < \rho < \rho_B = 5.6\ 10^{-8}$ g cm^{-3}
  - ✓first core
  - ✓outflow
  - ✓fragmentation
- H_2 dissociation $\gamma = 1.1$ $\rho_B < \rho < \rho_C = 2.0\ 10^{-3}$ g cm^{-3}
  - ✓second collapse

Temp-density relation of IS gas.
(Tohline 1982)

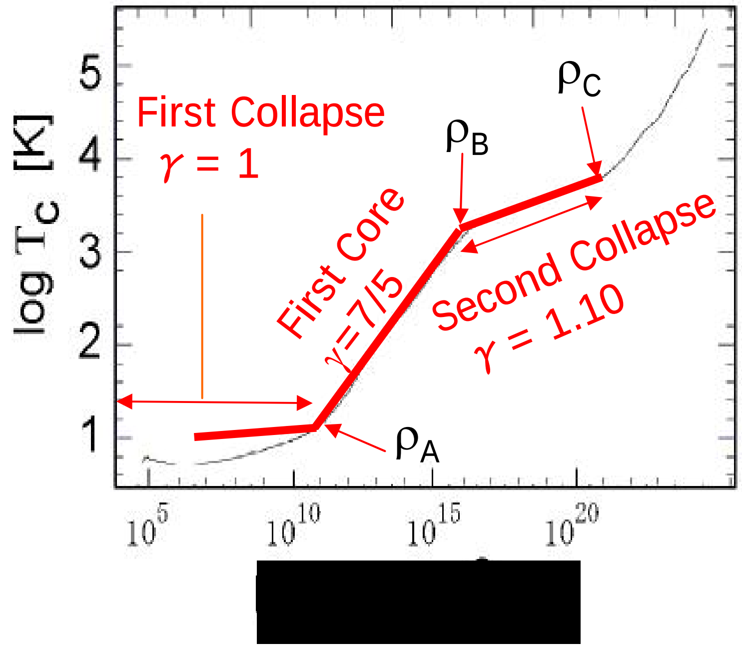

cf. Masunaga & Inutsuka (2000)

Runaway Collapse

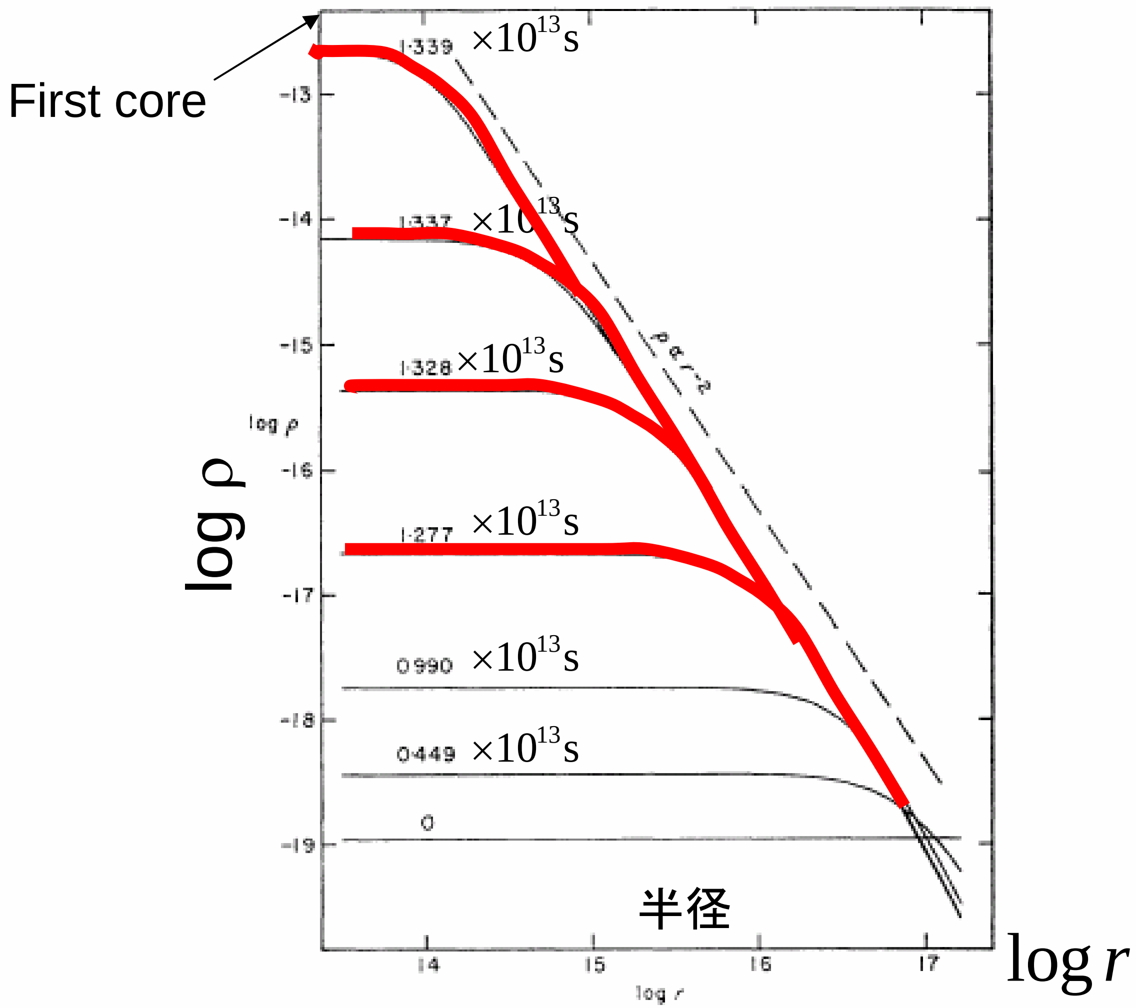

FIG. 1. *The variation with time of the density distribution in the collapsing cloud (CGS units). The curves are labelled with the times in units of* 10^{13} *s since the beginning of the collapse. Note that the density distribution closely approaches the form* $\rho \propto r^{-2}$.

Isothermal spherical collapse shows:

(1) Convergence to a power-law structure

$$\rho(r) \propto r^{-2}$$

(2) Increase of central density in a finite time.

(3) Only a central part contracts.

This is called "runaway collapse."

Larson 1969, MNRAS, 145,271

[redacted]

How about a Rotating Magnetized Cloud?

1. In case with B and Ω, a runaway contracting disk is made. As a consequence,
   (a) A flat first core is born.
   (b) Outflow is driven by a twisted B-field and a rotating disk.
   (c) B-field transfers the angular momentum from the contracting disk to the envelope.
3. Star formation process is controlled by the rotation speed of the first core.
   (a) A slow rotator evolves similarly to the $B=\Omega=0$ cloud.
   (b) A first core with Ω in a finite range,
   (c) A fast rotator fragments, which leads to binary formation.

Tomisaka (1998) ApJ **502**, L163-L167

Initial Condition

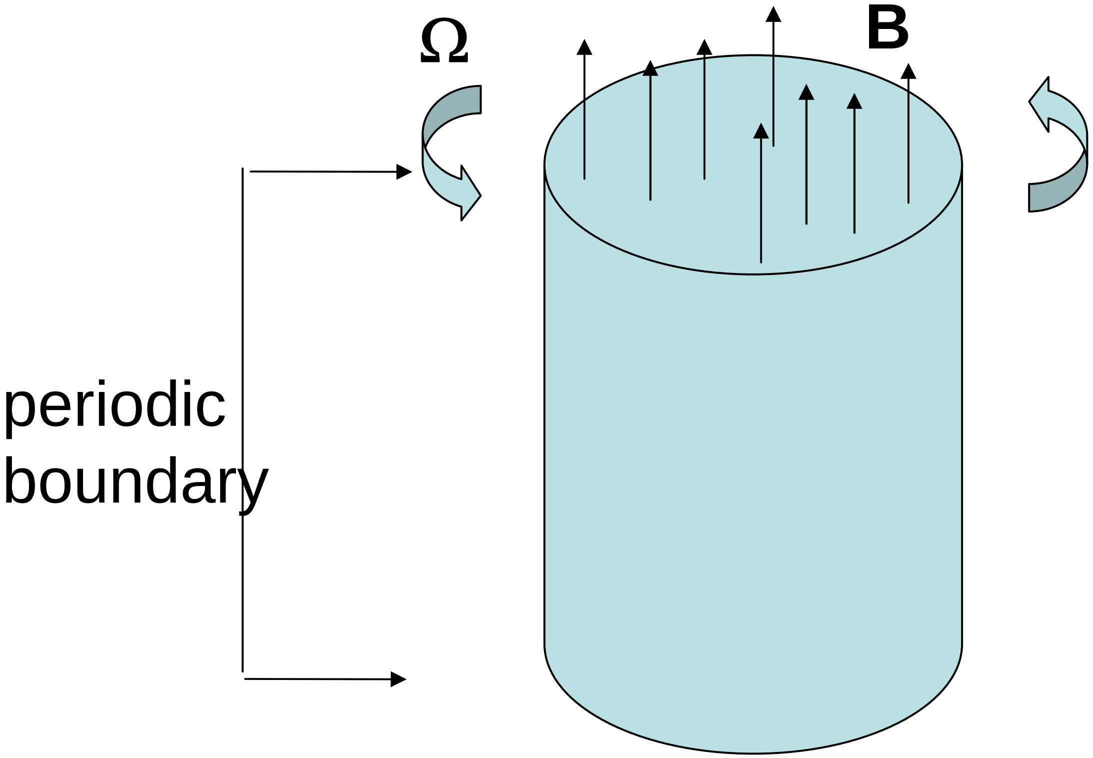

Numerical Method

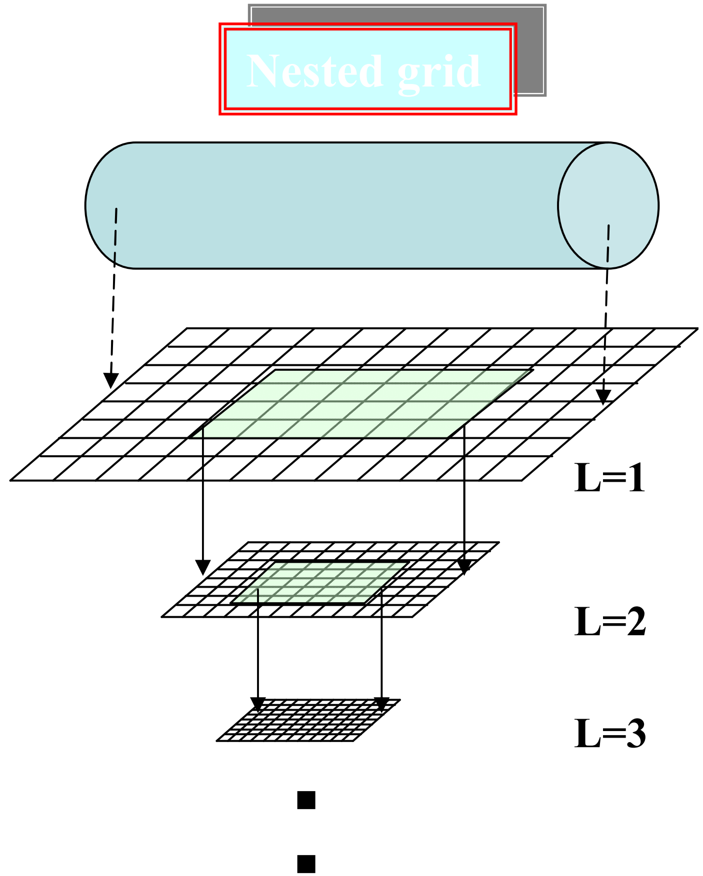

axisymmetric ρ perturbation

nonaxisymmetric ρ perturbation

The coarsest grid

Nested 4-times finer grid

Ω ρ Ω ρ

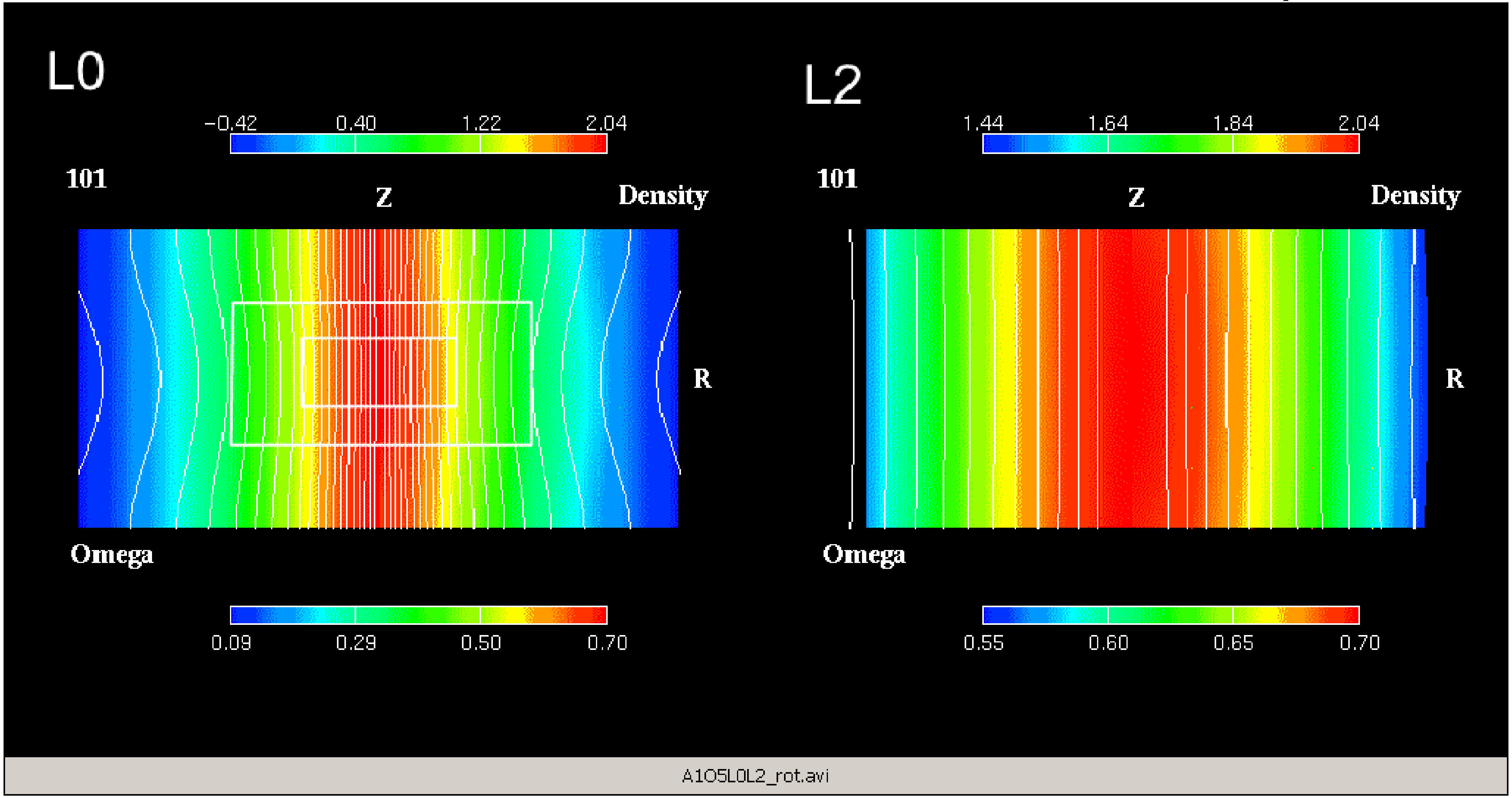

Nested 2^8-times finer grid

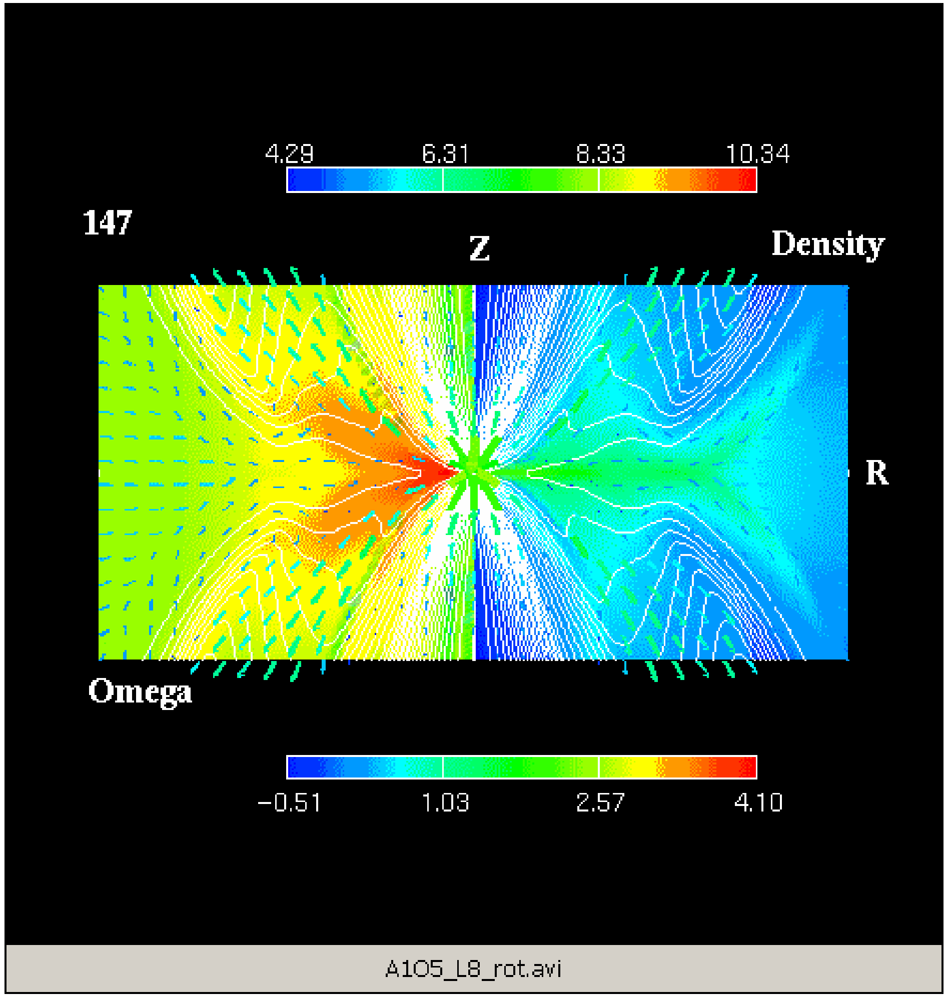

(1)Just after the central density exceeds ρ_A (first core formation), outflow begins to blow.

(2) In this case, gas is accelerated by the magnetocentrifugal wind mechanism.

(3) 10% of gas in mass is ejected with almost all the angular momentum.

ビデオ クリップ

Angular Momentum Redistribution in Dynamical Collapse

Tomisaka (2000) *ApJ* **528** L41-L44

- In outflows driven by magnetic fields:
  - The angular momentum is transferred effectively <u>from the disk to the outflow</u>.
  - If 10 % of inflowing mass is outflowed with having 99.9% of angular momentum, j_* would be reduced to 10^{-3} j_{cl}.

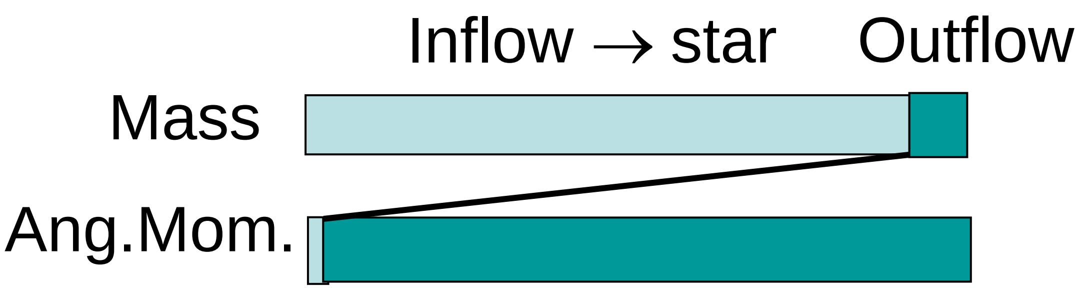

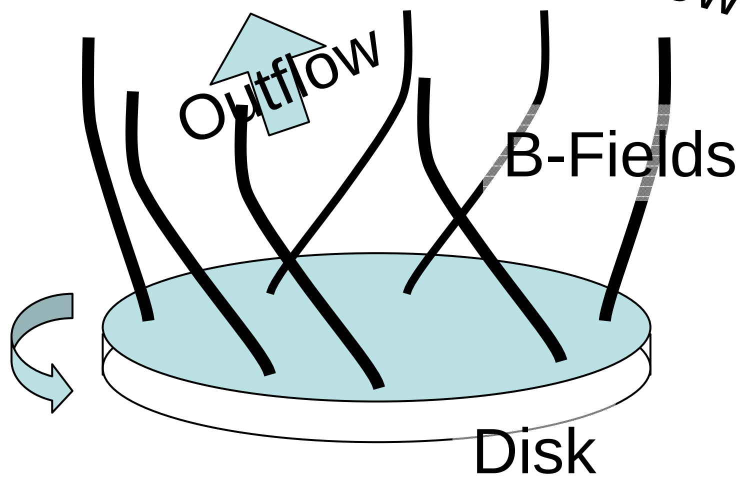

Angular Momentum Problem

- Specific Angular Momentum of a New-born Star

$$j_* \approx 6\times10^{16}\left(\frac{R_*}{2R_\odot}\right)^2\left(\frac{P}{10\mathrm{day}}\right)^{-1}\ \mathrm{cm^2s^{-1}}$$

- Orbital Angular Momentum of a Binary System

$$j_{\mathrm{bin}} \approx 4\times10^{19}\left(\frac{R_{\mathrm{bin}}}{100\mathrm{AU}}\right)^{1/2}\left(\frac{M}{M_\odot}\right)^{1/2}\ \mathrm{cm^2s^{-1}}$$

- Specific Angular Momentum of a Parent Cloud Core

$$j_{\mathrm{cl}} \approx 5\times10^{21}\left(\frac{R}{0.1\mathrm{pc}}\right)^2\left(\frac{\Omega}{4\mathrm{kms^{-1}pc^{-1}}}\right)\mathrm{cm^2s^{-1}}$$

$$\left.\begin{array}{l} \\ \\ \\ \end{array}\right\} \quad j_{\mathrm{cl}} >> j_* \quad j_{\mathrm{cl}} >> j_{\mathrm{bin}}$$

- Centrifugal Radius

$$R_c = \frac{j^2}{GM} \approx 0.06\mathrm{pc}\left(\frac{j}{5\times10^{21}\mathrm{cm^2s^{-1}}}\right)^2\left(\frac{M}{M_\odot}\right)^{-1}$$

$$R_c >> R_* \quad R_c >> R_{\mathrm{bin}}$$

Tomisaka 2000 ApJL **528** L41--L44

Angular Momentum Distribution

(1) Mass measured from the center

$$M(\rho > \rho_1) \equiv \int_{\rho > \rho_1} \rho dV$$

(2) Angular momentum in $M(\rho > \rho_1)$

$$L(\rho > \rho_1) \equiv \int_{\rho > \rho_1} \rho r v_\phi dV$$

(3) Specific Angular momentum distribution

$$j(< M) \equiv \frac{L(\rho > \rho_1)}{M(\rho > \rho_1)}$$

Run-away Collapse

High-density region is formed by gases with small *j*.

Accretion Stage

Magnetic torque brings the angular momentum from the disk to the outflow.

Outflow brings the angular momentum.

Angular Momentum Transfer

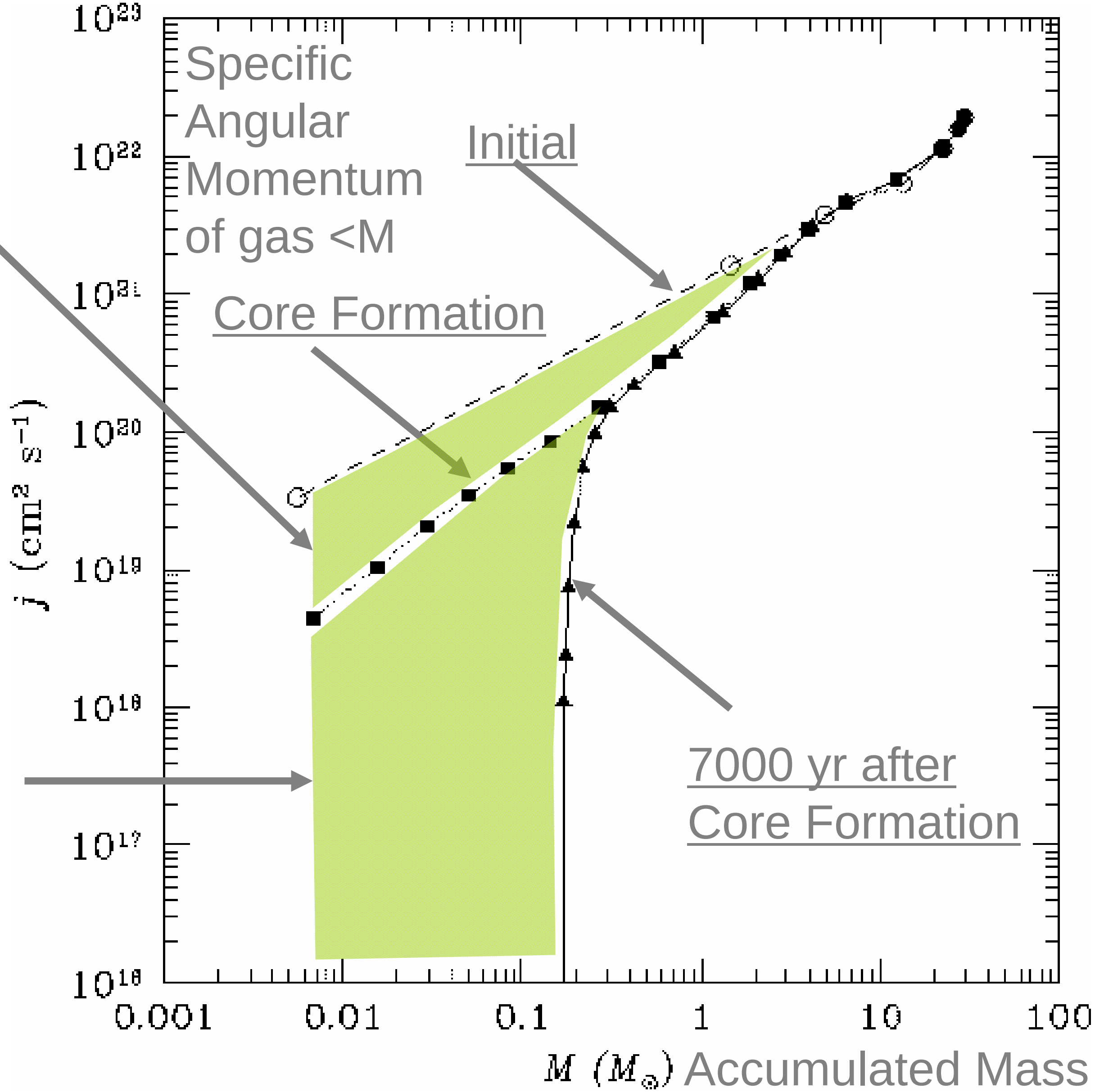

Molecular Outflow

L1551 IRS5

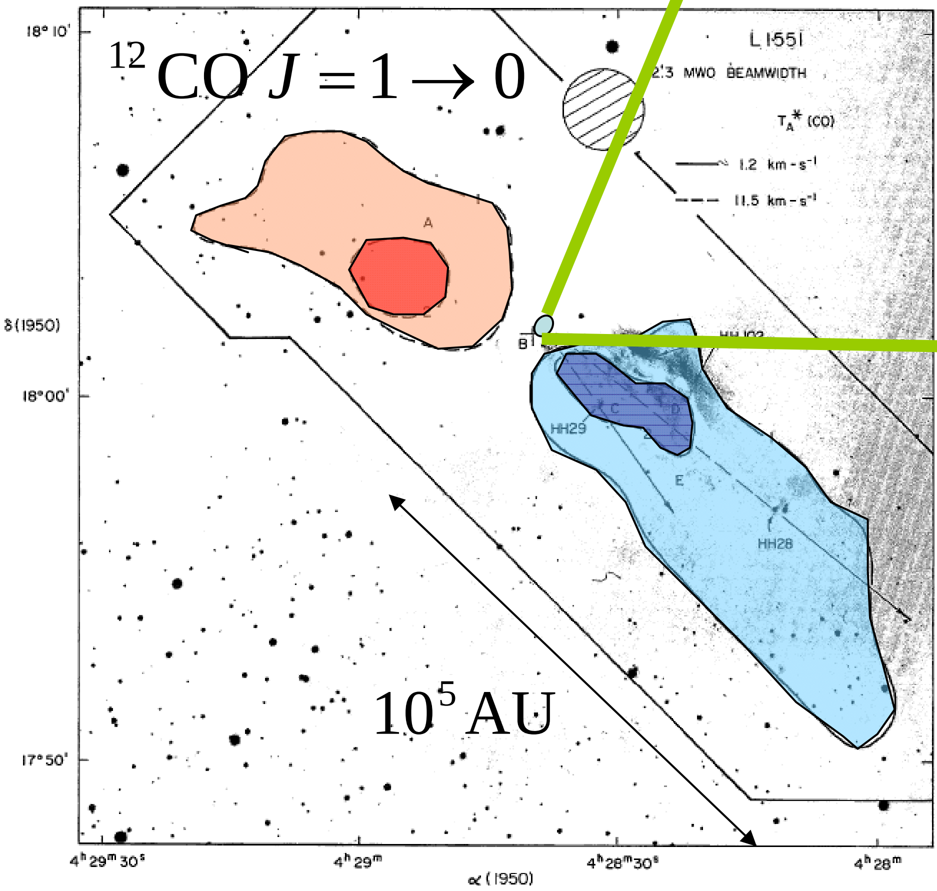

^{12}CO $J = 1 \rightarrow 0$

10^5 AU

Snell, Loren, &Plambeck 1980

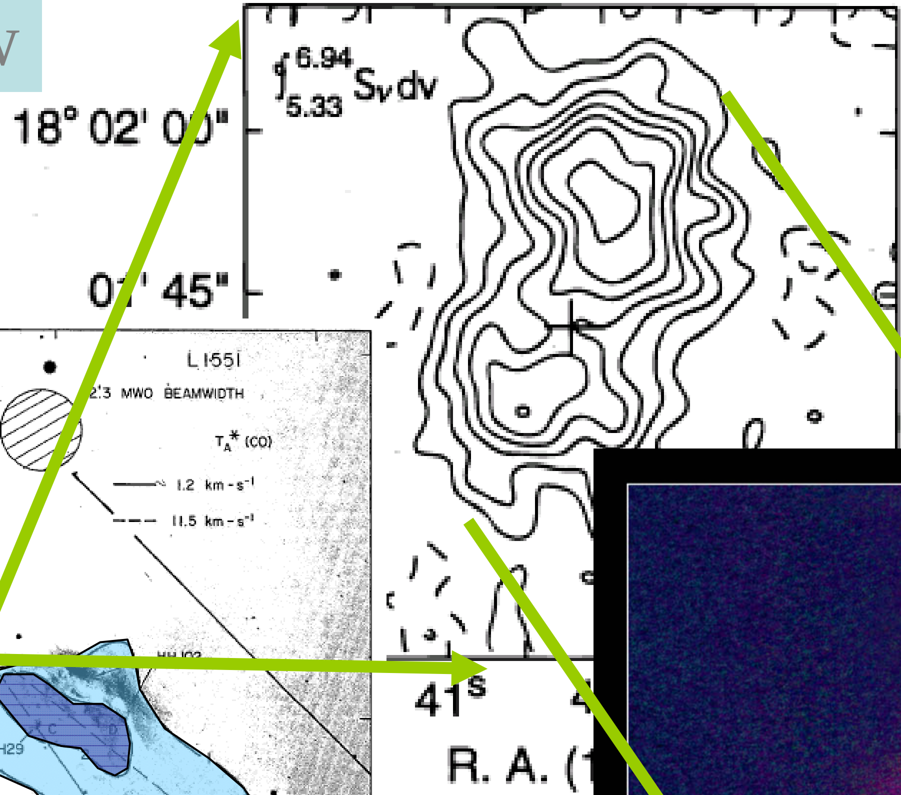

H^{13}CO^{+}

Saito, Kawabe, Kitamura&Sunada 1996

Optical Jets

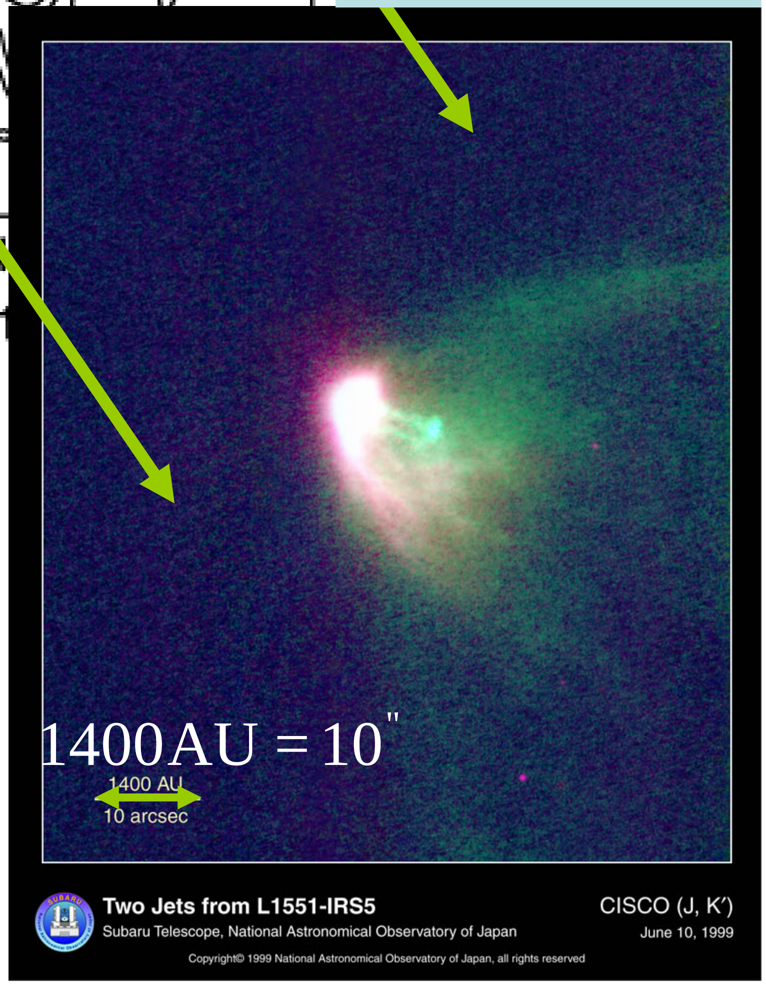

1400 AU = 10''

Binary: To understand Star Formation, study BINARY FORMATION.

Binary fraction is high.

TABLE 6. Multiplicity of T Taur stars in the complete samp

Sample	# Targets	# Companions in completeness region	bsf[b] (%)
Total	64	22	34±7
Oph–Sco	21	6	29±12
Tau–Aur	43	16	37±9
WTTS	22	8	36±13
CTTS	42	14	33±9
$\mathcal{M} < 1\mathcal{M}_\odot$	32	13	41±11
$\mathcal{M} > 1\mathcal{M}_\odot$	32	9	28±9

[a]The complete sample, discussed in Sec. 5.1, includes all observations sensitive to the "completeness region," i.e., that revealed all companion stars within the projected linear separation range 16 to 252 AU and within the magnitude difference range 0 to 2.0 mag.
[b]The restricted binary star frequency (bsf) incorporates only companion stars within the completeness region, and is therefore a lower limit to the true binary star frequency in the separation range 16 to 252 AU. Nonetheless, it is useful for comparisons of various groups of T Tauri stars, which are discussed in the sections listed in Column 5.

ΔK<2mag

if completely surveyed, bsd ~60%

Ghez et al 1993

Period distribution of nearby binaries

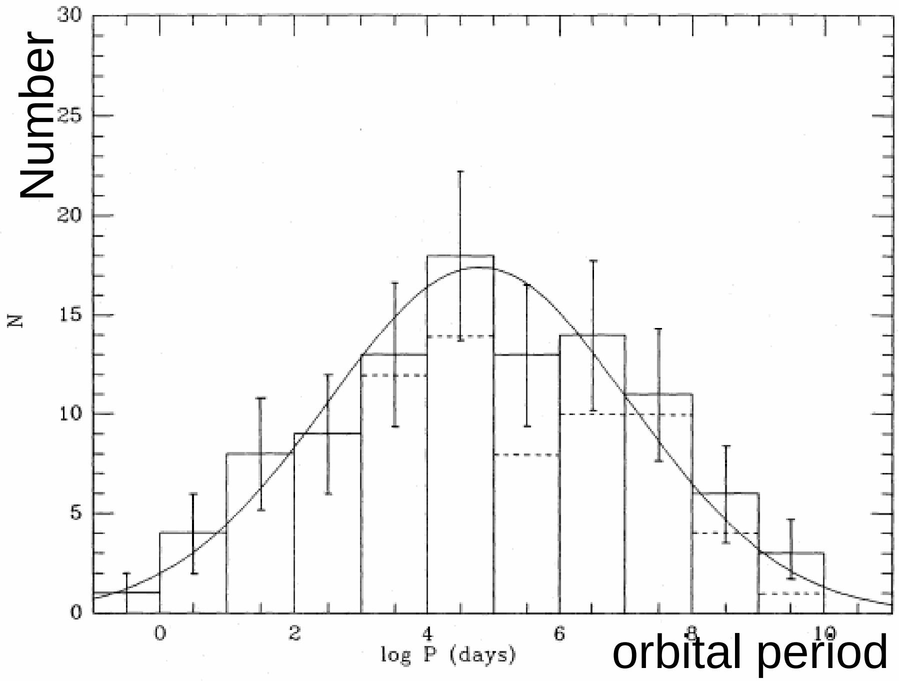

Fig. 7. Period distribution in the complete nearby G-dwarf sample, without (dashed line) and with (continuous line) correction for detection biases. A Gaussian-like curve is represented whose parameters are given in the text

Gaussian around ~180yr

Duquennoy & Mayor 2001

Binary Fraction

This suggests binary/multiple systems are formed in early phase.

(1) may depend on the mass of the stars

- Herbig/AeBe 68±11% (SSB) (Baines et al. 06)
- similar to T Tau

(2) may be deferent between PMS and MS.

Narrow wind obs.

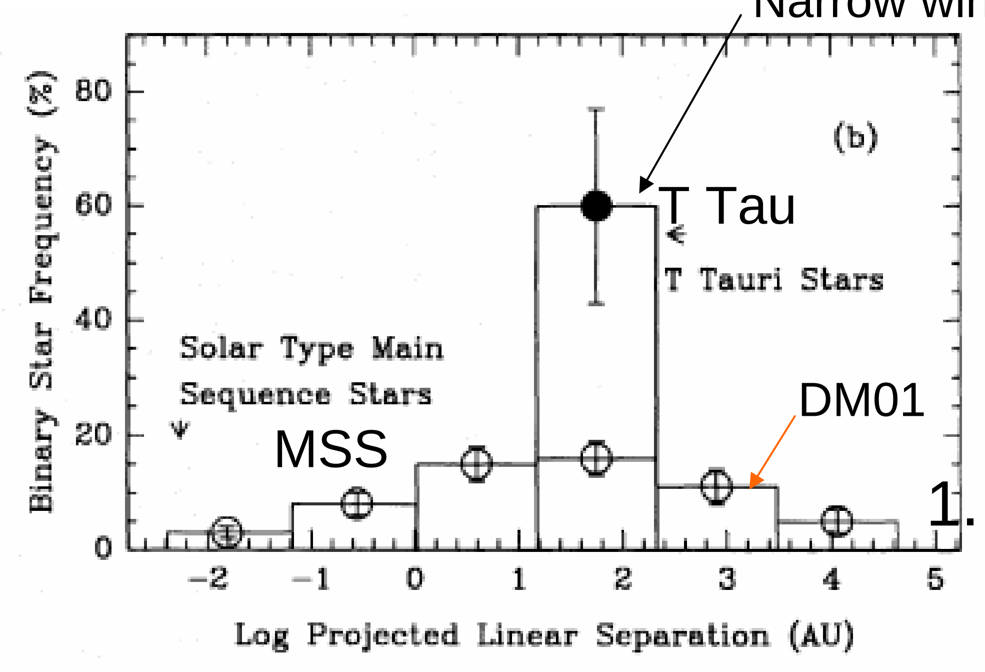

(3) may depend on the local stellar density

Liu et al. 2003

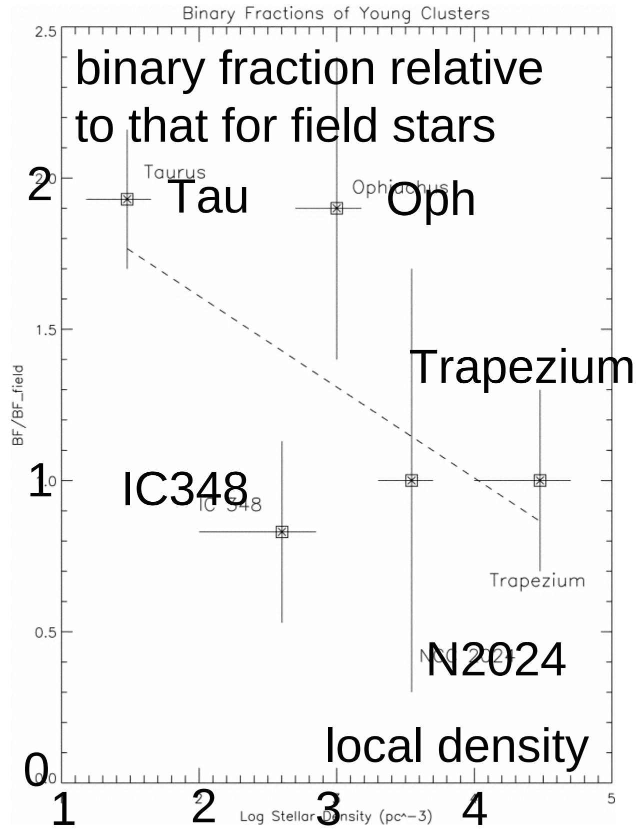

1. Binary fraction is a decreasing function of local stellar density

Ghez et al 1993

3D MHD Simulation of Rotating Magnetized Cloud Collapse

Machida, Tomisaka, Matsumoto 04
Machida, M.,H., Tomisaka, 05
Machida, M. Tomisaka, H. 05
Machida, M.,H., Tomisaka, 06

Model and Numerical Method

- Assume barotropic eq. state.
  - mimicing the result of 1D RHD (eg. Masunaga, Inutsuka 2000).

$$p = c_s^2 \rho + c_s^2 \rho_{crit} \left(\rho / \rho_{crit}\right)^{7/5}$$

$$p \approx \begin{cases} c_s^2 \rho \ \dots \ (\rho \le \rho_{crit}) \\ K\rho^{7/5} \dots (\rho > \rho_{crit}) \end{cases}$$

$$n_{crit} = 5 \times 10^{10}\,\mathrm{cm}^{-3}$$

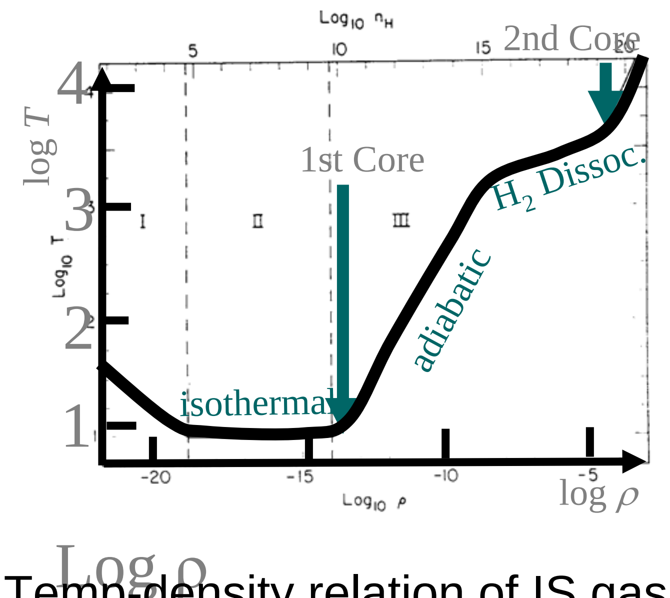

Temp-density relation of IS gas. (Tohline 1982)

- Ideal MHD

$$\begin{cases} \dfrac{\partial \rho}{\partial t} + \nabla \cdot (\rho \mathbf{v}) = 0, \\ \rho\left(\dfrac{\partial \mathbf{v}}{\partial t} + \mathbf{v}\cdot\nabla\mathbf{v}\right) = -\nabla p - \rho \nabla \phi, \\ \dfrac{\partial \mathbf{B}}{\partial t} + \nabla \times (\mathbf{v} \times \mathbf{B}) = 0, \\ \Delta \phi = 4\pi G \rho \end{cases}$$

Numerical Method (cont.)

- Non-homologous Collapse
  - Dynamic ranges of size and density scales are huge.

$$\rho_{\mathrm{ISM}} \sim 10^{2}\,\mathrm{cm}^{-3} \qquad \rho_{\mathrm{2ND\ CORE}} \sim 10^{17}\,\mathrm{cm}^{-3}$$
$$L_{\mathrm{ISM}} \sim 0.1\mathrm{pc} \qquad L_{\mathrm{2ND\ CORE}} \sim 10^{11}\,\mathrm{cm}$$

Nested grid

- "Nested Grid" Technique
  - Coarser grid: covers global structure
  - Finer grid: small-scale structure near the center.
    - # of cells : 128(x) × 128(y) × 32(z) × 17 (level)
    - equivalent to simulations with ∼ 1.5×10^{20} grids at the center.

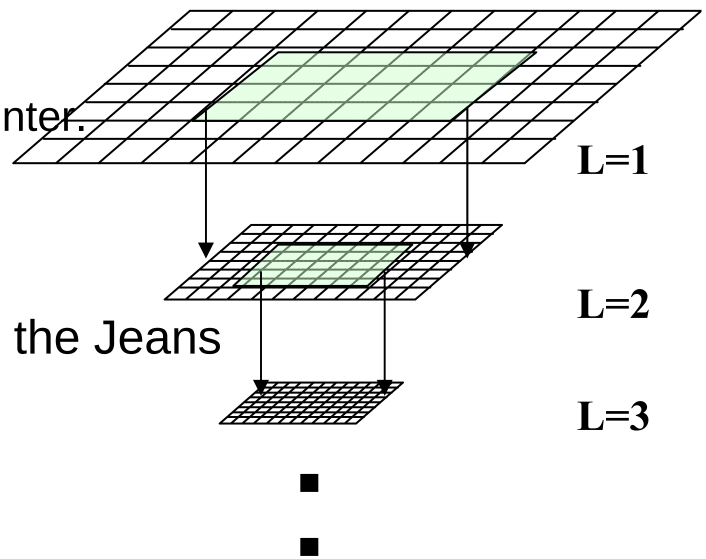

L=1

L=2

L=3

L=17

- New Finer Grid is Generated to Guarantee the Jeans Condition (Truelove et al. 1997)
  - To achieve physically correct answer:

$$\Delta x < \lambda_{\mathrm{J}} / 4 = [(4\pi G\rho)^{1/2} / c_s] / 4$$

  - Simulations continues till the "Jeans Condition" is violated at the deepest level of grid (17th Level).

Initial Condition

- An isothermal cylindrical cloud
  - in hydrostatic balance
    (Stodolkiewicz
    - $\mathbf{\Omega}$ // $\mathbf{B}$ // F
    - $B \propto \rho^{1/2}$;

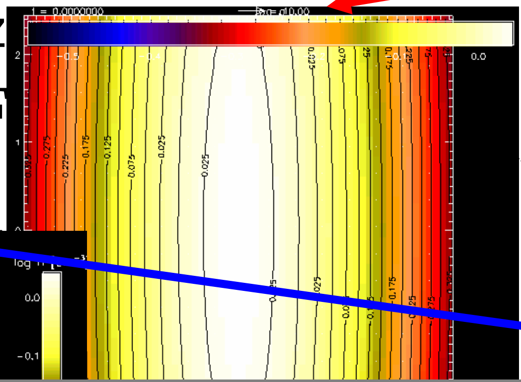

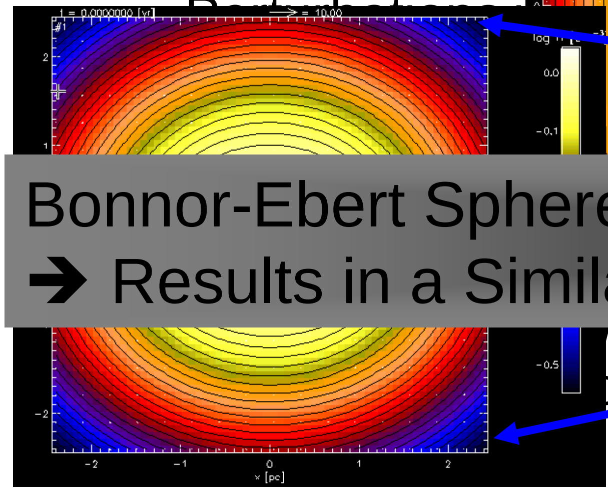

Bonnor-Ebert Sphere with Rigid-body Rotation & Uniform B-Field
➔ Results in a Similar Result.

well as
ode

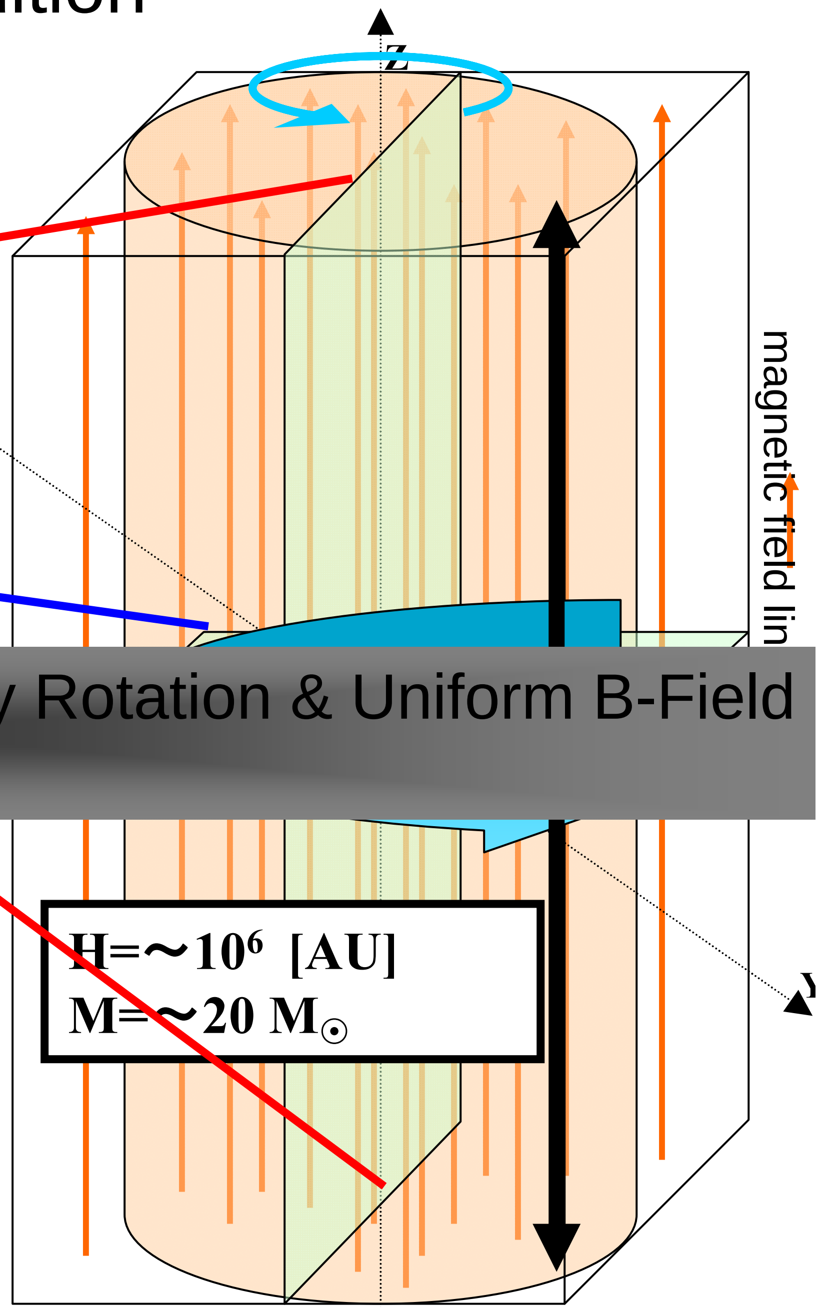

- Parameters:
  - B-field strength and angular rotation speed: $A\phi$,

$$\alpha = \frac{B_{0c}^2/4\pi}{c_s^2 \rho_{0c}} \quad \omega = \Omega\left(4\pi G \rho_{0c}\right)^{-1/2}$$

3.Results

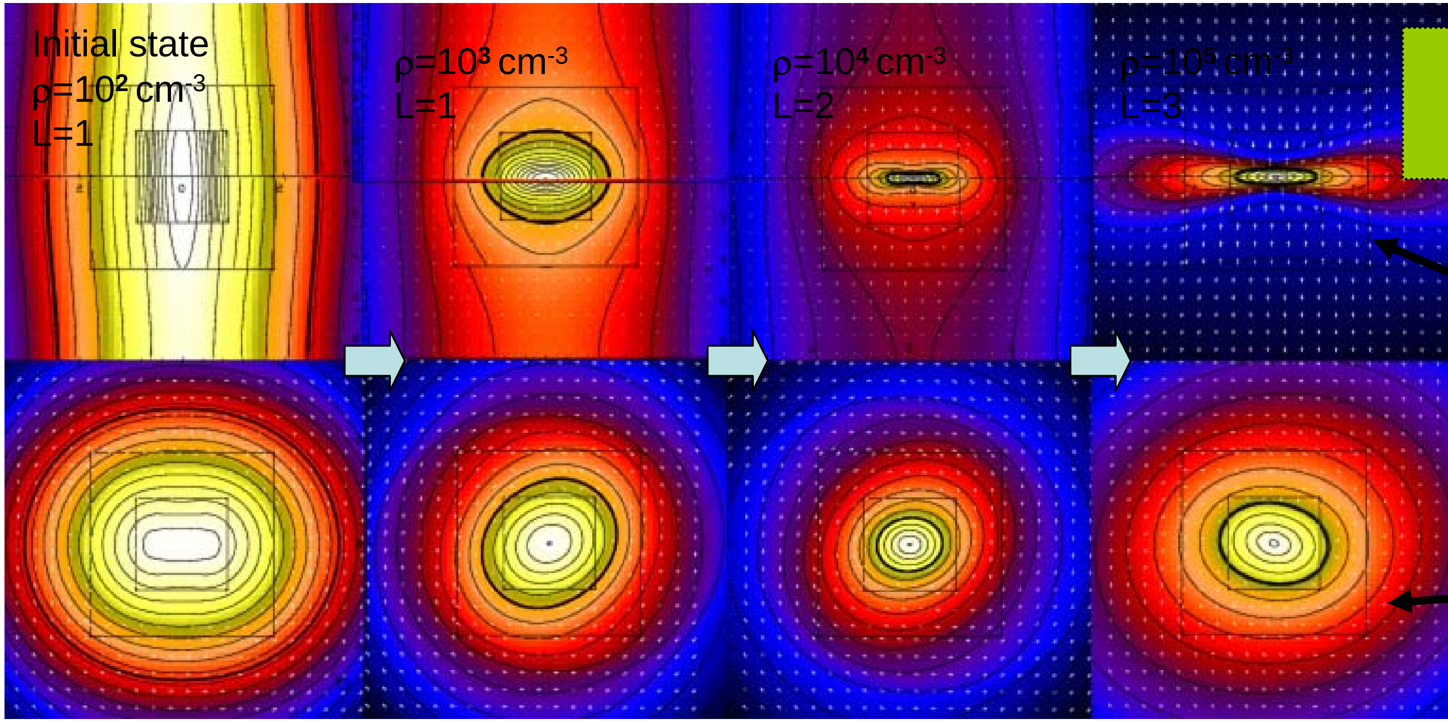

Side view

x=0 plane

Pole-on view
z=0 plane

(A_{m2}, α, ω)=(0.2, 1, 0.5)

Model with strong magnetic field and high rotation speed

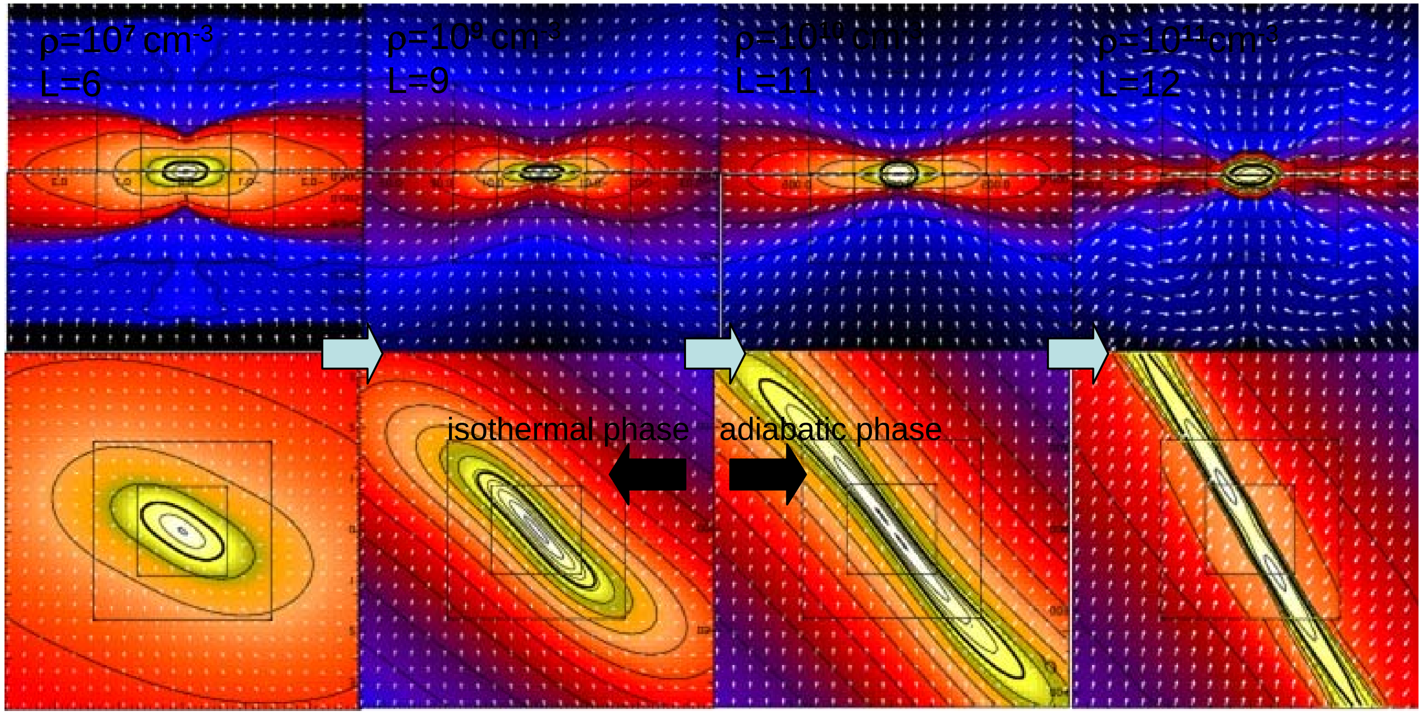

Only after the sufficiently thin disk is formed, the non-axisymmetric perturbation can grow

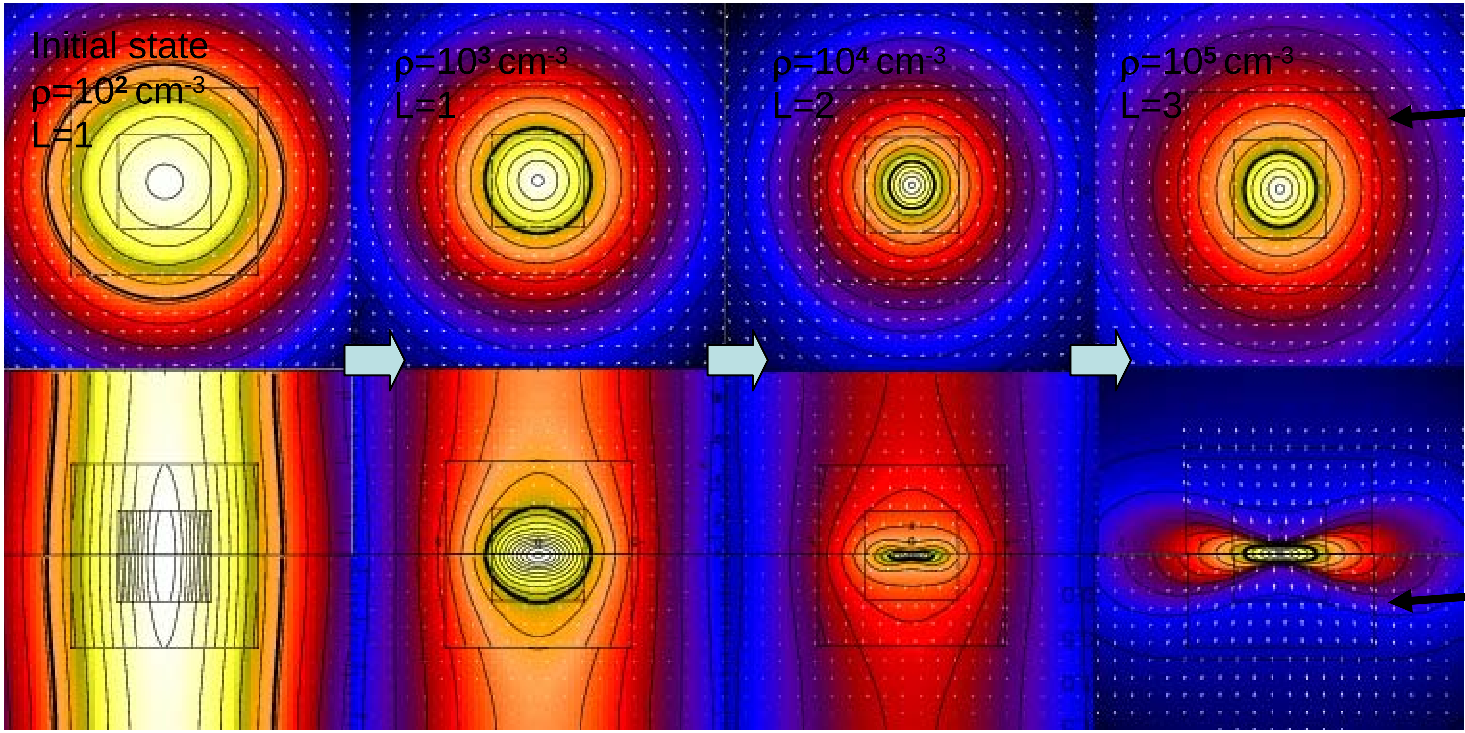

Pole-on view

z=0 plane

Model with weak magnetic field and high rotation speed

Side view

x=0 plane

Typical Model

(A_{m2}, α, ω)=(0.01, 0.01, 0.5)

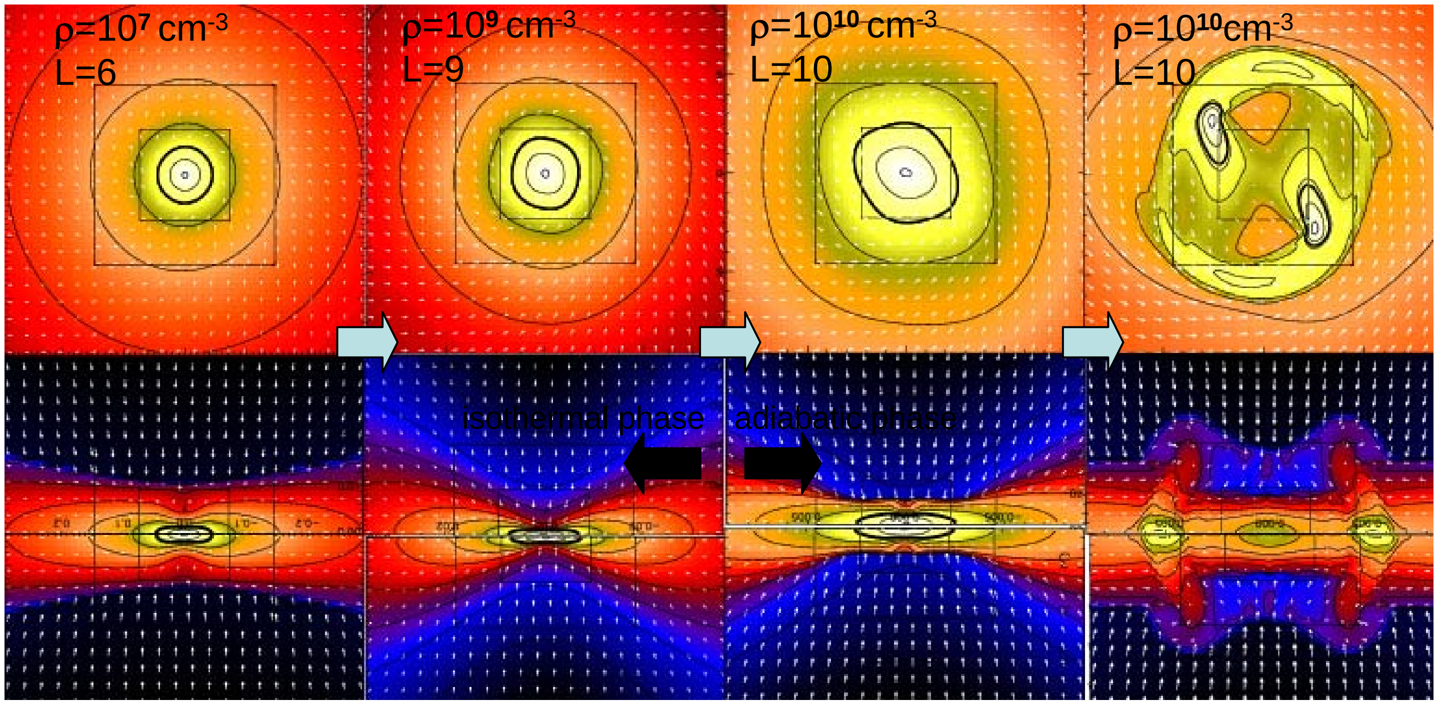

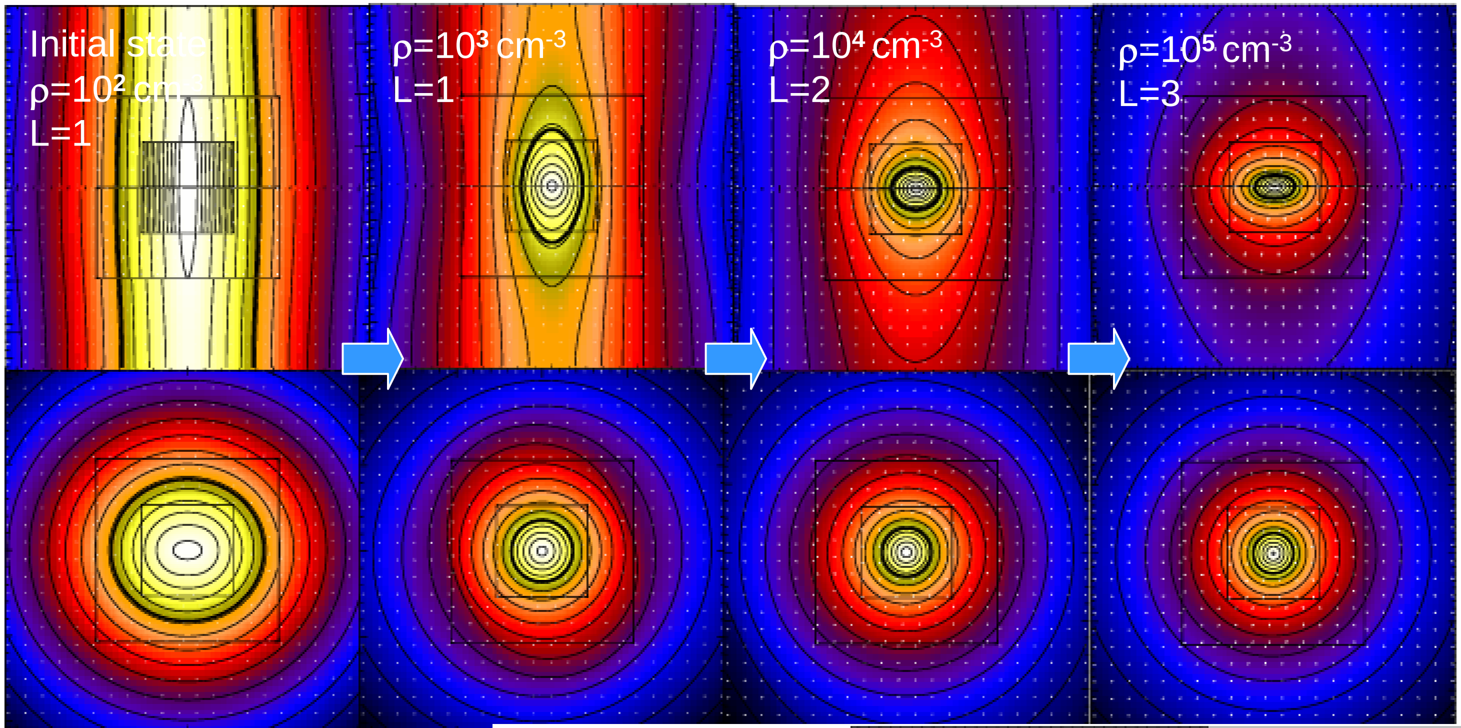

This corresponds to strong B-field & slow rotation.

Disk -->
Spherical core

Core Model

(A_{m2}, α, ω)=(0.01, 1, 0.1)

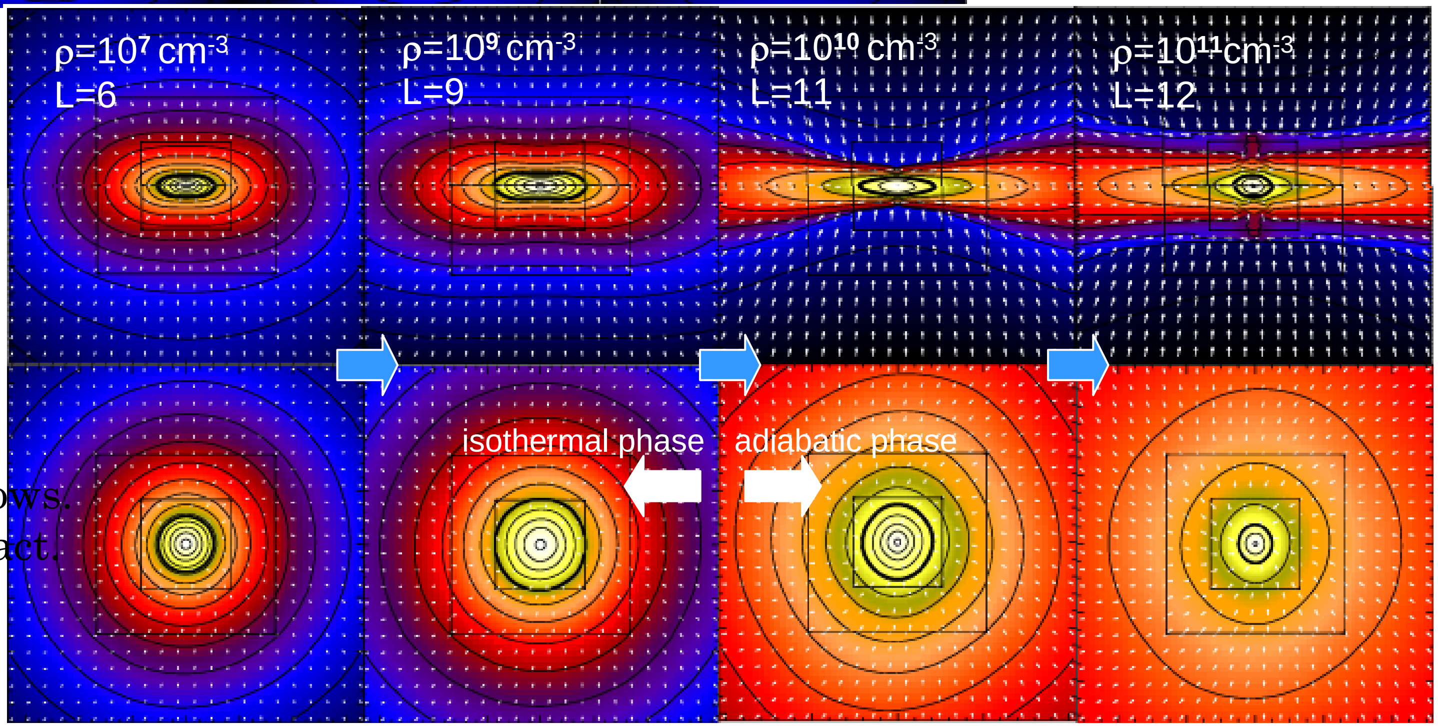

In this model, the non-axisymmetry hardly grows. Core continues to contract.

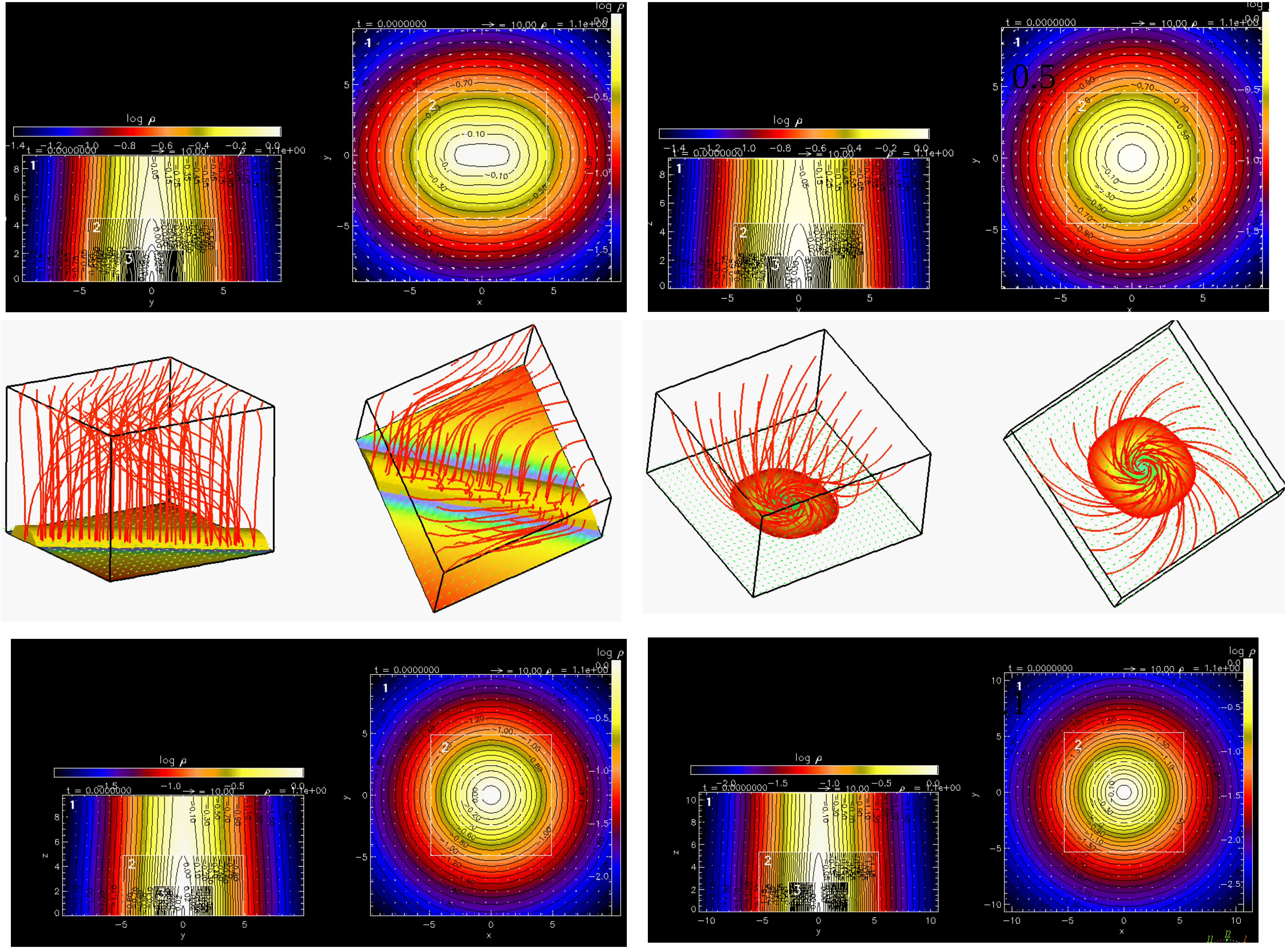

log ρ
t = 0.0000000
→ = 10.00 ρ = 1.1e+00
0.5
1

B-Ω Flux-Spin Relation

Machida et al. 2005a,b

--Evolutionary Path--

Support deficient.
➔ Spherical collapse.

$$B_c \propto \rho_c^{2/3} \quad \Leftarrow B_c R^2 = \text{const}$$
$$\Omega_c \propto \rho_c^{2/3} \quad \Leftarrow \Omega_c R^2 = \text{const}$$
$$\Downarrow$$
$$\Omega_c / \rho_c^{1/2} \propto B_c / \rho_c^{1/2} \propto \rho_c^{1/6}$$
$$\Omega_c / B_c \simeq \text{const}$$

Magnetic braking

$$B_c / \rho_c^{2/3} \simeq \text{const}$$
$$\Omega_c / \rho_c^{2/3} \searrow \qquad \text{J-loss}$$
$$B_c / \Omega_c \nearrow$$

$$B_c \Big/ \left(8\pi c_s^2 \rho_c\right)^{1/2} - \Omega_c \Big/ \left(4\pi G \rho_c\right)^{1/2}$$

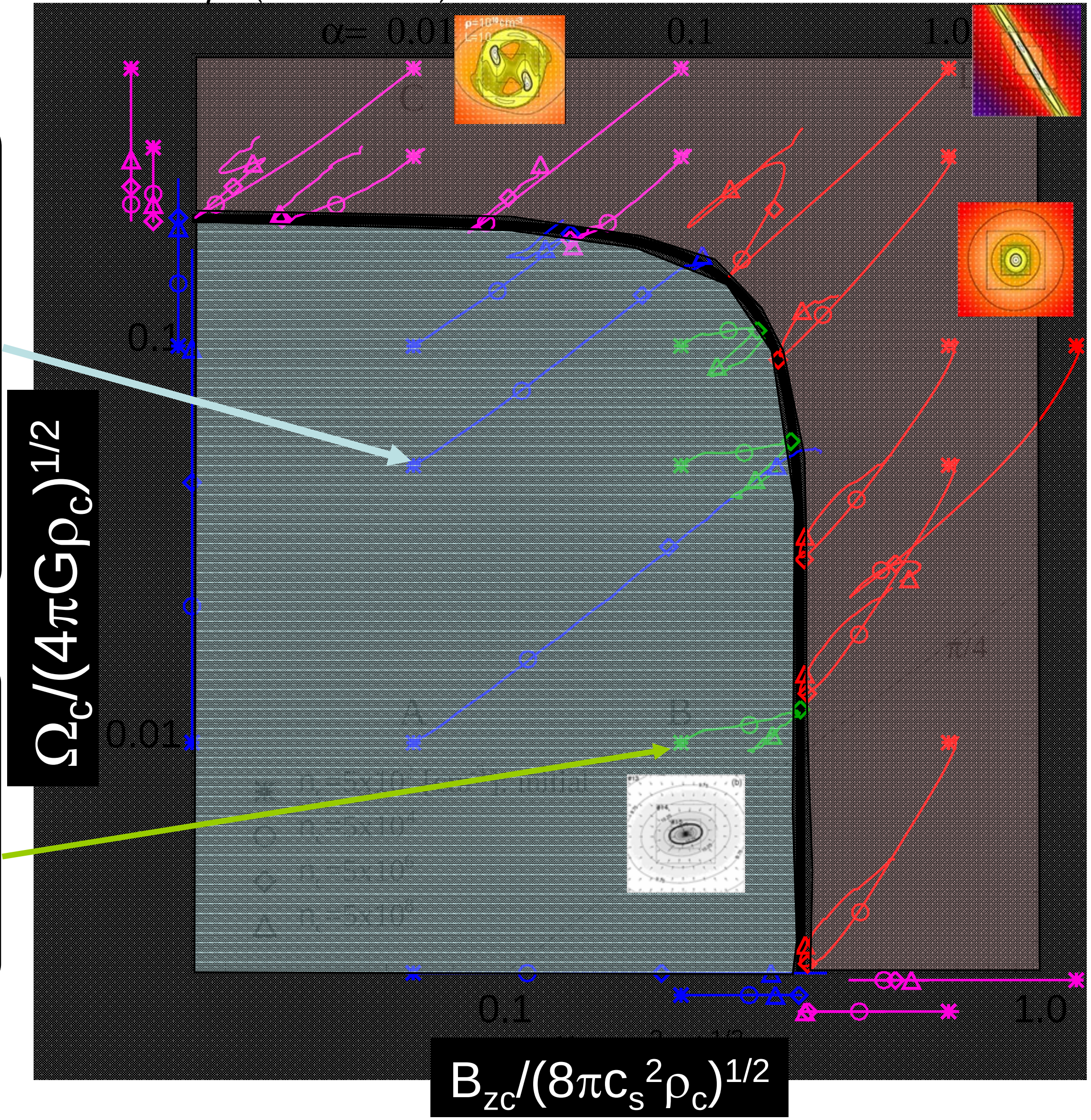

B-Ω Flux-Spin Relation

--Evolutionary Path--

$$B_c/(8\pi c_s^2\rho_c)^{1/2} - \Omega_c/(4\pi G\rho_c)^{1/2}$$

Support sufficient
➔Disk formation

$B_c \simeq \text{const}$

$\Omega_c \simeq \text{const}$ $\quad \rho_c \nearrow$

→move left-down

$\Omega_c / \rho_c^{1/2} \propto B_c / \rho_c^{1/2} \propto \rho_c^{-1/2}$

➔Radial collapse

$B_c / \sigma_c \simeq \text{const}$ ←frozen-in

$\Omega_c / \sigma_c \simeq \text{const}$ ←conserve J

$\sigma_c / \rho_c^{1/2} \simeq \text{const}$ ←self-grav. disk

→move slightly

Magnetic braking

$B_c / \Omega_c \nearrow$

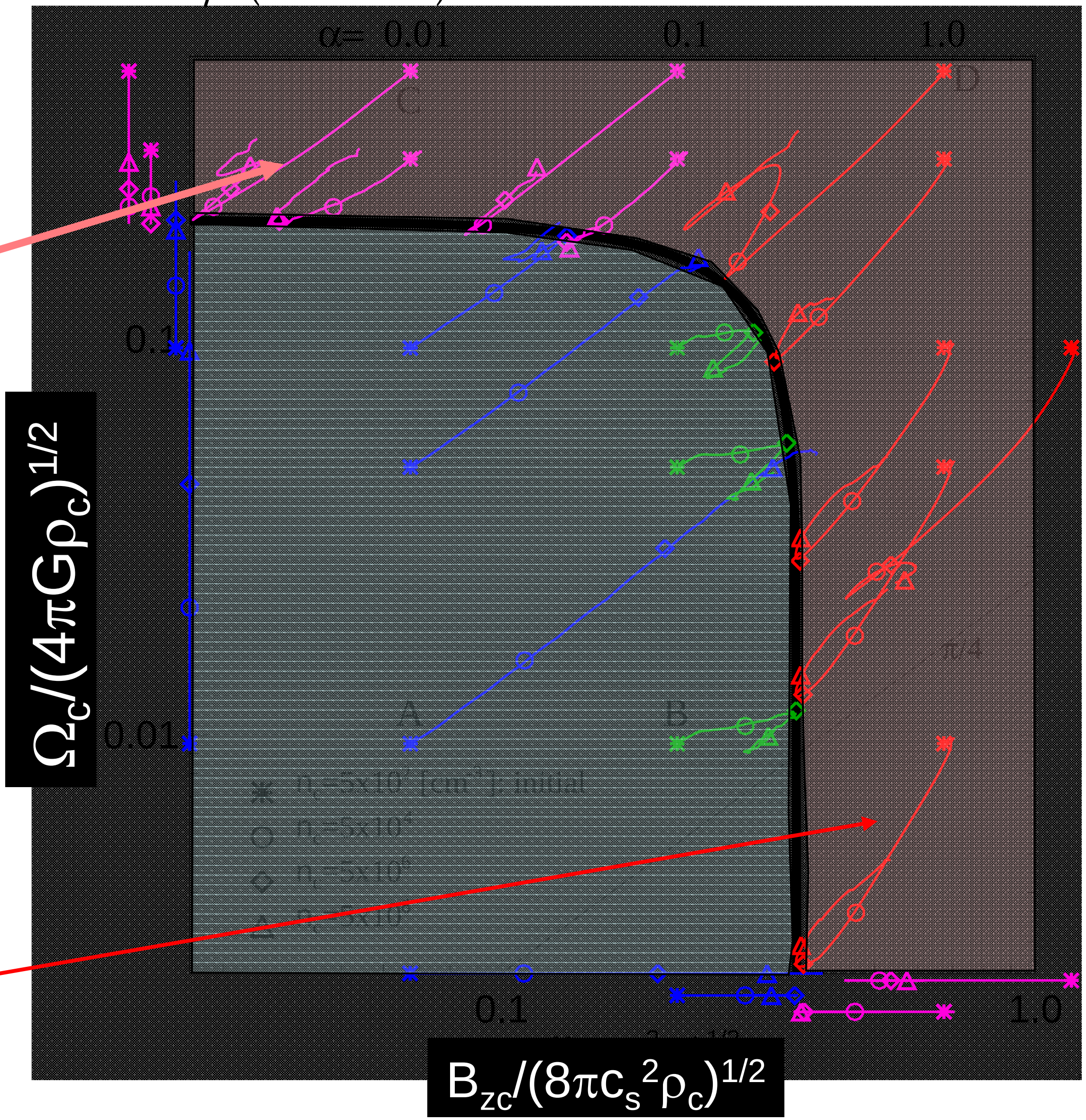

B-Ω Flux-Spin Relation

--Evolutionary Path--

- In the isothermal run-away collapse, contraction proceeds self-similarly or solution converges to a family of self-similar solutions.
- All the models converge to a line as

$$\frac{B_c^2}{(0.36)^2 8\pi c_s^2 \rho_c} + \frac{\Omega_c^2}{(0.2)^2 4\pi G \rho_c} = 1$$

empirical

- There exists a balance between B-field, centrifugal force, thermal pressure and gravity.

1. We know both the evolutionary path and fragmentation condition $\varepsilon_{ob}>3$ or $\Omega_c/(4\pi G\rho_c)^{1/2}>0.2$.
2. This gives a diagnosis of a cloud: fragments in the adiabatic stage or remains single ?

For the adiabatic core to fragment, it must rotate fast enough.

Large symbols initial states

Fragmentation

No fragmentation

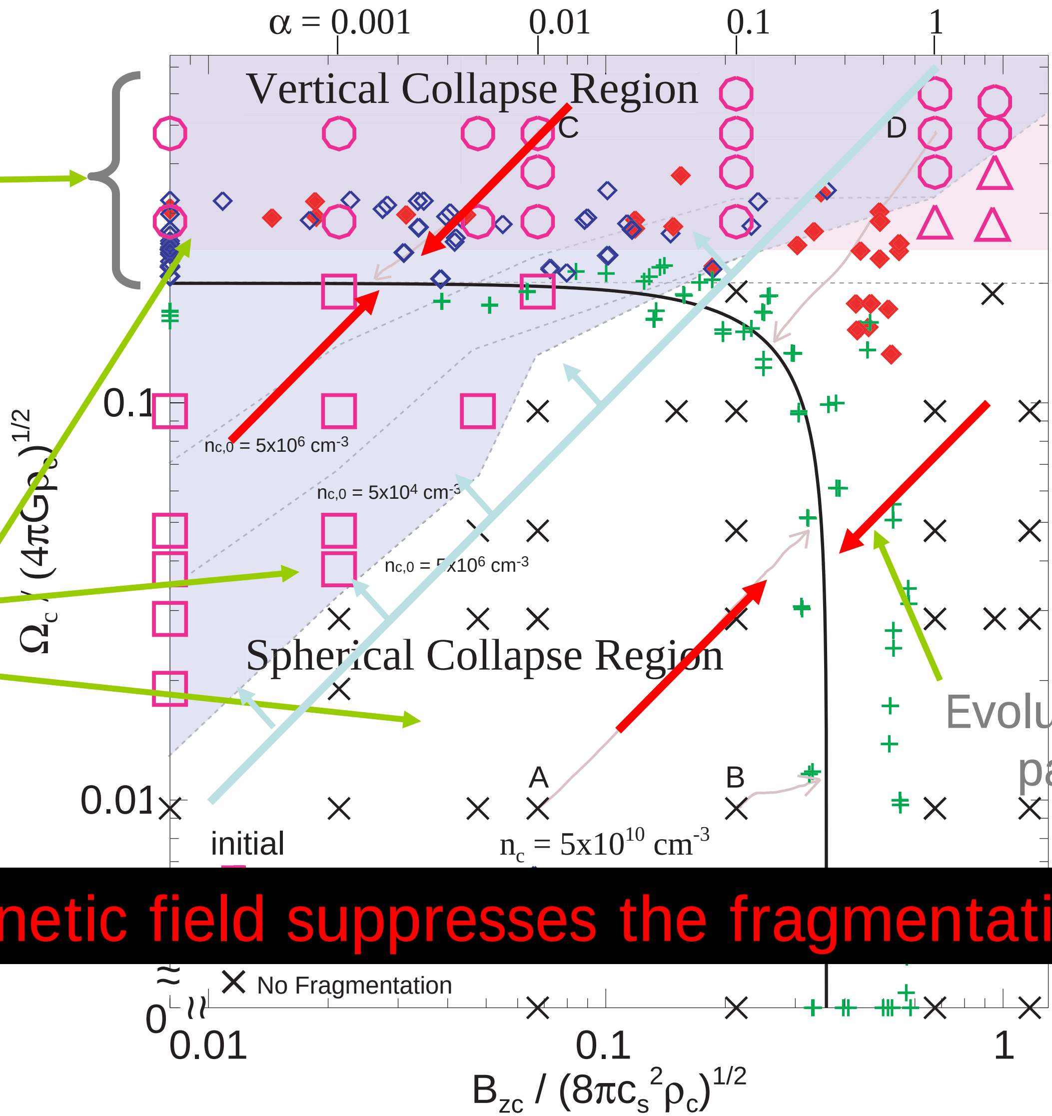

Evolutionary path

Small symbo

Adiabatic core

Magnetic field suppresses the fragmentation

To Fragment

$$\frac{\Omega_0}{B_0} > \frac{G^{1/2}}{2^{1/2} c_s} \sim 3\times10^{-7}\,\mathrm{yr}^{-1}\mu\mathrm{G}^{-1}\left(\frac{c_s}{190\mathrm{ms}^{-1}}\right)^{-1}$$

Prestellar core L1544

$$v_\phi \simeq 0.09\mathrm{km\ s}^{-1} @\, r = 15000\mathrm{AU}$$ Ohashi et al (1999)

$$\Rightarrow \Omega_0 \simeq 1.3\times10^{-6}\mathrm{yr}^{-1}$$

$$v_\phi \simeq 0.14\mathrm{km\ s}^{-1} @\, r = 7000\mathrm{AU}$$ Williams et al (1999)

$$\Rightarrow \Omega_0 \simeq 4.2\times10^{-6}\mathrm{yr}^{-1}$$

$$B_0 \simeq +11\pm 2\mu\mathrm{G}$$ Zeeman splitting Crutcher & Troland (2000)

$$\Rightarrow \quad \frac{\Omega_0}{B_0} \sim (1.2-3.8)\times10^{-7}\,\mathrm{yr}^{-1}\mu\mathrm{G}^{-1}$$

Marginal!!

Measurement both Ω and B at the same density
➔ future forecast!

Misaligned case

Machida, et al. (2006) ApJ. 645, 1227-1245

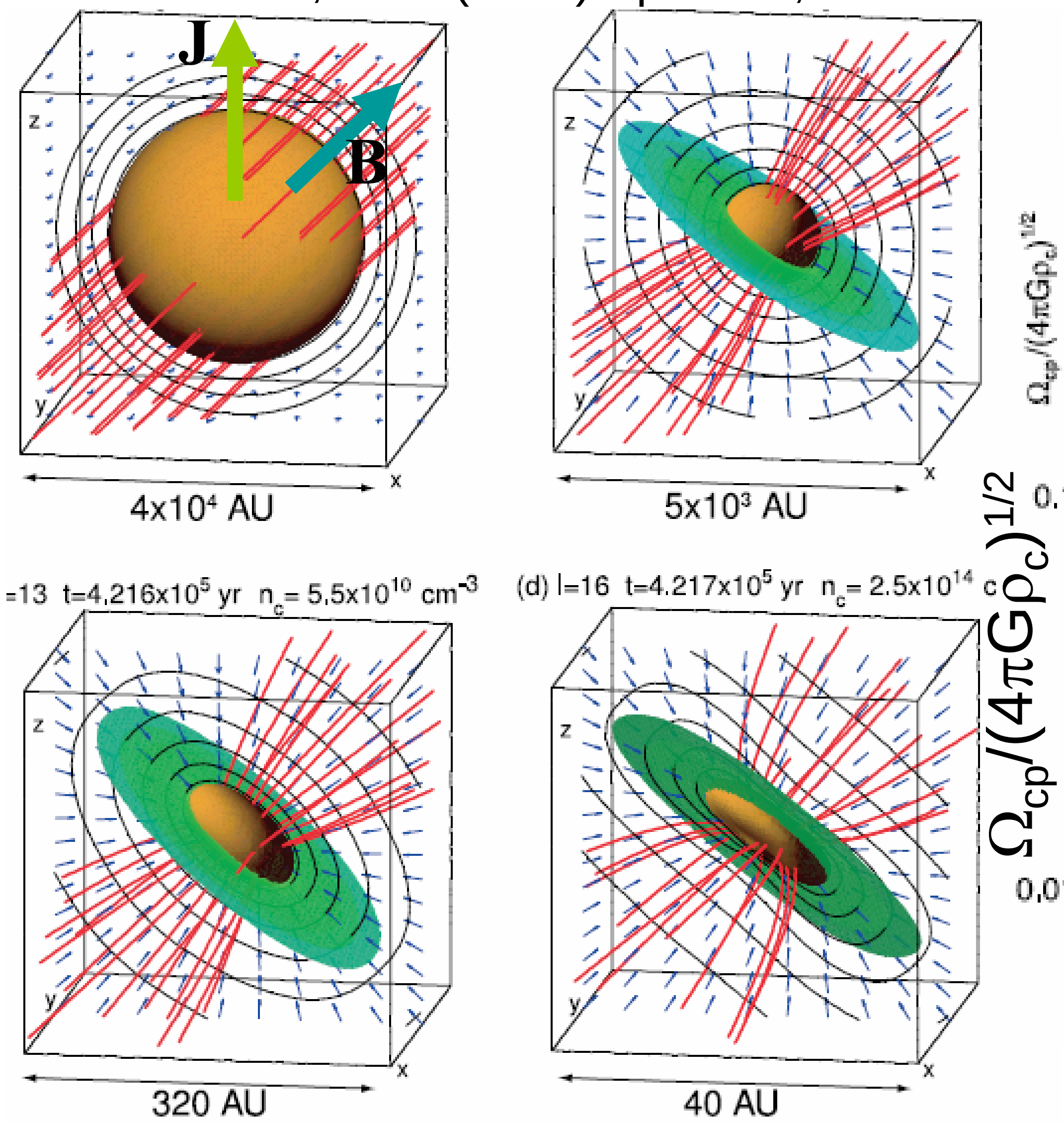

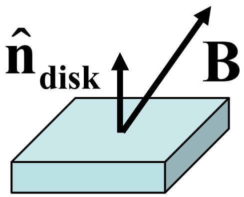

$$B_{cp} \equiv \mathbf{B}\cdot\hat{\mathbf{n}}_{\mathbf{disk}} \quad \Omega_{cp} \equiv \mathbf{\Omega}\cdot\hat{\mathbf{n}}_{\mathbf{disk}}$$

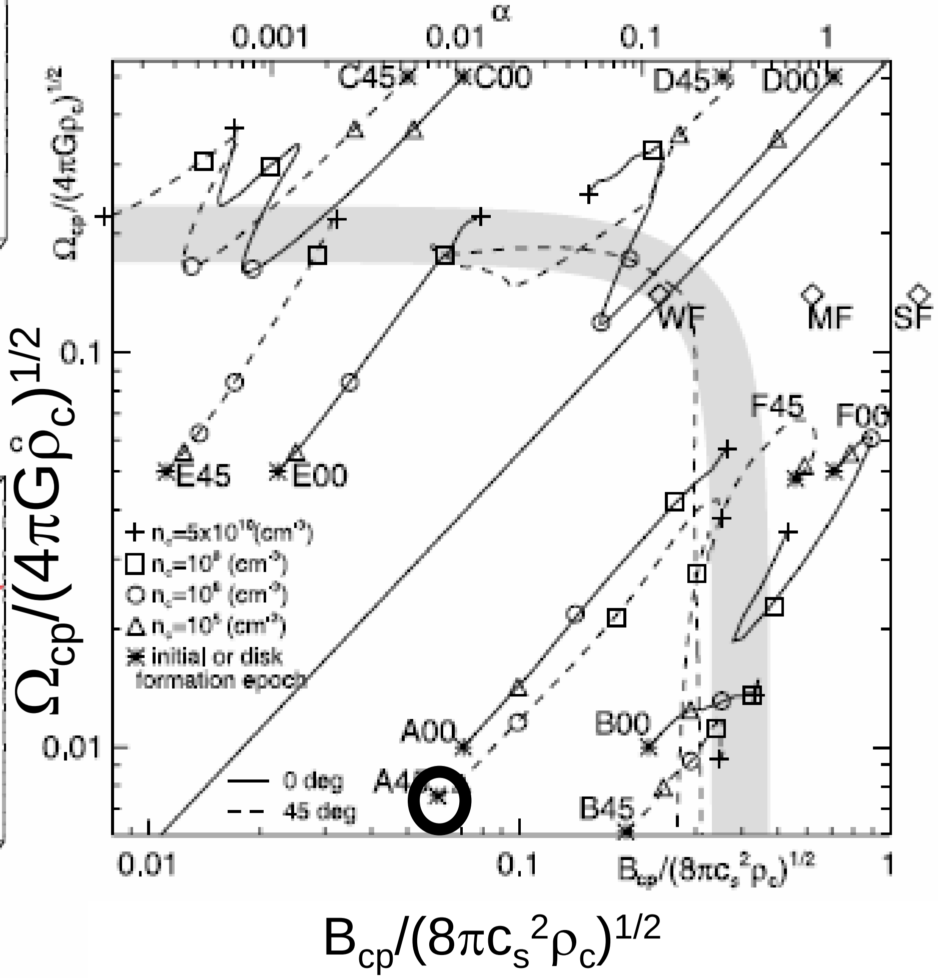

$\alpha = 0.01,\ \omega = 0.01$ Evolution is understood by the spin-flux relation.

Effect of Magnetic Fields
Misaligned Rotators: $B \not\parallel J$

Matsumoto & Tomisaka 2004 *Astrophysical Journal*, **616**, 266-282

- Promotion of disk formation
  - A pseudo-disk extending perpendicular to B is formed.

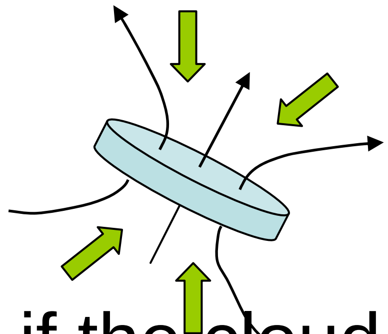

- Transfer the angular momentum if the cloud ➔ discourages disk formation
  - Ω perp. to B is promptly removed.
  - Ω parallel to B is transferred by magnetic torque.--- magnetic braking
    - Gravitational torque, Magnetic torque, Hydrodyn. Torque

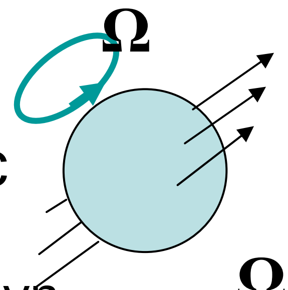

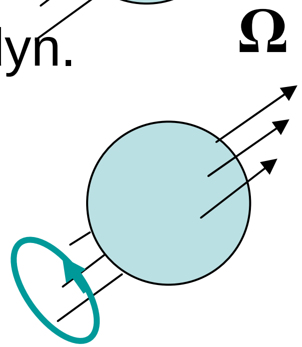

- Affect how Fragmentation Occurs

Alignment of Outflow and Magnetic Field

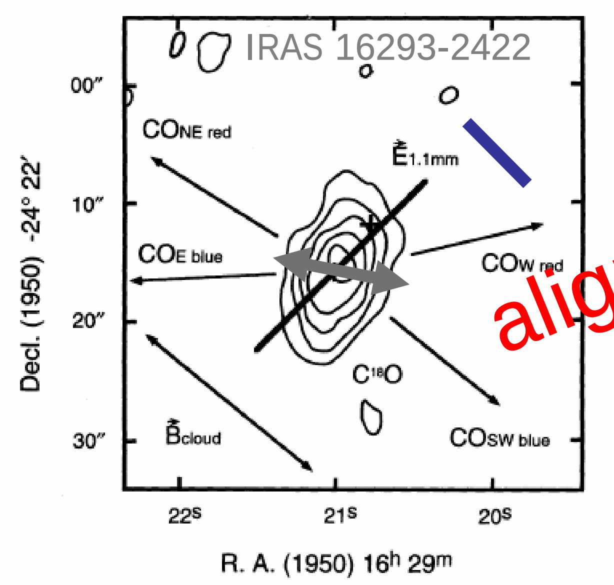

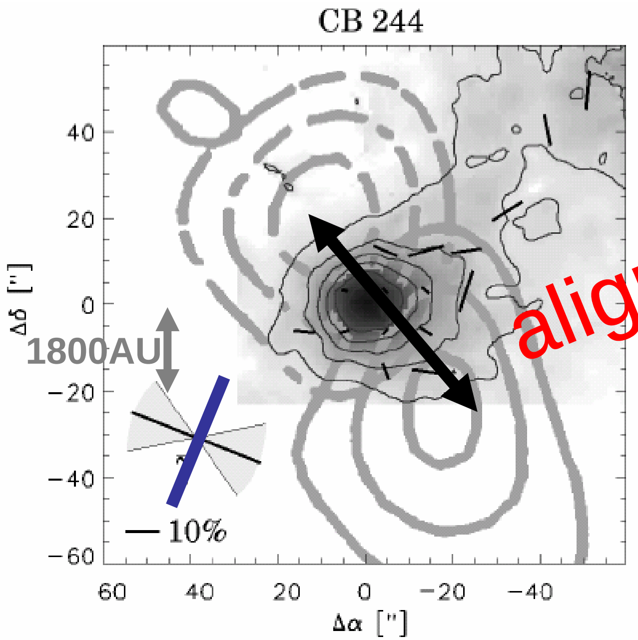

Wolf et al (2003)

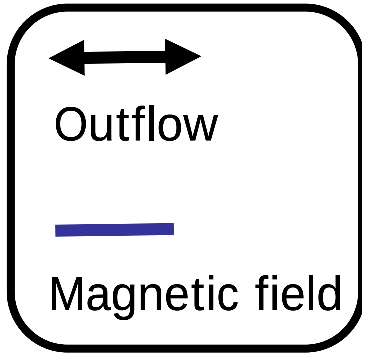

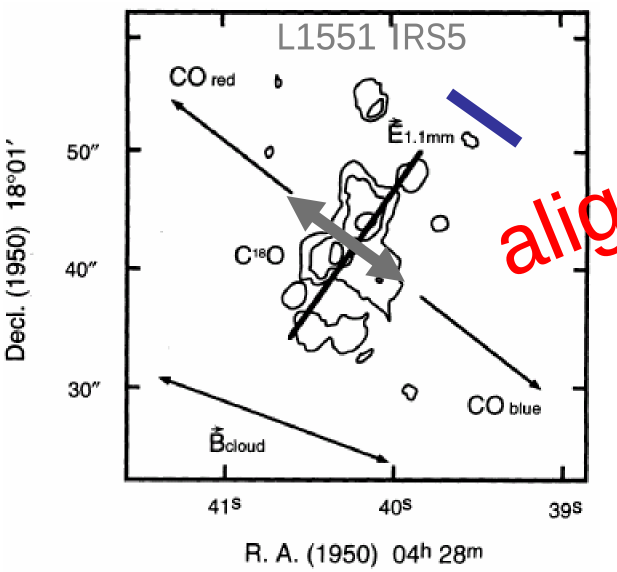

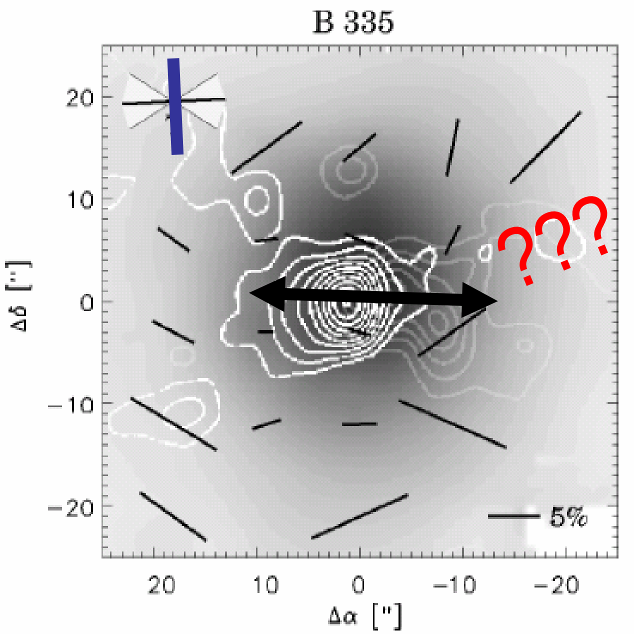

Tamura et al (1995) 1mm radio polarization

Polarization of thermal dust emission map SCUBA 850μm

Recent observations (1/2): *B*-fields, optical jets, and disks in Taurus

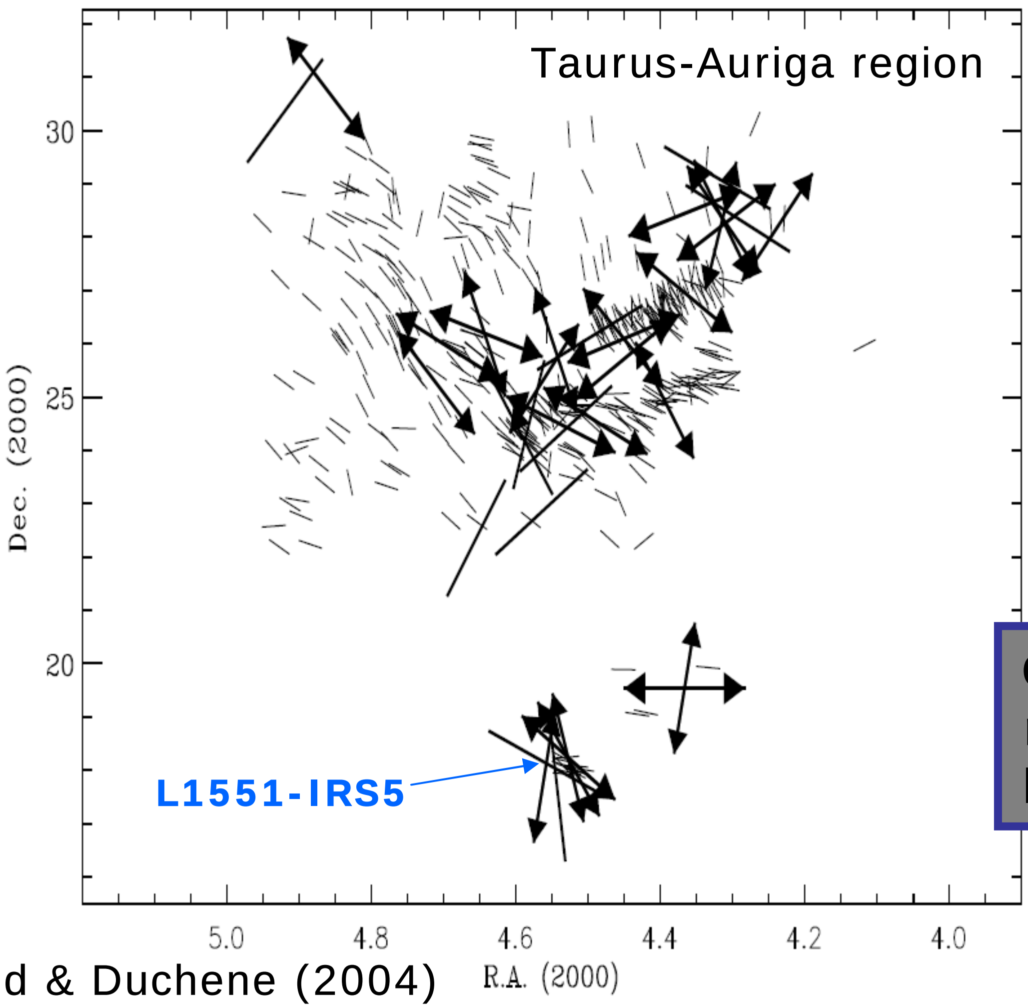

Menard & Duchene (2004)

Direction of magnetic fields inferred from polarized dust emission.

Direction of optical jets

Direction of disk normal

CTTS are oriented **randomly** with respect to local magnetic fields!

Angular Momentum

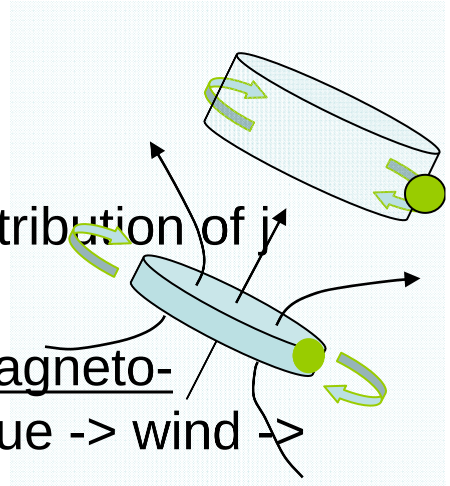

- Mechanism:
  - Magnetic — <u>Magnetic braking</u> (disk -> magnetic torque -> redistribution of j along one magnetic field line)
  - Molecular outflow ejected after the core formed. <u>magneto-centrifugal wind mechanism</u> (disk -> magnetic torque -> wind -> escape from the system)
  - Torque — Mechanical (pressure and gravitational) torque

- 3D MHD simulation (Dorfi 1982)
  - shows that component of J perpendicular to B is largely removed in the isothermal run-away collapse phase.

- Is a disk perpendicular to B or J?
  - Disk perpendicular to B is formed.

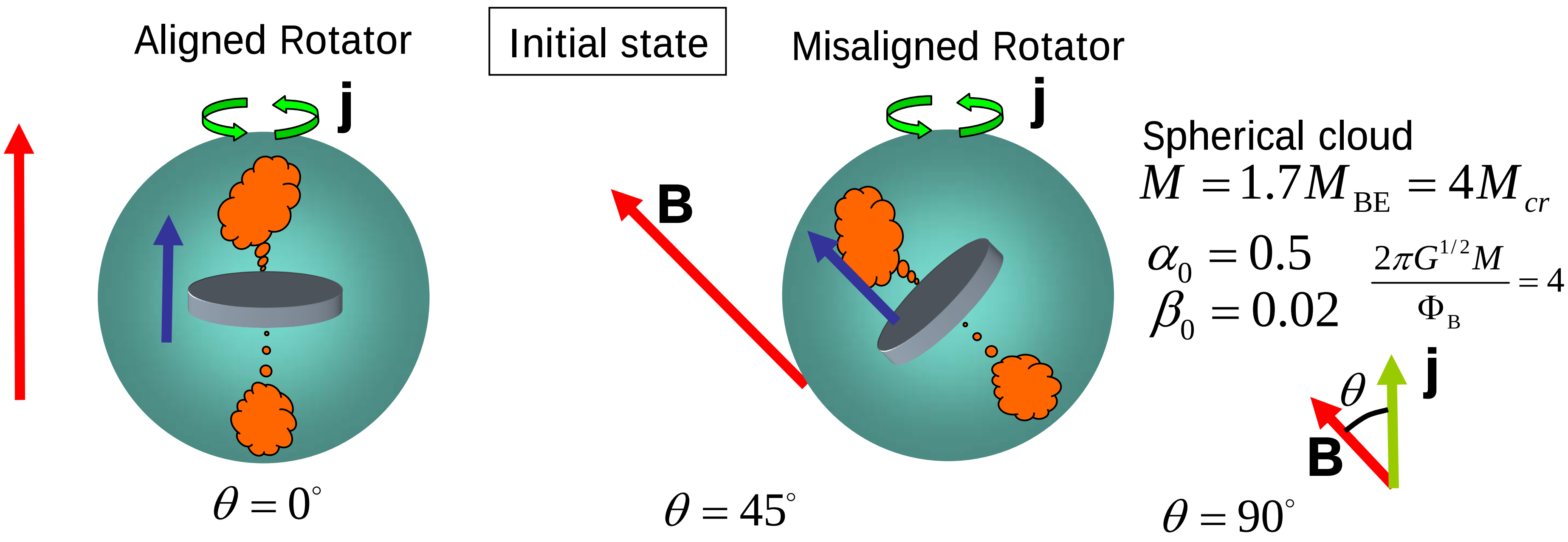

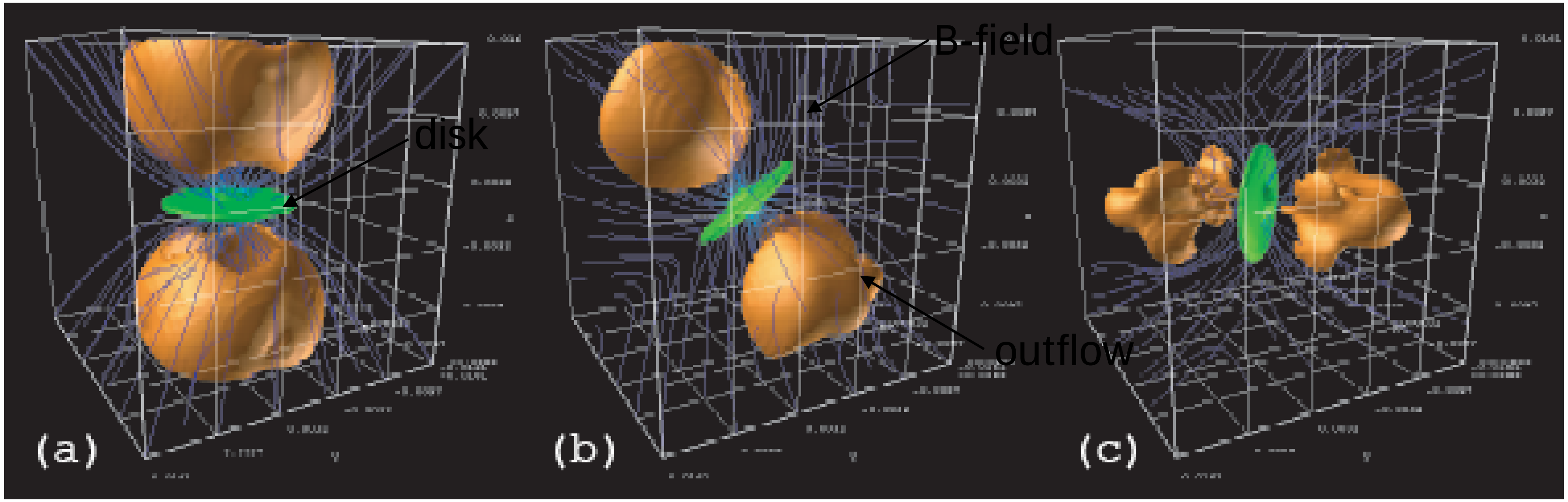

- Disk perpendicular to not J but B-field (!) is formed.

MF45 $\theta = 45^{\circ}$

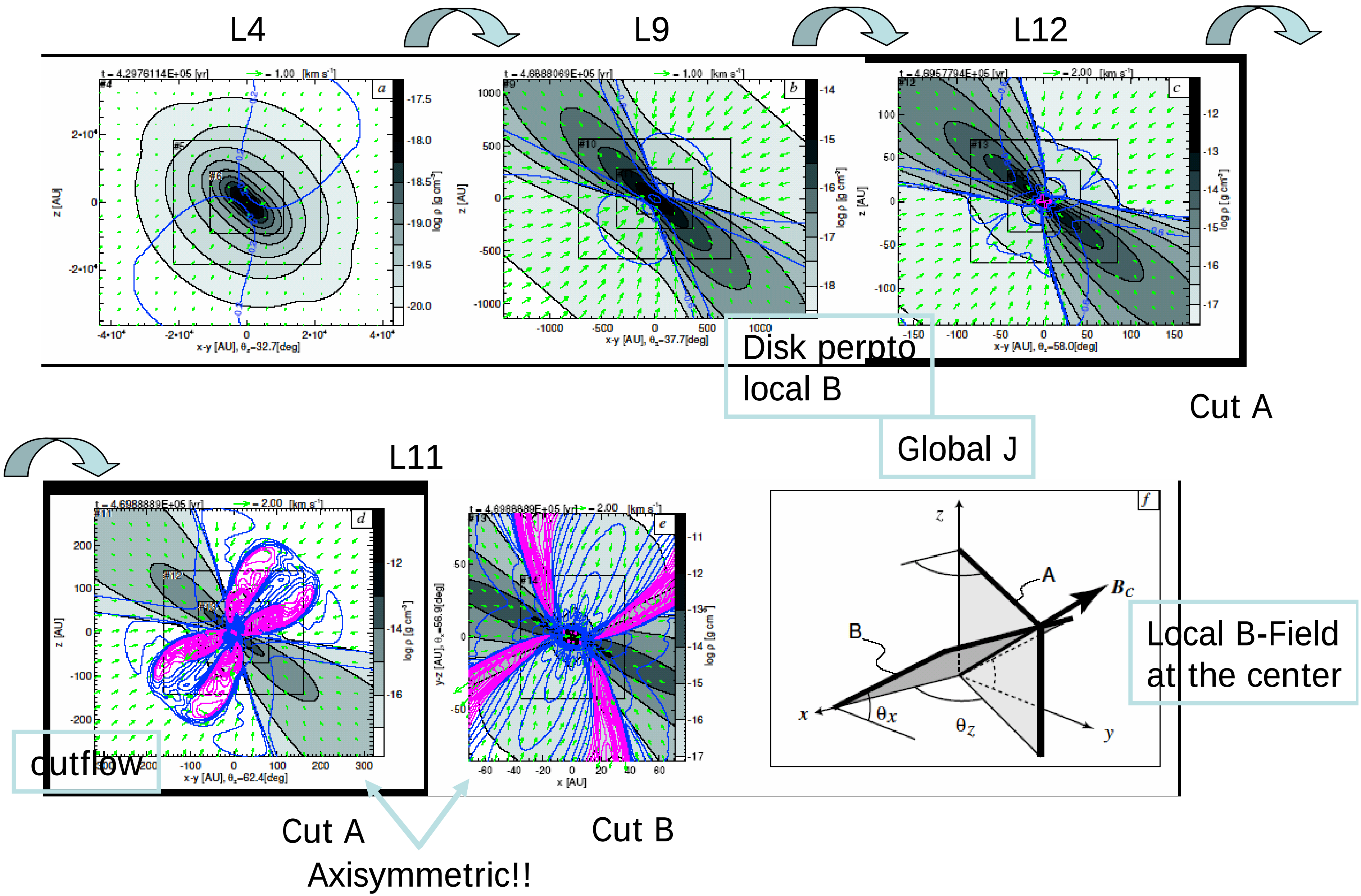

Disk, B Field and Rotation in Different Scales (Final state)

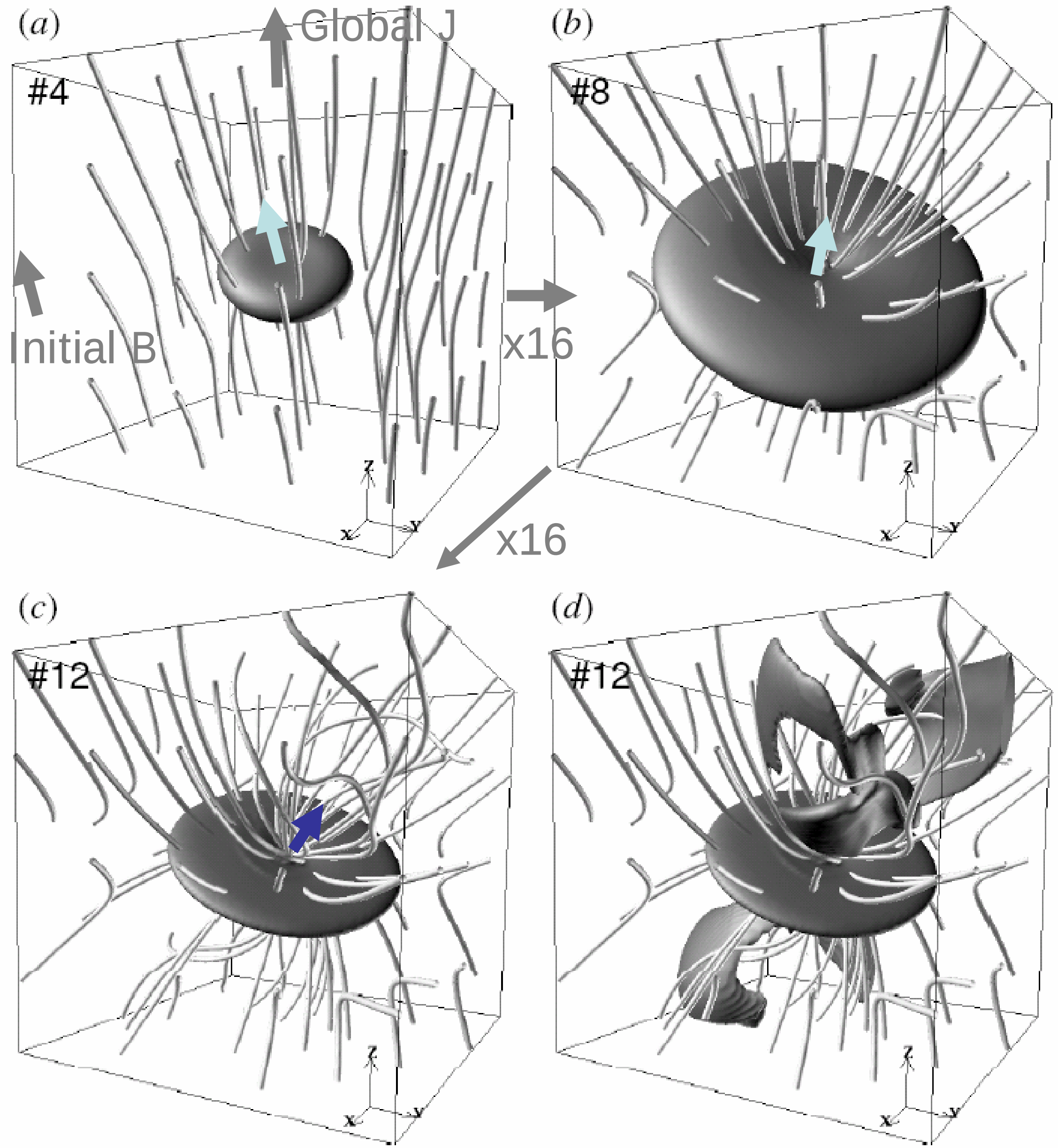

Disk oriantation, local B, and local J change their directions according to the scale.

Convergence

1. Loci of local $\mathbf{B_c}$, local $\mathbf{J_c}$, disk normal vector $\mathbf{n_c}$ are plotted viewing from the direction of global $\mathbf{J_g}$ (z-axis).
2. Precession or oscillation appears.
3. Finally, they converges to one direction.

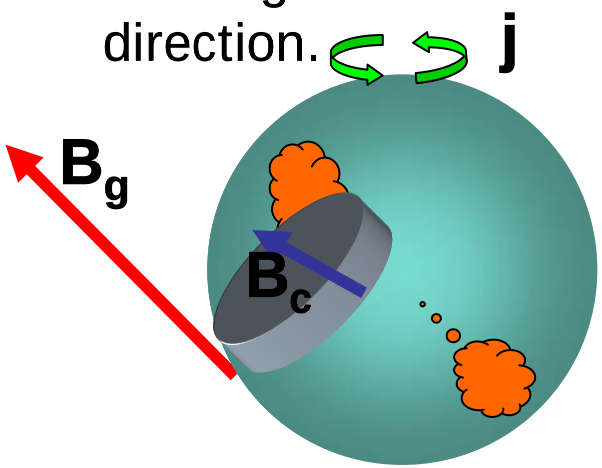

4. Angle between Bc and Bg is ~30 deg.

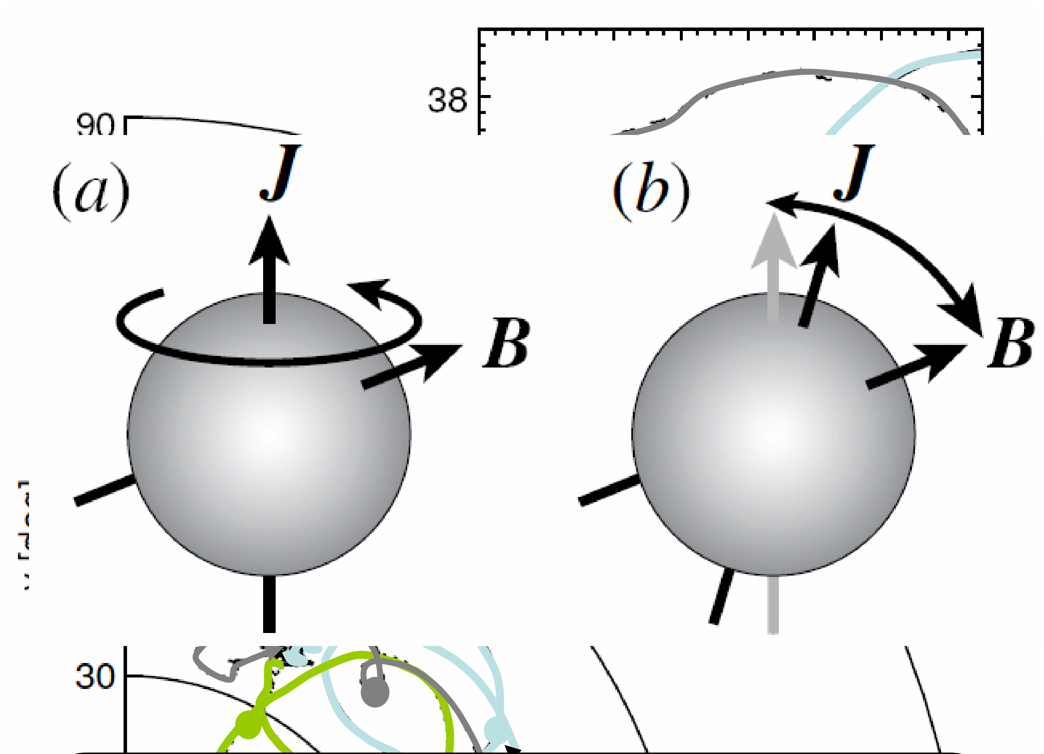

Explanation of precession.
(a) B-Field changes its direction owing to the rotation.
(b) Angular rotation vector inclines toward B-vector by the magnetic braking.

Case of large θ (angle between J_G and B_G)

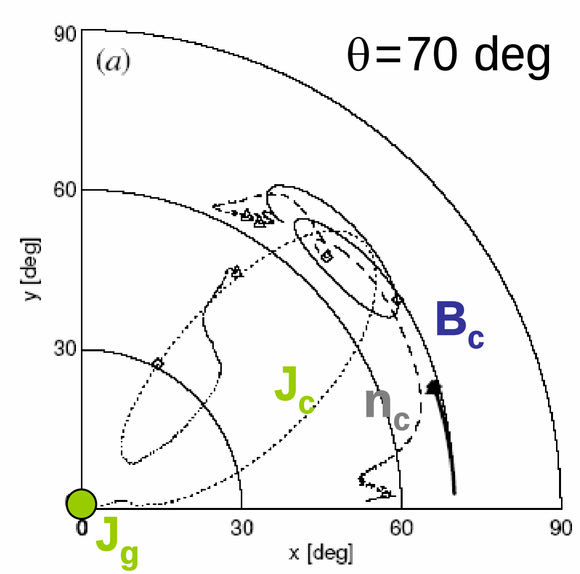

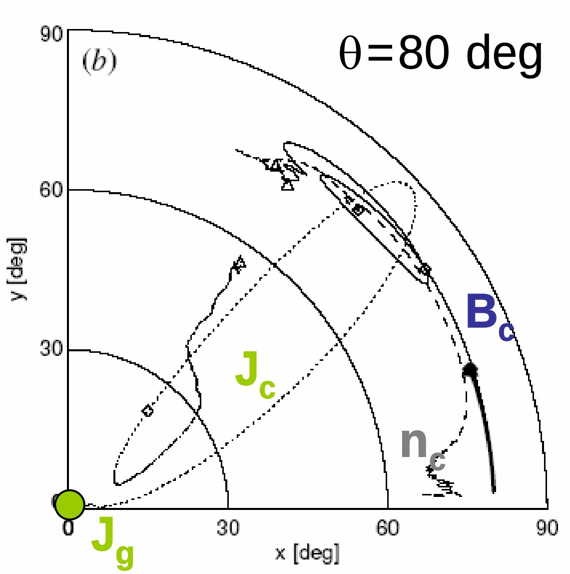

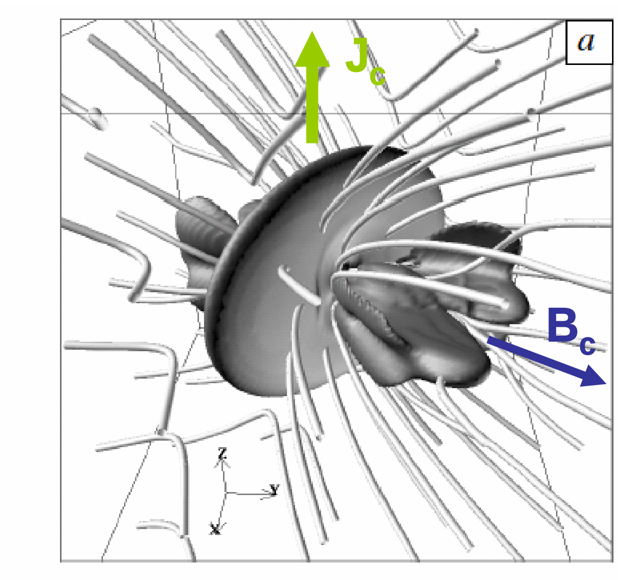

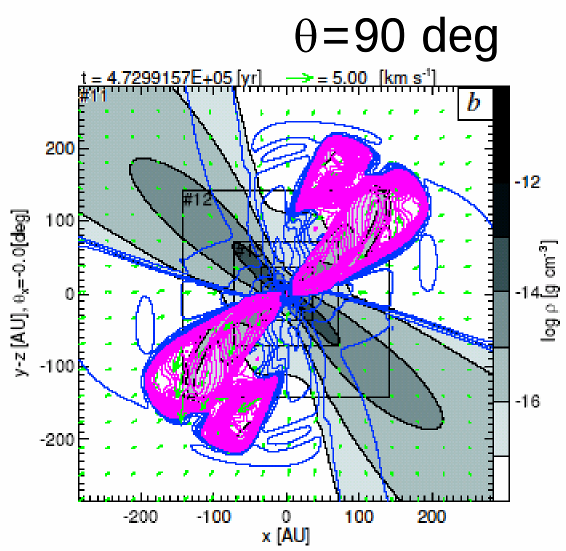

θ=70 deg and θ=80 deg

Local B_c, $\mathbf{J_c}$, and disk normal direction are converged!!

⇩

B-Field removes the perpendicular component of **J** to **B**.

θ~35 deg between $\mathbf{B_c}$ and $\mathbf{B_g}$

Perpendicular rotator

$\mathbf{J_c} \nparallel \mathbf{B_c}$

Even in this case, the outflow is ejected in the direction of B-field.

Magnetic Braking and Angular Momentum of $\rho > 0.1\rho_{max}$

- Angular momentum is effectively <u>transferred by the magnetic braking</u>.
- Especially model of θ = 90deg, J is effectively removed from the central part

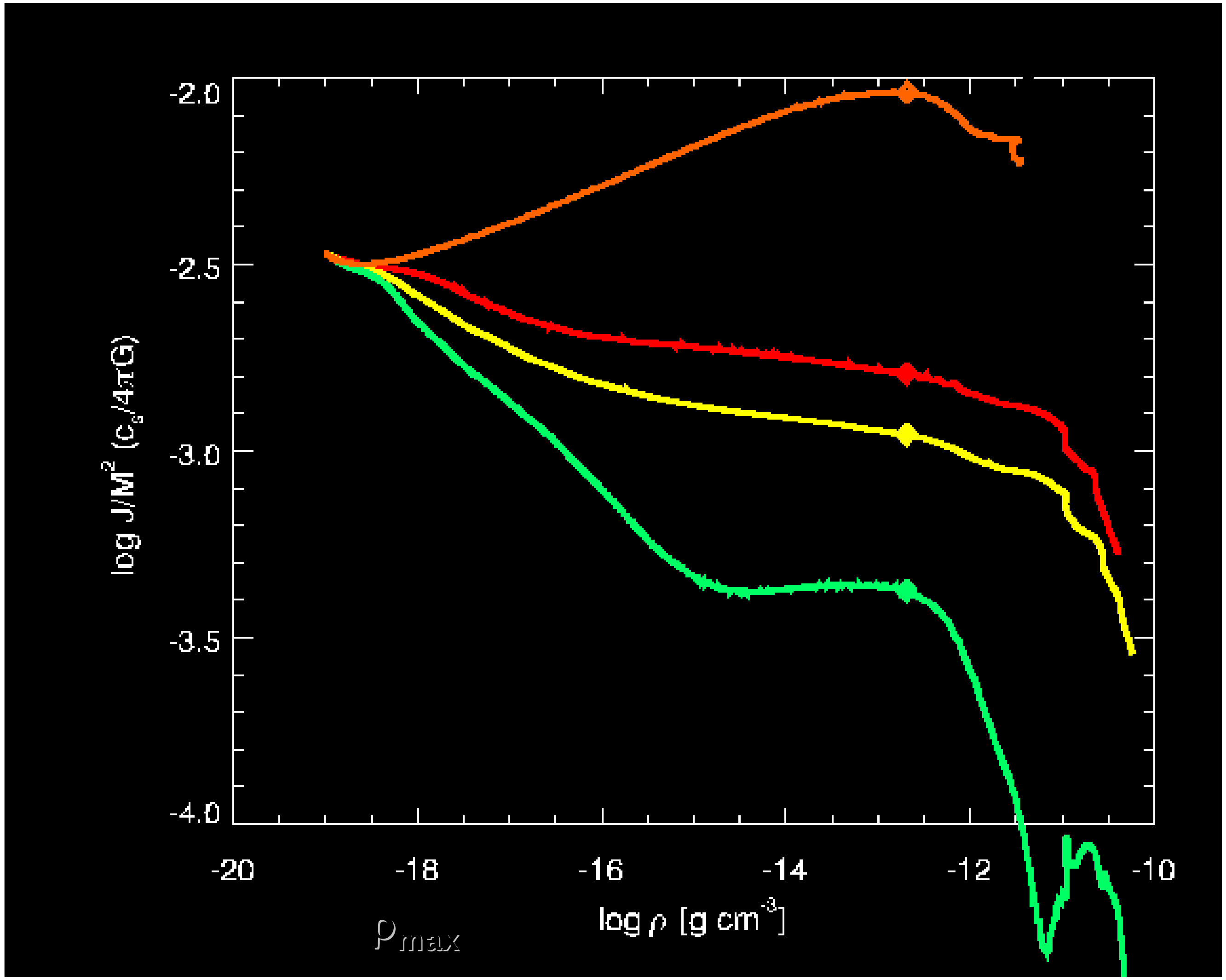

Amb. Diff?

Reconstruction of Polarization vectors at 5000 AU scale (B_{ave} = 82.8μG)

MF45
B_0=18.6μG

Matsumoto et al. 2006 ApJ. 637, L105

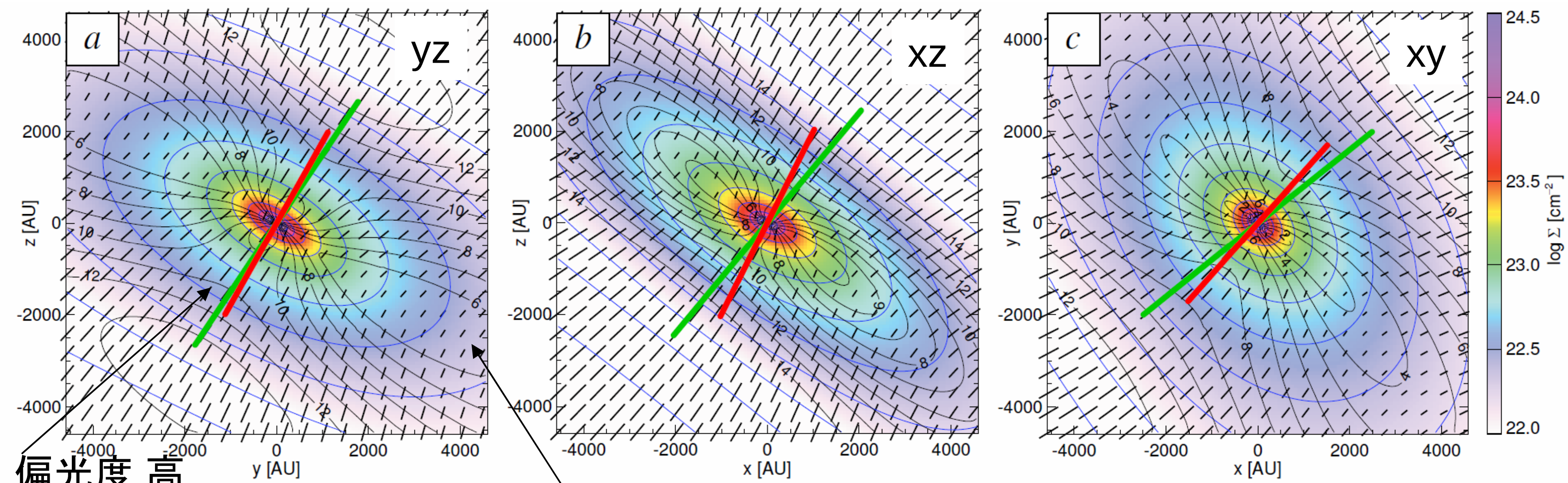

Green : mean direction of polarization vector
Red : direction of the outflow (50AU scale **B**)
Colors: column density

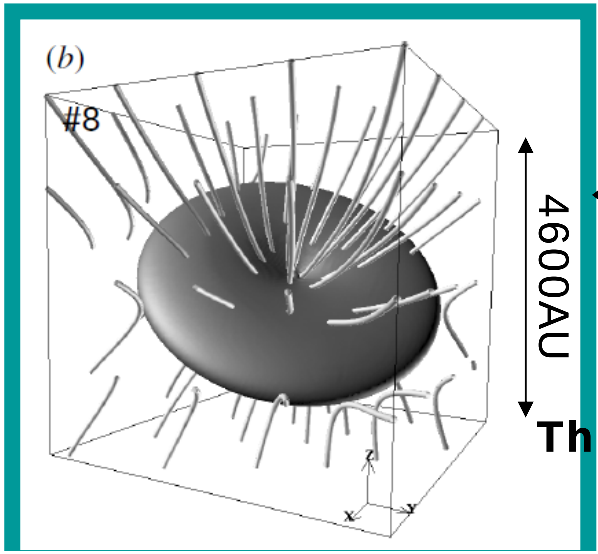

← Three-dimensional structure

Tree-dimensional angle between magnetic field and outflow is 12.4 deg.

The outflow is well aligned with the polarization vector.

Reconstruction of Polarization vectors at 5000 AU scale (B_{ave} = 50.1μG)

WF45
B_0 = 7.42μG

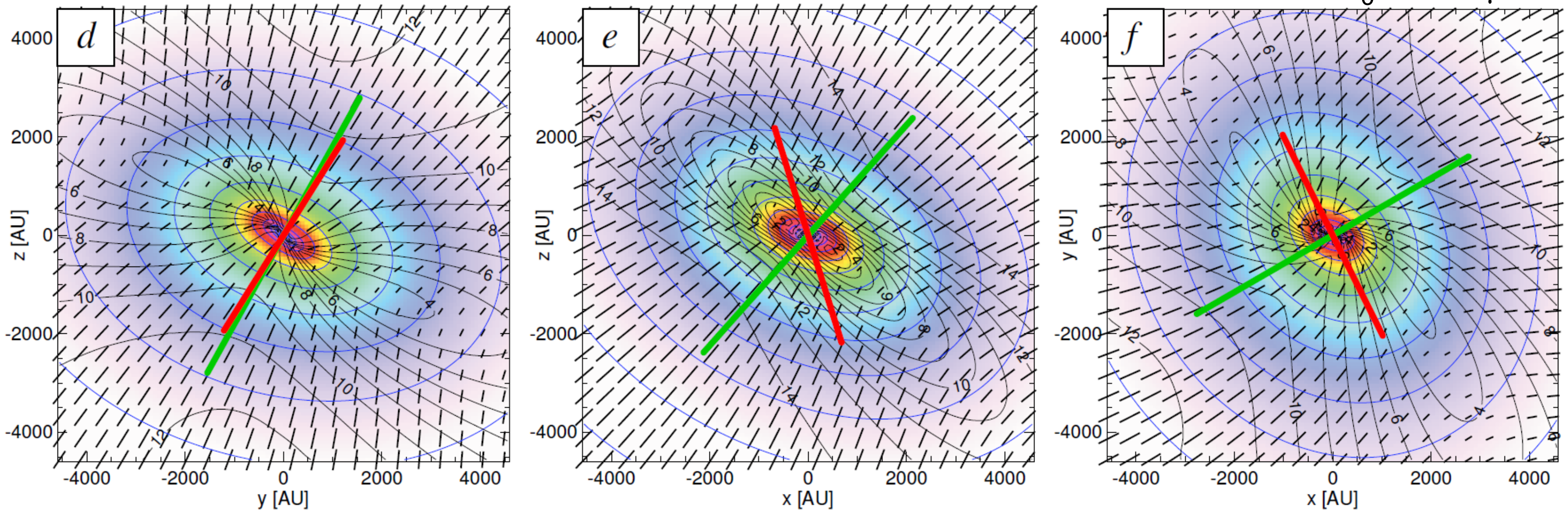

Green : mean direction of polarization vector
Red : direction of the outflow
Colors: column density

Three-dimensional angle between magnetic field and outflow is 53.5 deg.

The alignment depends on the line of sight

Directions of B, Ω, and disk normal vectors: variation in scale.

MF45
$B_0 = 18.6\mu G$

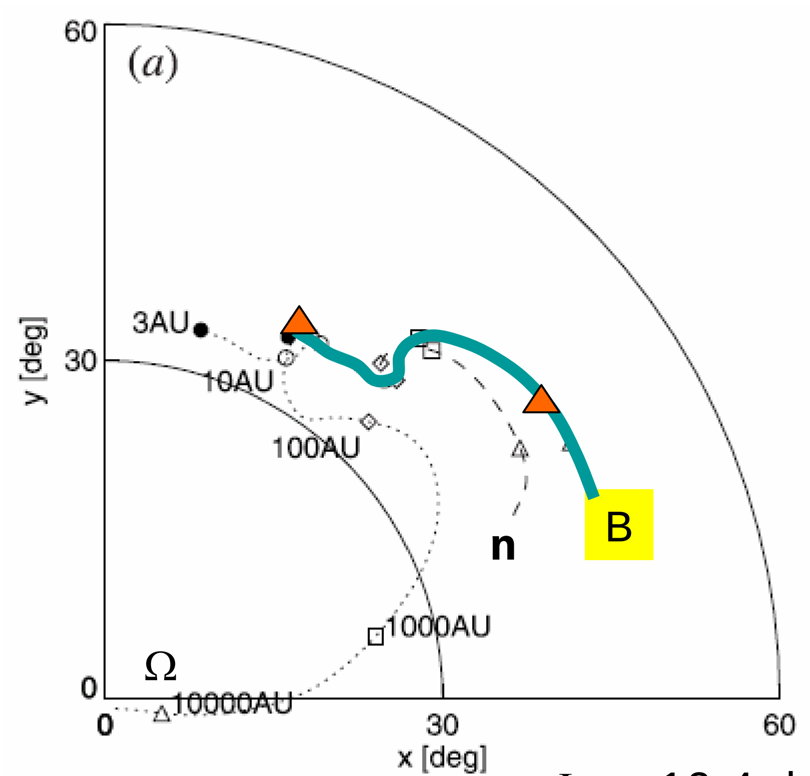

$\Phi_{3D} = 12.4$ deg.

WF45
$B_0 = 7.42\mu G$

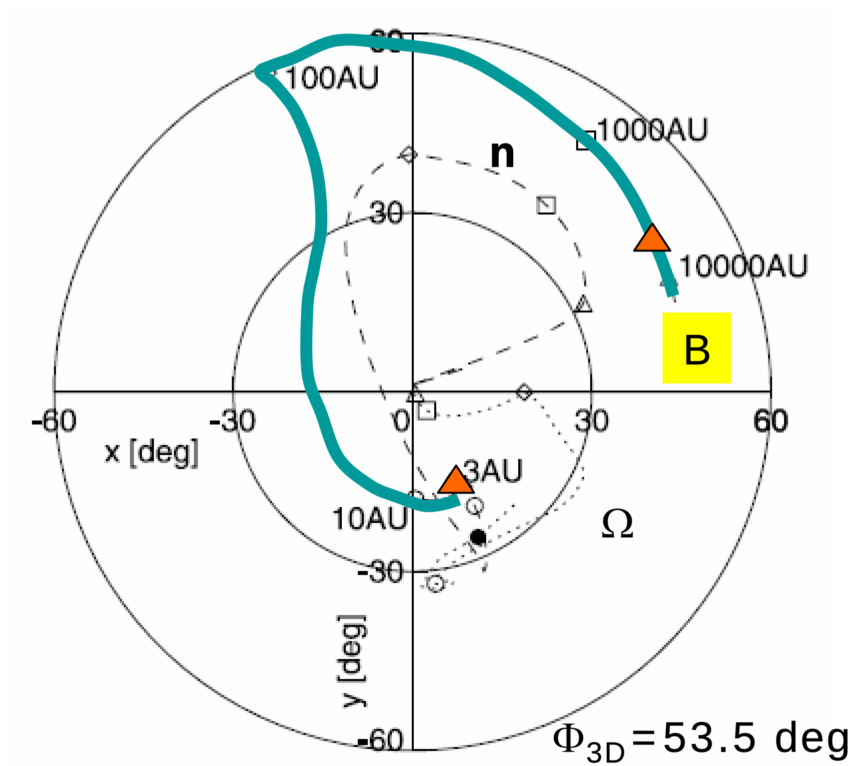

$\Phi_{3D} = 53.5$ deg.

FIG. 15.—Radial distribution of the mean magnetic field (*solid line*), mean angular momentum (*dotted line*), and normal vector of the disk (*dashed line*) in the final stage of model WF45.

Can we infer the central magnetic field near future? … by *ALMA*?

Target: B335 @ 250 pc
Resolution: 0.1” (25 AU)

WF45
$B_0 = 7.42 \mu G$

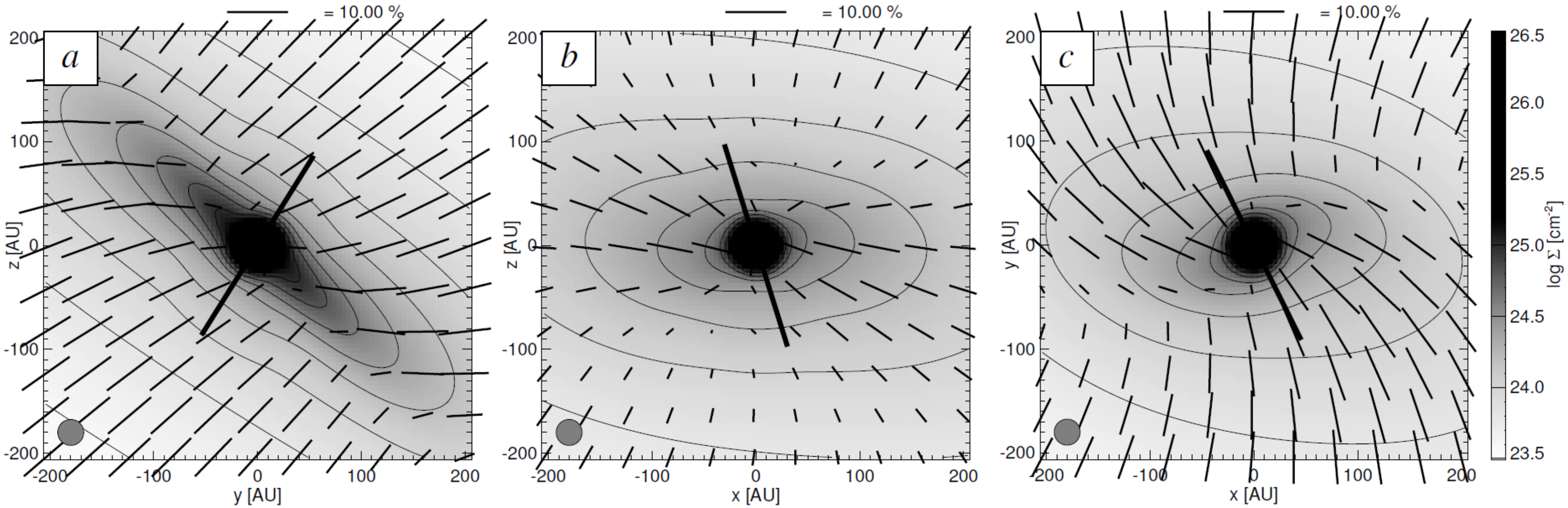

Yes, we can resolve the magnetic fields around the protostar.
The outflow traces the direction of magnetic field at the cloud center.

Summary

- Fragmentation of Aligned Rotator
  - A critical Ω to B ratio for the cloud to fragment

$$\frac{\Omega_0}{B_0} > \frac{G^{1/2}}{2^{1/2} c_s} \sim 3\times10^{-7}\,\mathrm{yr}^{-1}\mu\mathrm{G}\left(\frac{c_s}{190\mathrm{ms}^{-1}}\right)^{-1}$$

- Non-aligned Rotator
  - Local $\mathbf{B_c}$, $\mathbf{J_c}$, disk normal $\mathbf{n_c}$ directions are converged each other in the dynamical contraction.
  - Local $\mathbf{B_c}$ has an angle with $\mathbf{B_g}$ ~ 30-35deg if θ<80 deg.

Direction of the Disk

Machida, et al. (2006) ApJ. 645, 1227-1245

- Rotation-dominant:
  - disk $\perp \mathbf{J}$
- Magnetic-dominant:
  - disk $\perp \mathbf{B}$
- Boundary is given

$$\frac{\Omega_0}{B_0} = 0.39 \frac{G^{1/2}}{c_s}$$

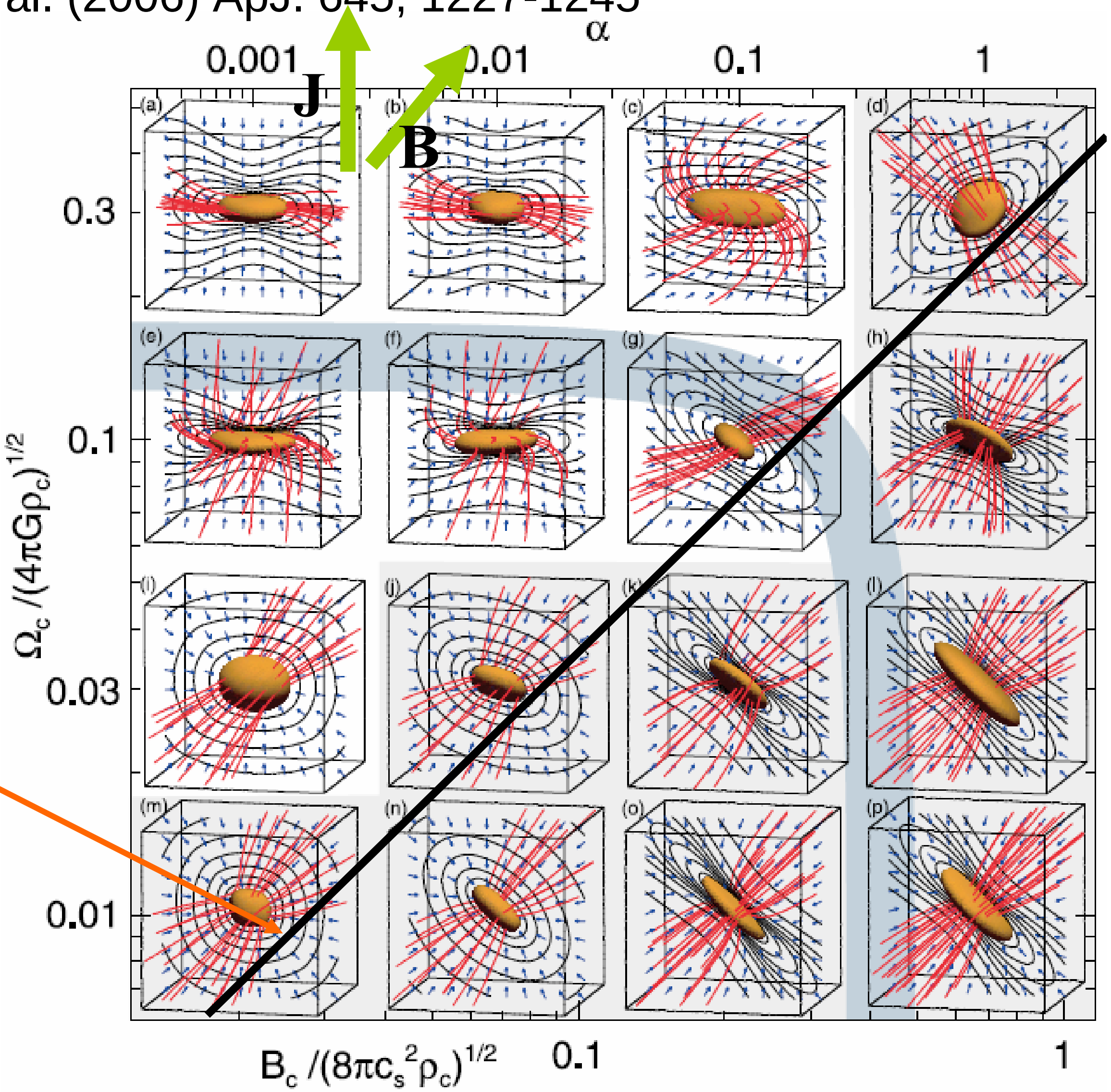

Qualitative

Summary for Part 1

- Magnetic field (B) and angular momentum (J) play cooperatively a role to form e.g. outflows.
- B reduces the power of J to form fragmentation.
- Disk is formed either by J or B depending on the dominant force: J or B.
- Misaligned weak field initial configuration fits observations of outflow-global B misalignment.

Evolution of a Rotating First Core

Saigo & Tomisaka (2006, ApJ, 645, 381-394)

Saigo, Matsumoto, Tomisaka (2007, in prep.)

- I have showed that B-field controls the angular momentum of the first core.
- Fragmentation develops quickly in a <u>hydrostatic state</u> (first core) <u>rather than in a contracting circumstance</u> (runaway phase)
- Fragmentation in a first core may bring binary or multiple stars.

  ←binaries are more popular than single stars.
- Ideal MHD should be reconsidered.

Temp-density relation of IS gas. (Tohline 1982)

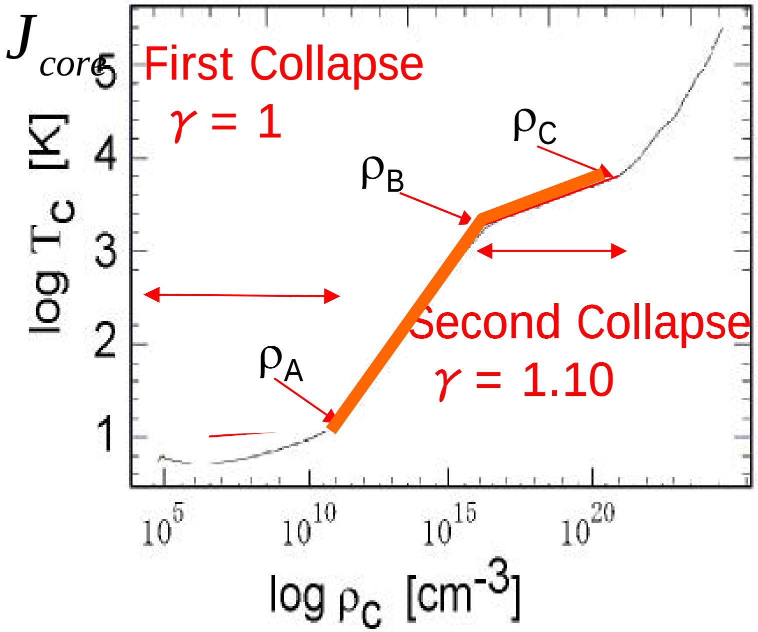

Masunaga & Inutsuka (2000)

Hydrostatic Equilibrium

- Hydrostatic Axisymmetric Configuration for Barotropic Gas

$$\left(\rho r \Omega^2, 0, 0\right) - \nabla P - \rho \nabla \psi = 0,$$

$$\Delta \psi = 4\pi G \rho$$

$$p \approx \begin{cases} K_1 \rho^{7/5} & \ldots \quad (\rho \le \rho_{dis}) \\ K_2 \rho^{1.1} & \ldots \quad (\rho > \rho_{dis}) \end{cases}$$

dissociation density

- Angular Momentum Distribution
  - same as a uniform-density sphere with rigid-body rotation
  - total mass M_{core} and total ang. mom. J_{core}

$$j(M(R)) = \frac{5}{2}\left(\frac{J_{core}}{M_{core}}\right)\left\{1 - \left(1 - \frac{M(R)}{M_{core}}\right)^{2/3}\right\}$$

- Self-consistent Field Method (SCF) Hachisu(1986), Tohline, Durisen

$$\left(M_{core}, J_{core}\right) \to \rho_c$$

  - to understand the evolution of first core

$$\left(\rho_c, M_{core}\right) \to J_{core}$$

Examples of Hydrostatic Configuration

$\Omega \nearrow \quad M \nearrow$

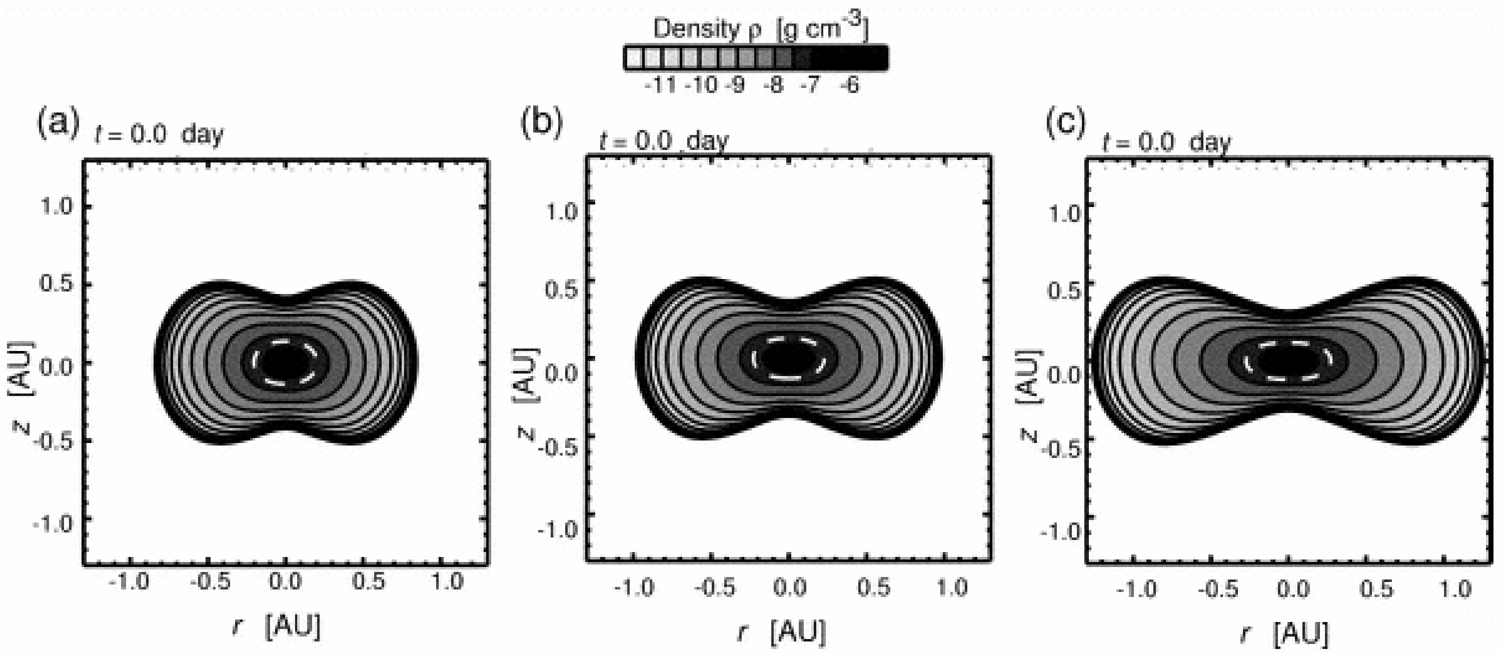

Three models have the same central density $\rho_c = 4\rho_{diss}$, but different angular momenta as 2.25×10^{49} (left), 4.18×10^{49} (middle), and 9.99×10^{49} g cm^2 (right), and masses as 2.77×10^{31} (left), 3.45×10^{31} (middle), and 4.97×10^{31} g (right).

Mass-Density Relation ($\Omega = 0$)

- <u>Below $\rho \lesssim \rho_{dis}$</u> mass increases with central density ρ_c.
  - Mass is prop. to Jeans mass
    $$M_J \propto T^{3/2} \rho^{-1/2} \propto \rho^{1/10}$$
    (Chandrasekhar 1949)
  - Mass accretion drives the core from lower-left to upper-right.

$\rho_{dis} = 5 \times 10^{-8}\,\mathrm{g cm^{-3}}$

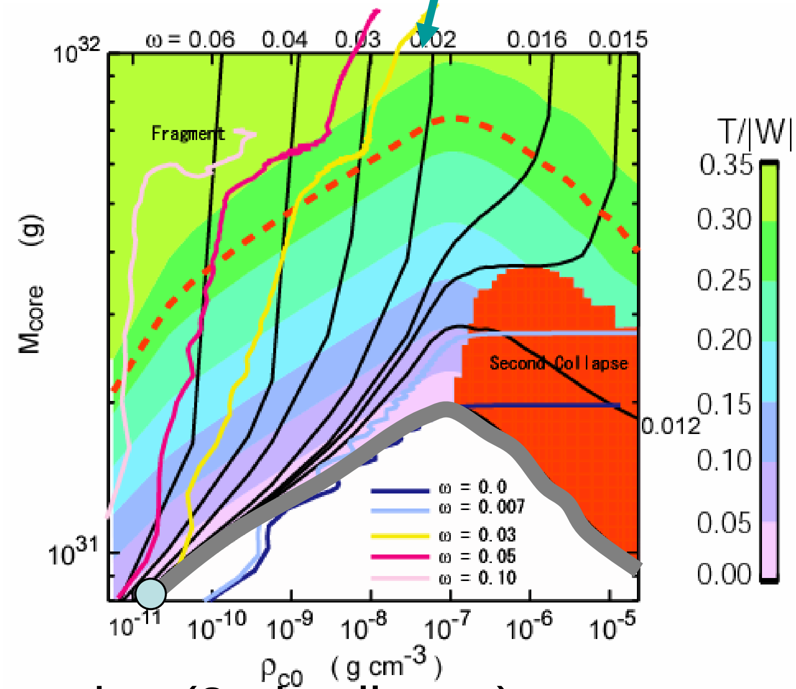

- <u>Above $\rho \gtrsim$ a few ρ_{dis}</u> mass decreases due to soft EOS.
  - Further accretion destabilizes the cloud and drives dynamical contraction (2nd collapse).

■ Maximum mass of the 1st core is 0.01 $M_{\odot}$.

Hydrodynamical Simulation

- run-away (1st collapse) → 1st core
  - 1st core grows by mass accretion from contracting envelope.
- Initial Condition
  - Bonnor-Ebert sphere (+ envelope (R~50,000AU))
  - n_c~$10^4 H_2 cm^{-3}$, T=10K
  - Rotation $\omega=\Omega t_{ff}$=0~0.3
  - increase the BE density by 1.1~8 times
  - Perturbations m=2 and m=3 $\delta\rho/\rho$=10%
- Numerical method
  - HD nested grid
  - barotropic EOS

Non-rotating model

1. Unless the cloud is much more massive than the B-E mass, the first core evolves to follow a path expected by quasi-hydrostatic evolution.

2. Maximum mass of a first core is small ~0.01M$_{\odot}$.

3. Quasi-static evolution gives a good agreement with HD result.

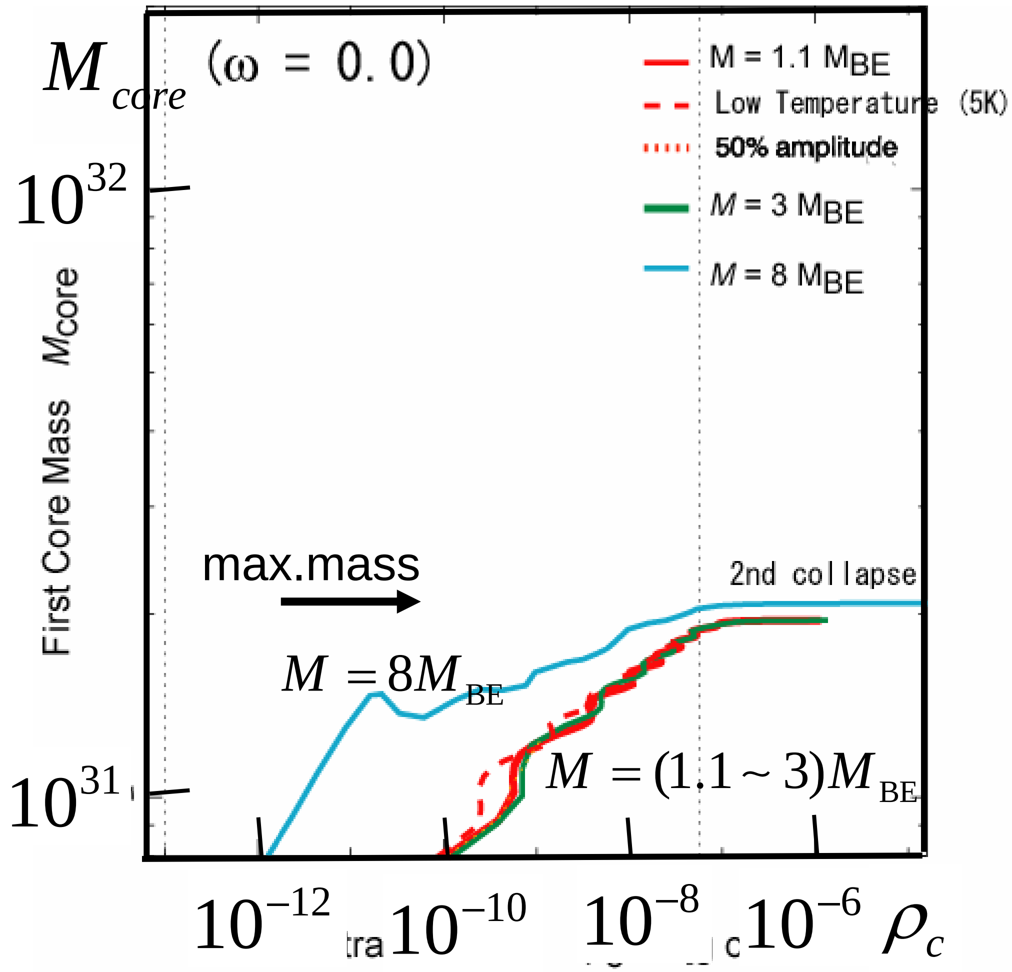

Mass-Density Relation ($\Omega > 0$)

- rotation rate of parent cloud

$$\omega = \frac{j}{M}\left(\sqrt{2}c_s / G\right)$$

- ω<0.015
  - similar to non-rot. case.
  - second collapse

- ω>0.015
  - Mass increases much
  - well below $\rho_c \ll \rho_{dis}$

$\rho_{dis} = 5\times10^{-8}\,\mathrm{gcm}^{-3}$

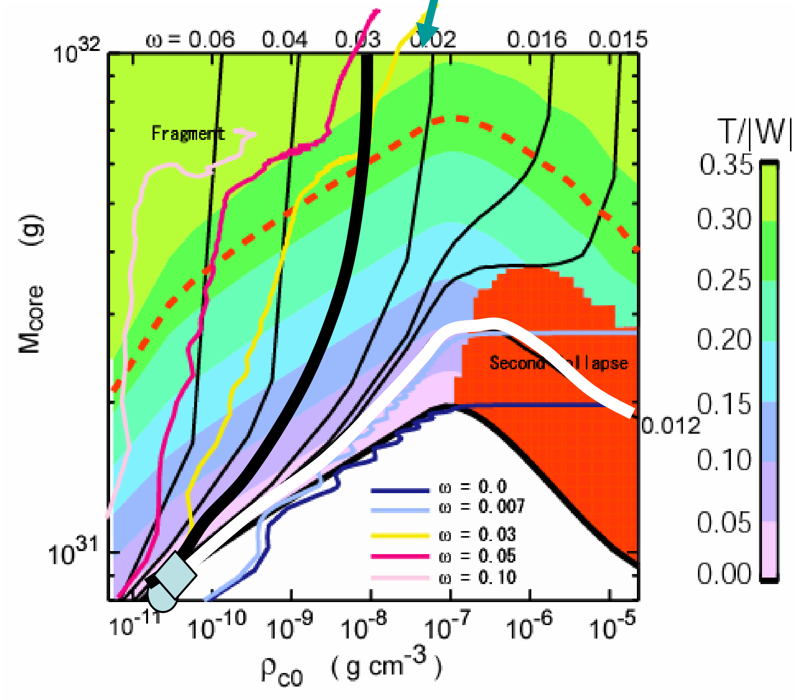

Rotating Cloud (ω=0.05)

- First, the 1st core increases its mass (upwardly in M_{cl}-ρ_c plane).
  - follows a hydrostatic evolution path.
  - Shape: round spherical disk.
- Then, the first core begins to contract (rightward in the plane)
  - This phase, spiral arms appear.
  - J is transferred outwardly.
- Core+disk continues to contract.

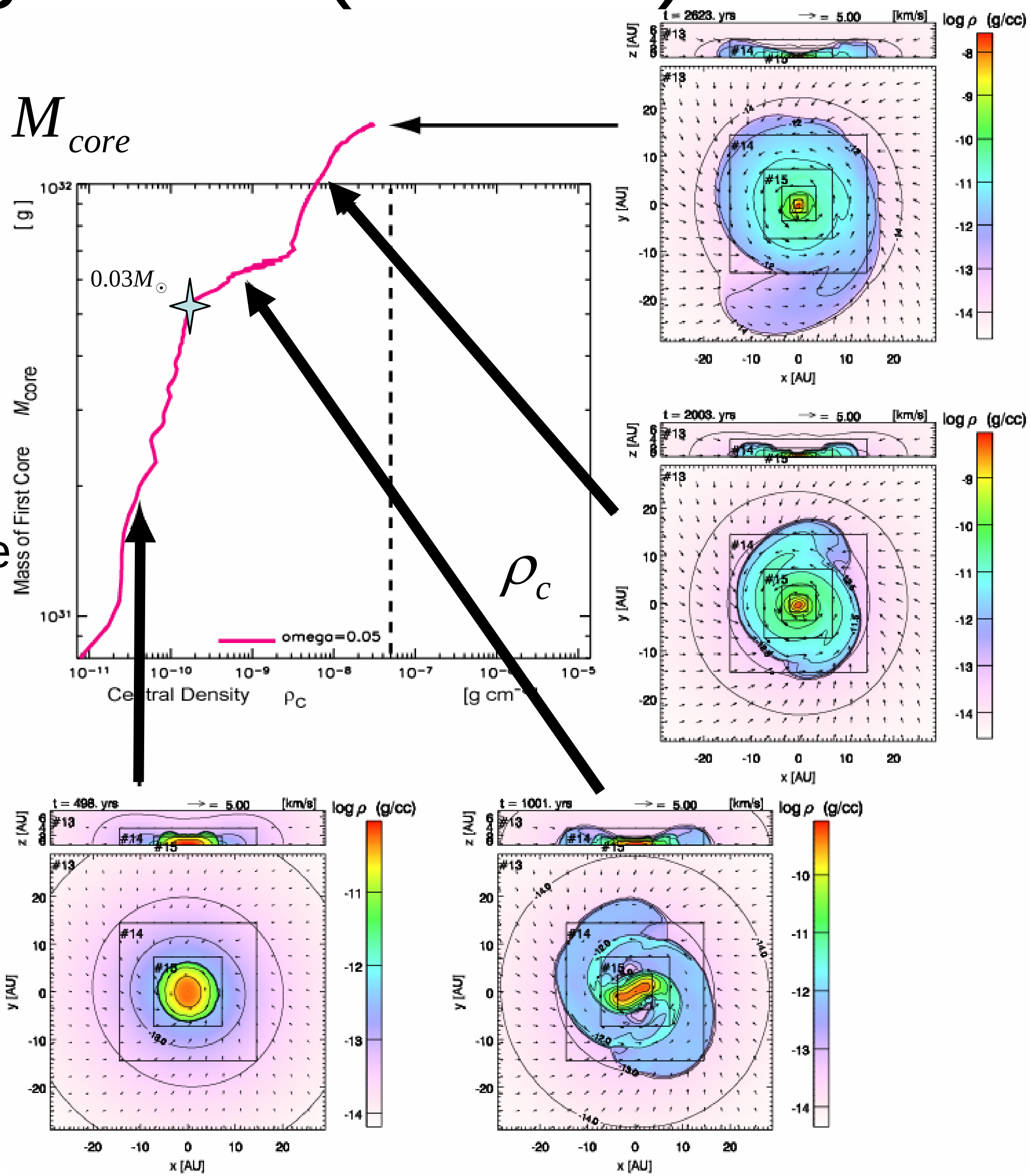

Central core of the 1st core

Begins 2nd collapse
after arrived at the unstable
region.

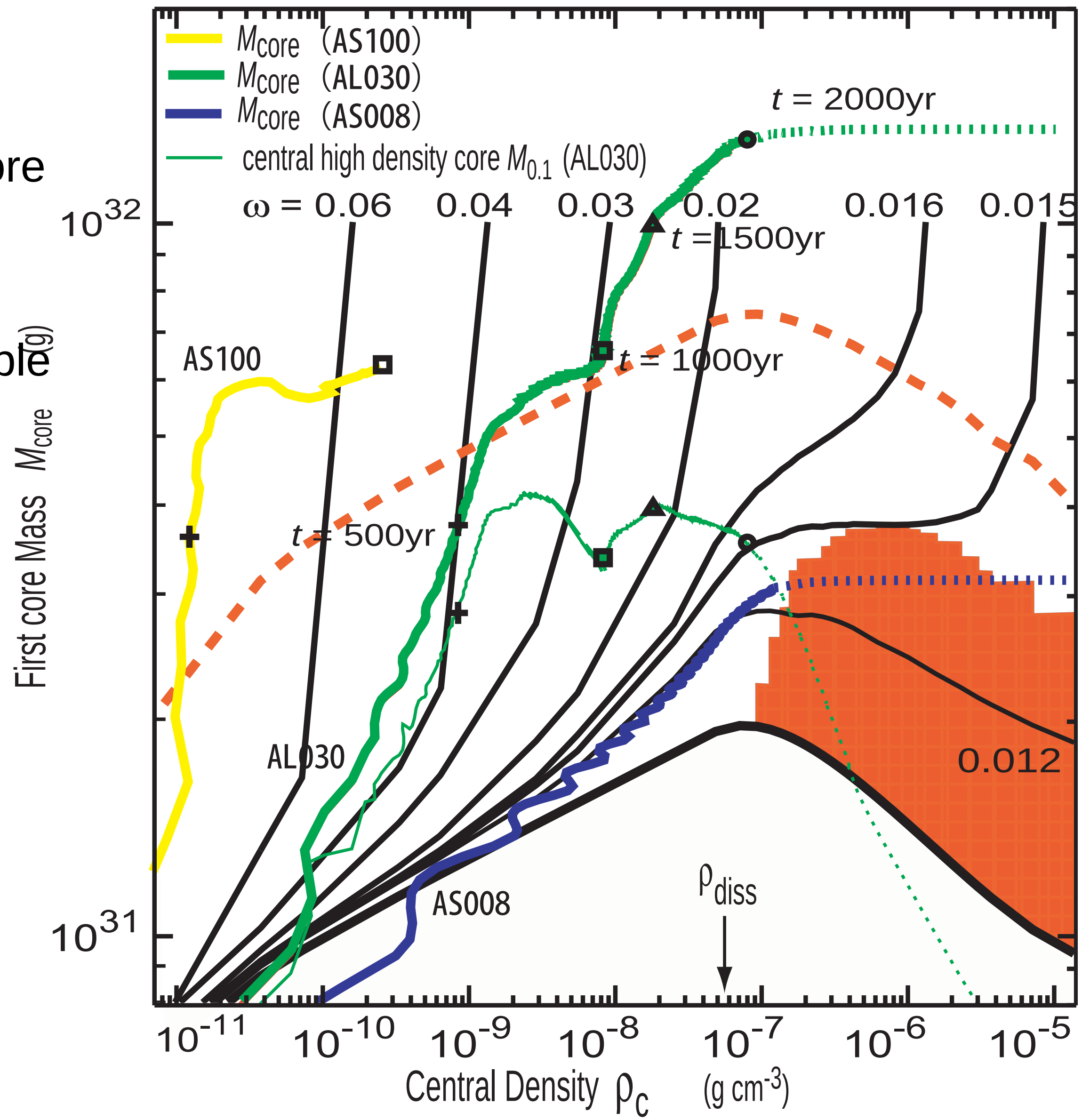

Nonaxisymmetric instability

- Rotational-to-gravitational energy ratio: $T/|W|$
  - A polytropic disk with $T/|W|>0.27$ ($\gamma=5/3$) is dynamically unstable under a wide range of conditions ($\gamma=5/3$: Pickett et al. 1996; $\gamma=7/5, 9/5, 5/3$ Imamura et al. 2000)
- $T/|W|$ increases with mass accretion.
- After $T/|W|$ exceeds the critical value,
  - nonaxisymmetric instability grows.
  - Angular momentum is transferred outwardly.
  - This may stabilize the disk again.

$$\rho_{dis} = 5\times10^{-8}\,\mathrm{gcm}^{-3}$$

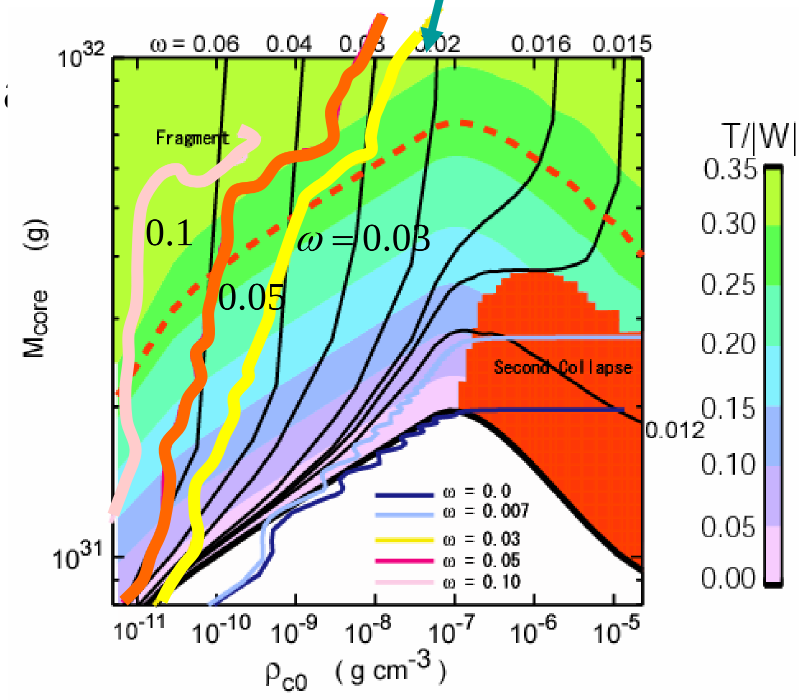

Fragmentation

- In a fast rotating cloud, fragmentation (more than 2 fragments) is observed in the 1st core.
- This occurs after non-axisymmetric instability is triggered.
-

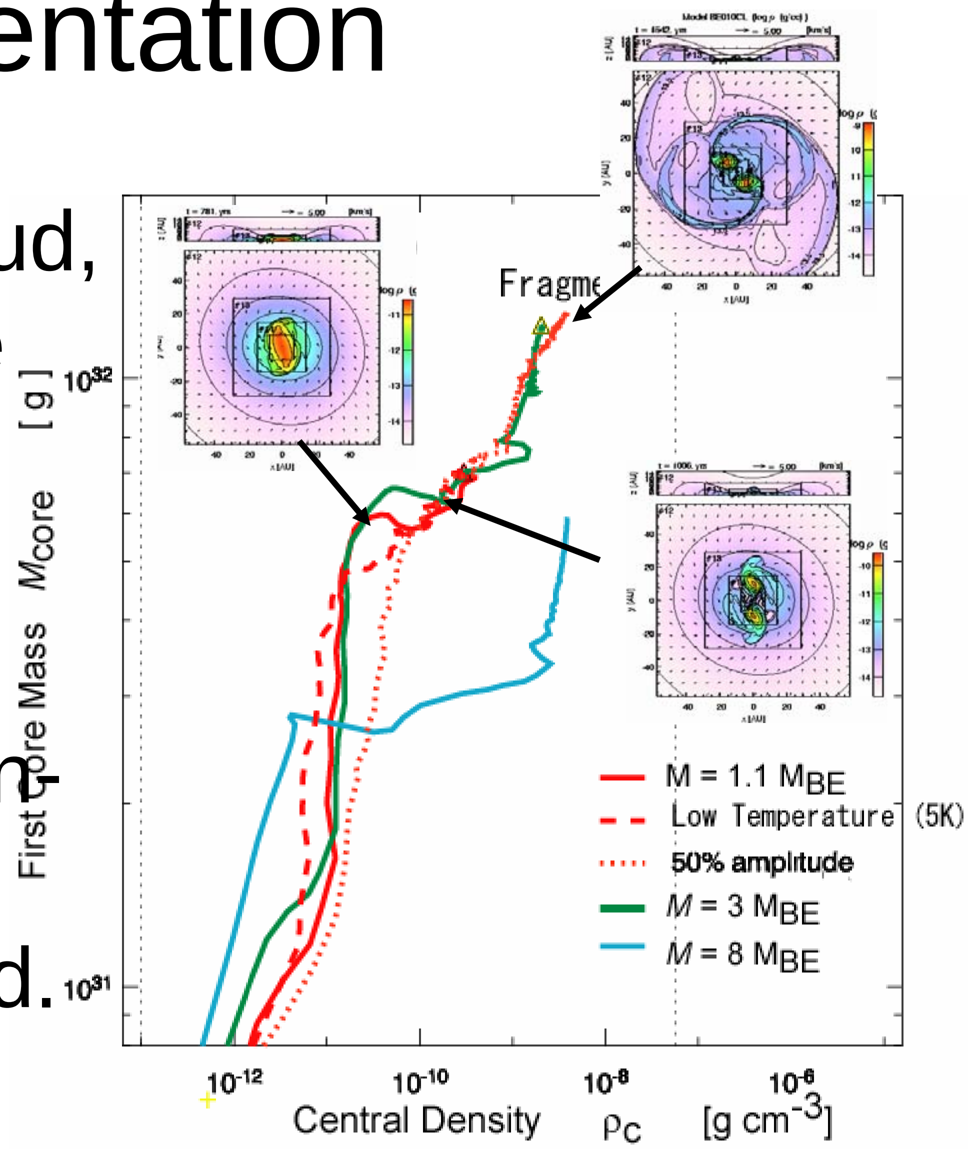

Typical Rotation Rate

- NH_3 cores ($n \sim 3\ 10^4 \mathrm{cm}^{-3}$) Goodman et al (1993)

$$\Omega \simeq (0.3-2)\times 10^{-6}\,\mathrm{rad\ yr}^{-1}$$

$$\tau_{ff} = \left(\frac{3\pi}{32G\rho}\right)^{1/2} \simeq 2\times 10^{5}\,\mathrm{yr} \longrightarrow \omega \simeq 0.06-0.4$$

- N_2H^+ cores ($\sim 2\ 10^5 \mathrm{cm}^{-3}$) Caselli et al. (2002)

$$\Omega \simeq (0.5-6)\times 10^{-6}\,\mathrm{rad\ yr}^{-1}$$

$$\tau_{ff} = \left(\frac{3\pi}{32G\rho}\right)^{1/2} \simeq 8\times 10^{4}\,\mathrm{yr} \longrightarrow \omega \simeq 0.04-0.5$$

Luminosity of the First Core

$$L = -\frac{dE_{tot}}{dt} = -\frac{d}{dt}\left(W + E_{kin} + E_{th}\right)$$

3D simulation

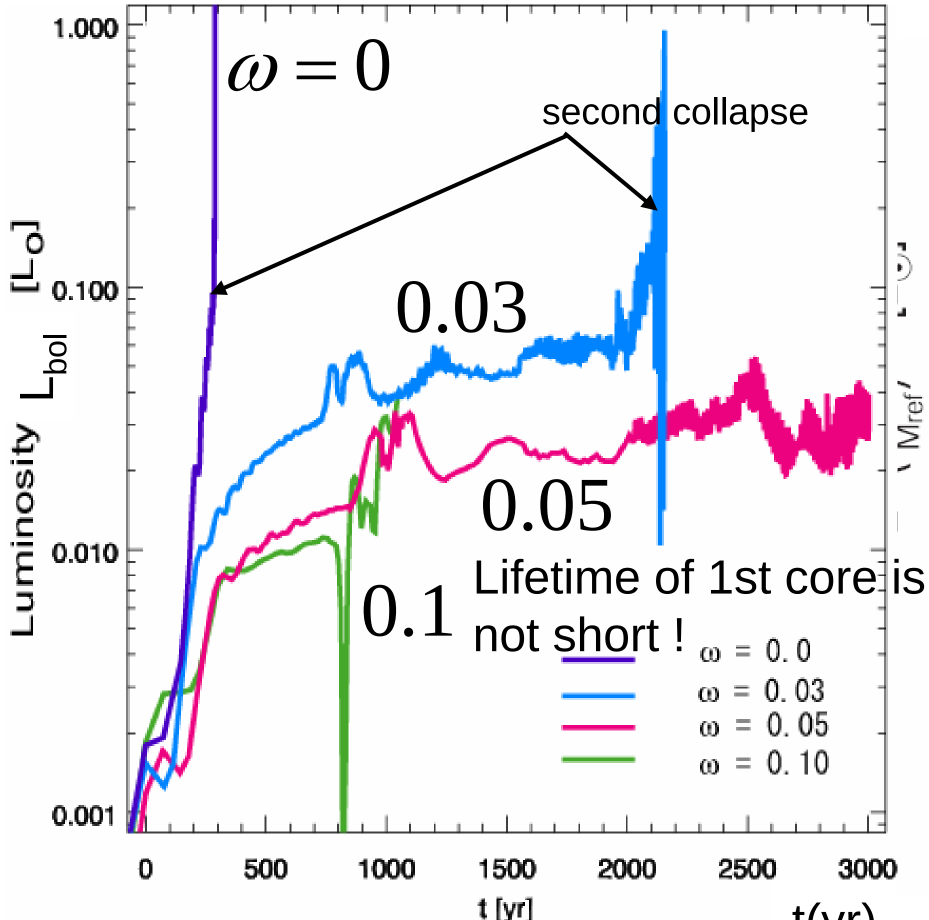

t(yr)

Quasi-static evolution

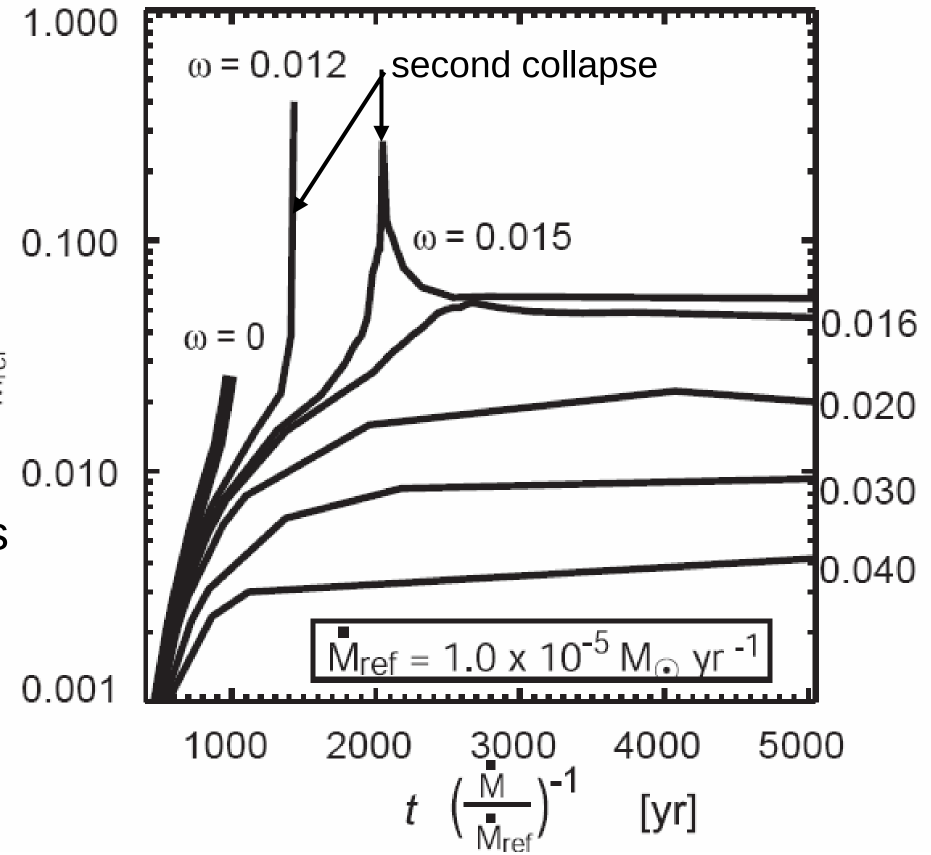

L is a decreasing function of ω.

$$\dot{M} \sim 2\times10^{-5} M_\odot \mathrm{yr}^{-1}$$
$$L \sim (3-5)\times10^{-2} L_\odot$$

Absolute value L and timescale are obtained after $\dot{M}$ is given. $L \propto \dot{M}$ $\quad t \propto \dot{M}^{-1}$

Mass Accretion Rate

- Mass accretion rate is between the LP solution and a SH disk solution.
- Much higher than that expected for SIS.

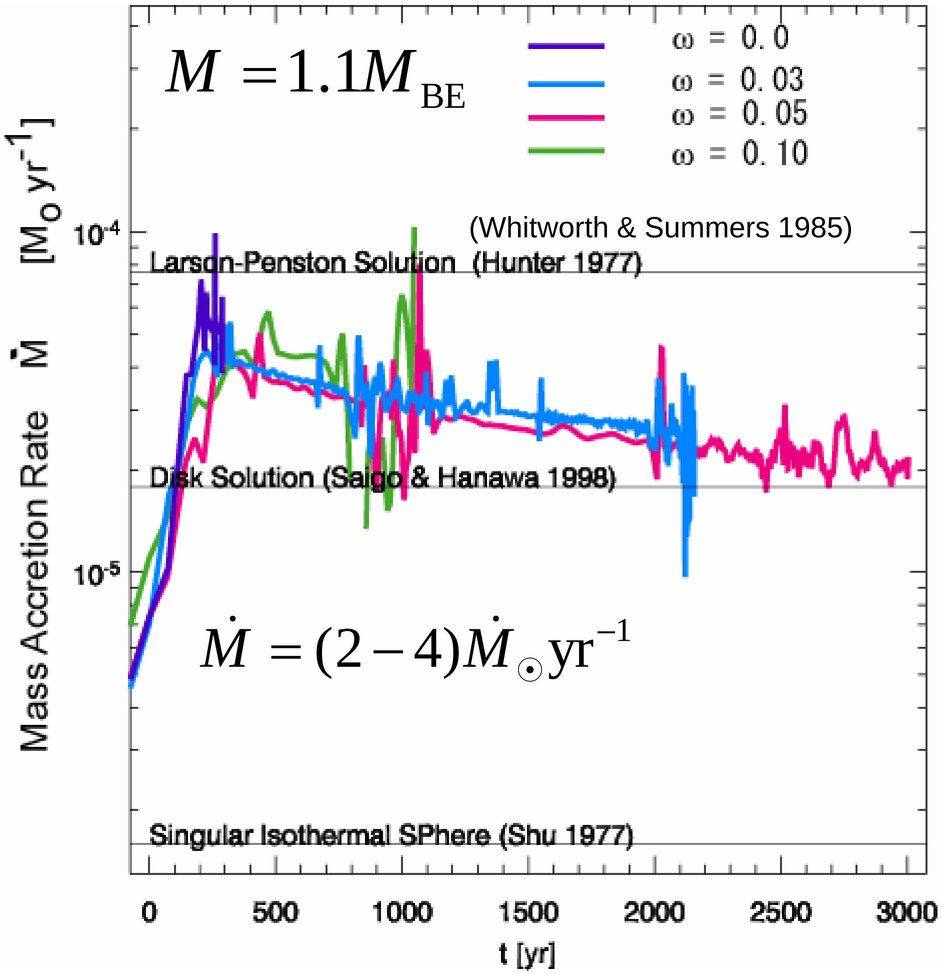

Summary of 2nd Part

- The evolution of a 1st core is well described with the quasi-static evolution.
- Slow (or no) rotation model exhibits the second collapse (ω<0.015).
  - Maximum mass of the 1st core ~0.02 $M_{\odot}$ (ω=0.015).
- Rotating cloud with ω>0.015, the 1st core contracts slowly.
  - After T/|W|>0.27, a dynamical nonaxisymmetric instability grows and spiral pattern appears.
  - Gravitational torque transfers the angular momentum outwardly.
  - The 1st core contracts further.
- In a rotating cloud with ω>0.1, we found the fragmentation of the 1st core.